

Puget Sound Nutrient Source Reduction Project

Volume 2: Model Updates and Optimization Scenarios, Phase 2



By

Cristiana Figueroa-Kaminsky, Anise Ahmed,
Teizeen Mohamedali, John Gala, and Hanis Zulmuthi

For the

Environmental Assessment Program

Washington State Department of Ecology
Olympia, Washington



June 2025, Publication 25-03-003

Publication Information

This document is available on the Department of Ecology's website at:
<https://apps.ecology.wa.gov/publications/SummaryPages/2503003.html>.

Related Information

- Activity Tracker Code: 06-509

Cover Photo: Eyes over Puget Sound, Marine Monitoring Unit, ECY. Algal bloom in Dugualla Bay/Skagit Bay on 7/28/2014.

Suggested Citation:

Figueroa-Kaminsky, C., A. Ahmed, T. Mohamedali, J. Gala, and H. Zulmuthi. 2025. Puget Sound Nutrient Source Reduction Project. Volume 2: Model Updates and Optimization Scenarios, Phase 2. Publication 25-03-003. Washington State Department of Ecology, Olympia.
<https://apps.ecology.wa.gov/publications/SummaryPages/2503003.html>.

Contact Information

Publications Coordinator
Environmental Assessment Program
Washington State Department of Ecology
P.O. Box 47600
Olympia, WA 98504-7600
Phone: 564-669-3028
Website: [Washington State Department of Ecology](http://www.ecology.wa.gov)¹

Any use of product or firm names in this publication is for descriptive purposes only and does not imply endorsement by the author or the Department of Ecology.

This project has been funded wholly or in part by the U.S. Environmental Protection Agency (EPA) under Multi-Purpose Grant Agreement AA-01J87501 and the Performance Partnership Agreement BG-96086013 with the Washington State Department of Ecology. The contents of this document do not necessarily reflect the views and policies of EPA, nor does mention of trade names or commercial products constitute endorsement or recommendation for use.

ADA Accessibility

The Department of Ecology is committed to providing people with disabilities access to information and services by meeting or exceeding the requirements of the Americans with Disabilities Act (ADA), Section 504 and 508 of the Rehabilitation Act, and Washington State Policy #188.

To request an ADA accommodation, contact the Environmental Assessment Program's Publications Coordinator by phone at 564-669-3028 or email at EAPpubs@ecy.wa.gov. For Washington Relay Service or TTY call 711 or 877-833-6341. Visit Ecology's website at <https://ecology.wa.gov/accessibility> for more information.

¹ www.ecology.wa.gov/contact

Department of Ecology's Regional Offices

Map of Counties Served



| | | | |
|---|---|---------------------------------------|---------------------------------------|
| Southwest Region 360-407-6300 | Northwest Region 206-594-0000 | Central Region 509-575-2490 | Eastern Region 509-329-3400 |
|---|---|---------------------------------------|---------------------------------------|

| Region | Counties served | Mailing Address | Phone |
|---------------------|--|--|--------------|
| Southwest | Clallam, Clark, Cowlitz, Grays Harbor, Jefferson, Mason, Lewis, Pacific, Pierce, Skamania, Thurston, Wahkiakum | PO Box 47775 Olympia, WA 98504 | 360-407-6300 |
| Northwest | Island, King, Kitsap, San Juan, Skagit, Snohomish, Whatcom | PO Box 330316 Shoreline, WA 98133 | 206-594-0000 |
| Central | Benton, Chelan, Douglas, Kittitas, Klickitat, Okanogan, Yakima | 1250 W Alder St Union Gap, WA 98903 | 509-575-2490 |
| Eastern | Adams, Asotin, Columbia, Ferry, Franklin, Garfield, Grant, Lincoln, Pend Oreille, Spokane, Stevens, Walla Walla, Whitman | 4601 N Monroe Spokane, WA 99205 | 509-329-3400 |
| Headquarters | Across Washington | PO Box 47600 Olympia, WA 98504 | 360-407-6000 |

Puget Sound Nutrient Source Reduction Project

Volume 2: Model Updates and Optimization Scenarios, Phase 2

by

Cristiana Figueroa-Kaminsky, Anise Ahmed, Teizeen Mohamedali, John Gala, and Hanis Zulmuthi

Environmental Assessment Program
Washington State Department of Ecology
Olympia, WA

June 2025 | Publication 25-03-003



DEPARTMENT OF
ECOLOGY
State of Washington

Table of Contents

| | Page |
|--|-----------|
| List of Figures | 3 |
| List of Tables..... | 6 |
| Acknowledgments | 7 |
| Abstract..... | 9 |
| Executive Summary | 10 |
| Background..... | 10 |
| Model updates and performance | 10 |
| Nutrient reductions and DO noncompliance | 11 |
| Introduction | 20 |
| Project Description | 25 |
| Methods..... | 27 |
| Model initialization and parameterization..... | 27 |
| Watershed updates..... | 28 |
| Open boundary..... | 28 |
| Marine point source updates..... | 29 |
| Other methods | 29 |
| Existing and reference loads | 31 |
| Opt2 scenarios..... | 40 |
| Selecting a single watershed framework | 42 |
| WWTP frameworks | 45 |
| Opt2 scenario loads..... | 47 |
| Results and Discussion | 53 |
| Performance of updated model..... | 53 |
| Overall approach | 53 |
| Watershed flow and water quality regressions | 54 |
| Hydrodynamics..... | 61 |
| Water quality..... | 65 |
| Phytoplankton productivity..... | 84 |
| Microbial respiration in bottom waters..... | 84 |
| Summary of performance | 85 |
| Overview of model limitations..... | 85 |
| Residence and flushing times..... | 86 |
| DO consumption in bottom layers | 87 |
| Sensitivity and uncertainty..... | 99 |
| Sensitivity to multiple parameter adjustment | 100 |
| Uncertainty in DO depletion estimates..... | 104 |

| | |
|--|------------|
| Uncertainty in comparison with DO numeric criteria | 105 |
| DO noncompliance | 107 |
| Noncompliance under existing conditions..... | 108 |
| Noncompliance under Opt2 scenarios..... | 109 |
| Conclusions | 126 |
| Recommendations..... | 129 |
| References | 130 |
| Glossary, Acronyms, and Abbreviations | 137 |
| Glossary | 137 |
| Acronyms and Abbreviations | 143 |
| Units of Measurement | 145 |
| Appendices..... | 146 |

List of Figures

| | Page |
|--|------|
| Figure 1. The Salish Sea Model domain and intermediate scale model grid (A) in Greater Puget Sound (B), northern Puget Sound (C), and South Sound (D). | 22 |
| Figure 2. Components of the Salish Sea Modeling effort to support the Puget Sound Nutrient Source Reduction Project. | 24 |
| Figure 3. Map showing the location of the eight basins that are used to group input loads and model results, along with the location of watershed and marine point source inputs. | 32 |
| Figure 4. Bar plots showing average annual daily flows as well as average annual daily anthropogenic (anthro.) total nitrogen (TN) and total organic carbon (TOC) loads entering WA waters of the Salish Sea in 2000, 2006, 2008, and 2014. | 35 |
| Figure 5. Bar plots showing average annual daily flows and average annual daily anthropogenic nitrogen loads (TN) and total organic carbon loads (TOC) entering different basins in 2000, 2006, 2008, and 2014 from both watersheds and marine point sources. | 36 |
| Figure 6. Daily anthropogenic total nitrogen (TN) loads entering WA waters of the Salish Sea in 2000, 2006, 2008, and 2014. | 38 |
| Figure 7. Daily anthropogenic total organic carbon loads entering WA waters of the Salish Sea in 2000, 2006, 2008, and 2014. | 39 |
| Figure 8. Plan view maps showing dissolved oxygen (DO) noncompliance days (left) and DO noncompliance magnitude (right) under existing 2014 conditions (top) and under Opt2 Scenario H1_C (bottom). | 41 |
| Figure 9. Annual anthropogenic watershed total nitrogen (TN, top) and total organic carbon (TOC, bottom) loads, by basin under existing 2014 conditions and the refined watershed framework for all Opt2 scenarios. | 44 |
| Figure 10. Annual anthropogenic total nitrogen (TN) watershed and marine point source loads entering different basins for each refined Opt2 scenario. | 48 |
| Figure 11. Diagnostic plots of model performance on the training data set for all variables for watersheds in different SSM basins. | 56 |
| Figure 12. Comparison of continuous SUNA nitrate-nitrite data with regression predictions at four major Puget Sound watersheds. | 58 |
| Figure 13. Comparison of 2023 to 2024 monthly average nitrate-nitrite regression-predicted and SUNA observed loads at four major Puget Sound watersheds. | 60 |
| Figure 14. NOAA water surface elevation observation stations. | 61 |
| Figure 15. Model predictions and observed data for water surface elevations. | 62 |
| Figure 16. Location of stations where currents were measured in 2006. | 63 |

| | |
|--|----|
| Figure 17. Eastward (U velocity, top panel) and northward (V velocity, bottom panel) depth-averaged current comparison between model prediction and observed data for Dana Passage (right panel) and Pickering Passage (left panel)..... | 64 |
| Figure 18. Time series plots of 2014 dissolved oxygen (DO) surface and bottom NWEM observations and SSM predictions..... | 67 |
| Figure 19. Time series plots for temperature (°C) at the surface (blue) and bottom (red) at selected stations for 2014..... | 69 |
| Figure 20. Time series plots for salinity (psu) at the surface (blue) and bottom (red) at selected stations for 2014..... | 70 |
| Figure 21. Time series plots for dissolved oxygen (DO, mg/L) at the surface (blue) and bottom (red) at selected stations for 2014..... | 71 |
| Figure 22. Year 2014 temperature profiles (°C) at selected stations for spring (left column), summer (center column), and fall (right column) conditions. | 72 |
| Figure 23. Year 2014 salinity profiles at selected stations for spring (left column), summer (center column), and fall (right column) conditions..... | 73 |
| Figure 24. Year 2014 dissolved oxygen (DO, mg/L) profiles at selected stations for spring (left column), summer (center column), and fall (right column) conditions. | 74 |
| Figure 25. Taylor (right) and target (left) plots for 2014 predicted and observed dissolved oxygen (DO) concentrations. | 76 |
| Figure 26. Taylor (right) and target (left) plots for bottom layers predicted and observed dissolved oxygen (DO) concentrations for all years (2000, 2006, 2008, and 2014) modeled. | 76 |
| Figure 27. Dissolved oxygen (DO) scatterplots for surface, middle, and bottom layers segregated into embayments and open estuary stations in 2014. | 77 |
| Figure 28. Map of selected locations for biochemical process DO consumption analysis... .. | 88 |
| Figure 29. Time series at selected locations of average simulated dissolved oxygen (DO) concentrations at SSM bottom two layers. | 89 |
| Figure 30. Sigma-t time series plots based on simulated data at selected locations. | 91 |
| Figure 31. Comparison of dissolved oxygen (DO) consumption from SSM’s bottom two layers at selected nodes by heterotrophic respiration (DDOC), nitrification (NITRIF), algal production minus algal respiration (DeltaDO_Algal) and sediment oxygen demand (SOD) in units of kg of O ₂ /hour. | 94 |
| Figure 32. Comparison of dissolved oxygen (DO) consumption from SSM bottom two layers at selected nodes by heterotrophic respiration (DDOC), nitrification (NITRIF), algal production minus algal respiration (DeltaDO_Algal) and sediment oxygen demand (SOD) in units of g O ₂ /m ² /day. | 95 |

Figure 33. Trendlines (smooth time series) of predicted percentages of dissolved oxygen (DO) removed by sediment oxygen demand (SOD) at selected nodes from entire water column (top) and from the two bottom layers (bottom) in 2014. ... 97

Figure 34. Time series of predicted dissolved oxygen (DO) consumed by biogeochemical processes at selected nodes in 2014. 98

Figure 35. Taylor plots for sensitivity runs for dissolved oxygen, nitrate-nitrite, ammonium, and chlorophyll-a. 103

Figure 36. Area of DO noncompliance and maximum magnitude of DO noncompliance under existing conditions (bottom bar) and under each refined Opt2 model scenario for the year 2014. 112

Figure 37. Total days of DO noncompliance under each refined Opt2 model scenario for the year 2014. 113

Figure 38. Cumulative days of DO noncompliance for 2014 existing (left), Opt2_5 (center), and Opt2_10 (right). 116

Figure 39. Cumulative days of DO noncompliance for all 10 refined Opt2 scenarios in Sinclair and Henderson Inlets. 117

Figure 40. Predicted 2014 time series at Henderson Inlet 303(d) assessment units under reference, existing, and Scenario Opt2_5 and Opt2_10. 120

Figure 41. Predicted 2014 time series at Sinclair Inlet 303(d) assessment unit under reference, existing, and Scenarios Opt2_5 and Opt2_10. 121

Figure 42 Predicted 2014 time series at Lynch Cove (Hood Canal) 303(d) grid assessment units under reference, existing, and Scenario Opt2_5 and Opt2_10. 122

Figure 43. Planview map showing improvement in bottom layer minimum dissolved oxygen (DO) concentrations in terms of magnitude (top panel) and percent (bottom panel) between 2014 existing conditions and Scenario Op2_5 (left panel) and Scenario Opt2_10 (right panel). 124

Figure 44. Planview map showing reduction in maximum sediment oxygen demand in terms of magnitude (top) and percentage (bottom) between 2014 Scenario Opt2_5 (left panel) and existing condition, and Scenario Opt2-10 (right panel) and existing condition, respectively. 125

List of Tables

| | Page |
|---|------|
| Table 1. Average annual daily flows and average annual daily total nitrogen (TN) and total organic carbon (TOC) marine point source and watershed loads entering WA waters of the Salish Sea for each of the four modeled years. | 34 |
| Table 2. Description of the refined watershed framework and associated annual anthropogenic (anthro.) loads used for all refined Opt2 scenarios. | 43 |
| Table 3. Refined Opt2 WWTP frameworks (each paired with a single watershed framework)..... | 46 |
| Table 4. Annual anthropogenic (anthro.) total nitrogen (TN) loads entering different basins for each refined Opt2 model scenario for the year 2014. | 49 |
| Table 5. Annual anthropogenic (anthro.) total organic carbon (TOC) loads entering different basins for each refined Opt2 model scenario for the year 2014..... | 50 |
| Table 6. Annual loads and percent load reductions in total nitrogen (TN) to WA waters of the Salish Sea associated with each refined Opt2 scenario for the year 2014..... | 51 |
| Table 7. Annual loads and percent load reductions in total organic carbon (TOC) to WA waters of the Salish Sea associated with each refined Opt2 scenario for the year 2014..... | 52 |
| Table 8. Comparison of 2014 model performance for Bounding Scenarios, Opt1, and Opt2..... | 79 |
| Table 9. Comparison of 2008 model performance for Bounding Scenarios and Opt2..... | 80 |
| Table 10. Comparison of 2006 model performance for Bounding Scenarios Report, Opt1, and Opt2..... | 81 |
| Table 11. Model performance statistics for Opt2 year 2000..... | 82 |
| Table 12. Values of several key parameters under the base calibration and alternative calibration for the year 2014. | 102 |
| Table 13. Statistics for 2014 base calibration and alternative parameterization runs..... | 102 |
| Table 14. Probability of correct matches between DO predictions and observations, and of errors when comparing with DO numeric criteria threshold. | 106 |
| Table 15. DO noncompliance under existing conditions for the years 2000, 2006, 2008, and 2014 for WA waters of the Salish Sea. | 108 |
| Table 16. DO noncompliance and anthropogenic total nitrogen (TN) loads under existing conditions and for each of the refined ten Opt2 model scenarios for the year 2014..... | 110 |
| Table 17. DO noncompliance associated with existing conditions and each of the refined ten Opt2 model scenarios for the year 2014 for each basin. | 111 |

Acknowledgments

The authors of this report thank the following people for their contributions to this study:

Scientists who reviewed the report in its entirety* or portions of it:

- Carl Cerco, U.S. Army Corps of Engineers (retired)*
- Ben Cope, U.S. Environmental Protection Agency*
- Tarang Khangaonkar, University of Washington Salish Sea Modeling Center and Pacific Northwest Laboratory (PNNL)*
- Evan Newell, Washington Department of Ecology (Ecology)*
- Jude Apple, Padilla Bay National Estuarine Research Reserve
- Chad Eshelman, Ecology
- Alex Fisher, Ecology
- Christopher Krembs, Ecology
- Kris Ryding, Ecology
- David Shull, Western Washington University (WWU)
- Sandra Weakland, Ecology

Entities/people who provided monitoring data or tools:

- Counties of Jefferson, King, Pierce, and Thurston produced data we used in this study.
- City of Bellingham
- Ecology's Environmental Information Management (EIM) database
- Squaxin Island Tribe
- USEPA Water Quality Exchange (WQX), which contains data produced by local Tribes
- USGS National Water Information System
- UW PRISM cruise data were collected and processed in collaboration with National Oceanic and Atmospheric Administration (NOAA).
- UW-HYAK staff who operate the high-performance computational cluster infrastructure used for model runs.
- WWU provided data at Shannon Point and collaborated with Ecology on sediment flux study

Washington State Department of Ecology staff:

- Jeremy Reiman, Ben Rau, and Melissa Gildersleeve, Water Quality Program (WQP)
- Dustin Bilhimer coordinated and developed the Puget Sound Nutrient Source Reduction Project (PSNSRP) from 2017 to 2023
- PSNSRP Steering Committee members
- WQP Permit Managers
- Lisa Euster, Ecology's Librarian, pursued all avenues to procure numerous references
- Steve Hood collaborated on drafting the initial set of Optimization Phase 2 scenarios
- Freshwater Monitoring Unit, Stephanie Estrella, provided data for this work
- Marine Monitoring Unit, Suzan Pool, provided data for this work
- Devon Nemire-Pepe and Christine Phillipsen edited, provided accessibility support, and published the report
- Diana Olegre, provided web support
- Michael Trunkhill provided graphic support
- Elisabeth Westgard provided graphic support
- Jamie Wasielewski, created SSM Opt2 WebMap
- Sheelagh McCarthy, Greg Pelletier, Mindy Roberts, and Brandon Sackmann, who contributed to earlier phases of this project (previously with Ecology)

Abstract

Multiple physical, chemical, and biological processes influence dissolved oxygen (DO) concentrations in the Salish Sea. DO levels in bottom waters of this region can be naturally low. Embayments and terminal inlets can experience reduced flushing and are vulnerable to lower DO in bottom waters due to anthropogenic nutrient loads. During periods of restricted flushing and little to no vertical mixing, sediment oxygen demand plays a proportionally dominant role in consuming bottom water DO.

The Salish Sea Model (SSM) was used to quantify the influence of reducing regional and local anthropogenic nitrogen and organic carbon loads from Washington watersheds and wastewater treatment plants (WWTP) to determine their effects on noncompliance with Washington's DO standards. Refinements to input load estimates, improved initial conditions, tidal and bottom friction effects, code updates, and limited parameterization modifications improved SSM DO skill performance metrics compared to previous efforts. Results regarding the influence of anthropogenic nutrient loads in lowering DO levels, particularly in bottom waters of vulnerable terminal inlets and embayments, mirror findings from previously published works.

DO noncompliance occurs in multiple locations, including portions of Hood Canal, Port Susan, Bellingham Bay, Case, Carr, Sinclair and Dyes Inlets, Quartermaster Harbor, and Penn Cove. Differences in daily DO minimum magnitudes between 2014 reference and existing conditions at noncompliant locations range from -0.3 to -1.3 mg/L, with a mean of -0.3 mg/L DO. Noncompliances in 2014 range from -0.1 to -1.1 mg/L, with a mean of -0.1 mg/L DO. The total estimated noncompliance area in 2014 is 467 km², excluding certain areas.

Watershed and WWTP load reduction scenarios result in zero noncompliances at nearly all locations (99.5% – 99.8%, relative to 2014 noncompliant areas). The maximum magnitude of remaining noncompliance is -0.1 DO mg/L (a 90.9% reduction).

Executive Summary

Background

The Salish Sea includes several interconnected marine waterways that cross into both Canada and the United States (U.S.), including Puget Sound, the Strait of Georgia, and the Strait of Juan de Fuca. Dissolved oxygen (DO) levels measured in bottom waters of Puget Sound are seasonally low, below levels needed for aquatic marine life to thrive in multiple locations. DO levels within Puget Sound can be naturally low. Embayments and terminal inlets experience reduced flushing, and so are more vulnerable to lower DO in bottom waters due to human nutrient loads. The 1972 Federal Clean Water Act requires states to establish water quality standards (Section 303(c)), identify impaired waters, and develop plans to clean up waters (Section 303(d)). Multiple embayments and terminal inlets are noncompliant with the DO standard. Ecology (2025) contains a map of all DO 303(d) listings in the Washington waters of the Salish Sea.

The Washington State Department of Ecology (Ecology) is conducting the Puget Sound Nutrient Source Reduction Project (PSNSRP) to address water quality concerns in Puget Sound. This collaborative process aims to reduce local and regional anthropogenic nutrients from point and nonpoint sources to meet DO water quality standards.²

Multiple physical, chemical, and biological factors affect DO levels in Puget Sound. These include topography, water depth, water circulation, meteorological conditions, transfer of gases and nutrients to and from the sediment bed, and the flow of water from the Pacific Ocean. Additionally, regional and local nutrient inputs from watersheds and marine point sources play a role. This complexity necessitates using a three-dimensional (3D) hydrodynamic and biogeochemical mechanistic model to adequately simulate DO and to isolate the impact of anthropogenic nutrients from local and regional sources on DO in Washington waters of the Salish Sea. Model simulated noncompliance with Washington State's DO standards occurs in multiple terminal inlets and embayments such as portions of Hood Canal, Port Susan, Bellingham Bay, Case, Carr, Sinclair and Dyes Inlets, Quartermaster Harbor, and Penn Cove.

Model updates and performance

The Salish Sea Model (SSM) is composed of a 3D hydrodynamic model (called Finite Volume Community Ocean Model or FVCOM) coupled with water quality kinetics (rooted in CE-QUAL-ICM), together referred to as FVCOM-ICM. Khangaonkar et al. (2018) provide an overview of the modeling system. The model includes flow and nutrient inputs from watersheds and marine point source outfalls that discharge directly to the Salish Sea. The model includes 16,012 grid cells that vary in diameter from 130 to 250 meters in the inlets and bays to 800 meters in the main basin of Puget Sound, up to 3000 meters in the Strait of Juan de Fuca, and up to 15 Km at

² Webpage for PSNSRP and collaborative process via the Puget Sound Nutrient Forum:
<https://www.ezview.wa.gov/DesktopDefault.aspx?alias=1962&pageid=37106>

the open boundary near the continental shelf. For noncompliance calculations, we use 303(d) grids (assessment units), which are about 1130 m long and 790 m wide. This phase of the work involved multiple updates and refinements to previous Ecology efforts related to applying the SSM in support of the PSNSRP (McCarthy et al. 2018; Ahmed et al. 2019, 2021).

Model updates included the following:

- The use of an updated FVCOM-ICM code and review of key parameters.
- Running the model 10 consecutive times (for the same year) in series to allow for the stabilization of key biogeochemical processes as part of the initialization process.
- Updates and refinements to watershed inputs to improve water quality input load estimates and the spatial distribution of these freshwater inflows.
- Updates to tidal constituents at the open boundary.
- Filling data gaps and improving inputs for some marine point sources.

As a result of these updates, model performance improved. We evaluated performance for water surface elevations, tidal currents, and key water quality parameters and processes for 2000, 2006, 2008, and 2014. SSM predictions are consistent with field observations, and the model reproduces seasonally low DO, particularly in inlets and bays. The model performs better in middle and bottom waters than surface waters, and model skill in embayments is similar to that in open channel locations.

The model demonstrates the level of performance needed to determine the impact of hypothetical reductions in human loads from watersheds and wastewater treatment plants.

Nutrient reductions and DO noncompliance

This work builds on earlier efforts and delves deeper into understanding how temporal and spatial anthropogenic nutrient reductions from local and regional sources can help us meet DO water quality standards. We refer to the present work as Optimization Phase 2 (Opt2). In this report, the evaluation of DO noncompliance is accomplished at the scale of the assessment units, rather than at each SSM model grid.

Model scenarios involved different nutrient reduction frameworks for watersheds and point sources discharging into marine waters. Point sources include wastewater treatment plants (WWTP) and industrial facilities. All model scenarios were run for the year 2014. Ecology selected 2014 as the key model year for Opt2 PSNSRP load variation scenarios because it includes the Brightwater facility (a newer WWTP that came online in September 2011 and discharges to Main Basin). Additionally, previous analyses had shown that 2014 was an average year in terms of water residence time for the Central Basin (PSEMP 2016). However, in this phase of the work, we found that 2014 had the fastest winter flushing time at the Puget Sound scale among the four years that we evaluated.

All load reduction scenarios were based on 2014 flows, and nutrient concentrations were reduced to reflect specific reduction frameworks. For watersheds, all species of nitrogen (ammonium, nitrate-nitrite, and organic nitrogen) and organic carbon (particulate and dissolved

organic carbon) were reduced. For WWTPs, dissolved inorganic nitrogen (DIN) was reduced and reported as total nitrogen reductions. Total organic carbon reductions were also made for WWTPs. Industrial facility loads were held at existing 2014 levels.

An initial set of Opt2 scenarios was tested, combining different “watershed frameworks” and “WWTP frameworks” to identify the optimal pairing based on the level of reductions associated with each framework and their relative effectiveness in reducing DO noncompliance. Results from initial scenarios informed the development of 10 refined Opt2 model scenarios, which were also run for 2014.

The 10 refined Opt2 scenarios involved pairing 10 different WWTP reduction frameworks with a single watershed reduction framework. This single watershed framework involved the following anthropogenic nutrient reductions:

- Holding loads for those watersheds entering the U.S. portions of the Strait of Juan de Fuca (SJF-US) and Strait of Georgia (SOG-US) to existing 2014 loads.
- 90% reductions in small watersheds discharging closest to Sinclair Inlet, Liberty Bay, Lynch Cove, and Henderson Inlet (all areas that showed persistent DO noncompliance under prior scenarios).
- 67.7% reductions in remaining large watersheds (size determined based on existing 2014 loads) entering Northern Bays, Whidbey Basin, Main Basin, and South Sound.
- 61.2% reductions in remaining small or medium watersheds entering Northern Bays, Whidbey Basin, Main Basin, and South Sound.
- 53.5% reductions in remaining watersheds entering Hood Canal and Admiralty Inlet.

WWTP frameworks involved applying different biological nitrogen removal (BNR) treatment levels during different seasons across varying groups of WWTPs. BNR treatment was specified in the SSM model input files in terms of the concentration limits of dissolved inorganic nitrogen (DIN) and carbonaceous biological oxygen demand (CBOD₅) in WWTP effluent. These BNR levels were applied by setting WWTP effluent DIN concentrations to 3 mg/L, 5 mg/L, and 8 mg/L relative to existing 2014 DIN concentrations. All levels of BNR treatment were associated with setting an effluent limit of 8 mg/L CBOD₅. These levels were based on a study that consisted of a technical and economic evaluation of nutrient removal at WWTPs that involved BNR levels of 3 to 8 mg/L of DIN (Tetra Tech 2011). Within this report, these three BNR levels are often expressed in shorthand as BNR3, BNR5, and BNR8 to represent effluent DIN concentrations of 3 mg/L, 5 mg/L, and 8 mg/L, respectively.

Table ES-1 presents the questions addressed by each of the 10 refined Opt2 scenarios and associated WWTP BNR levels. Figure ES-1 compares the anthropogenic TN loads entering different basins under each scenario from watersheds and marine point sources. This figure shows that marine point source loads vary only slightly among scenarios due to small variations in the BNR treatment applied to WWTP facilities in each scenario.

Figure ES-2 compares plan view maps of DO noncompliance between 2014 existing conditions and the refined scenario with the least reductions (Opt2_5) and the scenario with the most reductions (Opt2_10). Figure ES-3 illustrates areas where remaining predicted noncompliance,

calculated from model output, persists in localized areas within Sinclair and Henderson Inlets across most of the 10 scenarios. This illustrates that zero noncompliance at nearly all locations (99.5% – 99.8%, relative to 2014 noncompliant areas, see Table ES-2) can be achieved with nitrogen and organic carbon load reductions from watersheds and WWTPs discharging into marine waters.

Table ES-1. Refined Opt2 WWTP frameworks (each paired with a single watershed framework).

| Scenario ID | Question that it addresses | WWTPs at existing 2014 loads | BNR levels ^a at WWTPs |
|-------------|--|---|--|
| Opt2_1 | What is the effect of BNR 8/5/3 at all WWTPs on noncompliance? | None | All WWTPs at 8/5/3 |
| Opt2_2 | How does setting very small WWTPs at existing 2014 loads affect noncompliance? | Very small WWTPs ^b | All other WWTPs at 8/5/3 |
| Opt2_3 | How does increasing BNR treatment for those WWTPs discharging within or near Sinclair Inlet affect noncompliance? | None | Three WWTPs within or near Sinclair Inlet set at BNR 3/3/3. All other WWTPs at 8/5/3 |
| Opt2_4 | How does setting WWTPs discharging into the Straits of Juan de Fuca and Georgia, Admiralty Inlet, and Hood Canal, at existing 2014 loads, affect noncompliance? | WWTPs in Straits of Juan de Fuca and Georgia, Admiralty Inlet, and Hood Canal | All other WWTPs at BNR 8/5/3 |
| Opt2_5 | What is the combined effect on noncompliance of 1) setting very small WWTPs and 2) setting WWTPs discharging into the Straits of Juan de Fuca and Georgia, Admiralty Inlet, and Hood Canal at existing 2014 loads? | Very small WWTPs ^b and WWTPs in Straits of Juan de Fuca and Georgia, Admiralty Inlet and Hood Canal | All other WWTPs at BNR 8/5/3 |
| Opt2_6 | What is the combined effect on noncompliance of 1) setting WWTPs discharging into Straits of Juan de Fuca and Georgia, Admiralty Inlet, and Hood Canal at existing 2014 loads and 2) increasing BNR treatment for those WWTPs discharging within or near Sinclair Inlet? | WWTPs in Straits of Juan de Fuca and Georgia, Admiralty Inlet, and Hood Canal | Three WWTPs within or near Sinclair Inlet set at BNR 3/3/3. All other WWTPs at BNR 8/5/3 |
| Opt2_7 | What is the combined effect of 1) setting very small WWTPs at existing 2014 loads, 2) setting WWTPs discharging into Straits of Juan de Fuca and Georgia, Admiralty Inlet, and Hood Canal at existing 2014 loads, and 3) increasing BNR treatment for those WWTPs discharging within or near Sinclair Inlet? | Very small WWTPs ^b and WWTPs in the Straits of Juan de Fuca and Georgia, Admiralty Inlet, and Hood Canal | Three WWTPs within or near Sinclair Inlet set at BNR 3/3/3. All other WWTPs at BNR 8/5/3 |
| Opt2_8 | Can zero DO noncompliance be achieved everywhere with the largest (dominant) WWTPs in Main Basin at BNR 8/3/3 and those in the vicinity of Sinclair Inlet at BNR 3/3/3, but West Point (a dominant facility treating combined sewers) at 8/5/3? | Very small WWTPs ^b and WWTPs in the Straits of Juan de Fuca and Georgia, Admiralty Inlet, and Hood Canal | Three WWTPs within or near Sinclair Inlet set at BNR 3/3/3. All dominant Main Basin WWTPs ^c at BNR 8/3/3 (except West Point set at 8/5/3). All other WWTPs at 8/5/3. |

| Scenario ID | Question that it addresses | WWTPs at existing 2014 loads | BNR levels^a at WWTPs |
|--------------------|---|---|---|
| Opt2_9 | Can DO zero noncompliance be achieved everywhere with the largest (dominant) WWTPs in Main Basin at BNR 8/3/3 and those in the vicinity of Sinclair Inlet at BNR 3/3/3? | Very small WWTPs ^b and WWTPs in the Straits of Juan de Fuca and Georgia, Admiralty Inlet, and Hood Canal | Three WWTPs within or near Sinclair Inlet set at BNR 3/3/3. All dominant Main Basin WWTPs ^c at BNR 8/3/3. All other WWTPs at 8/5/3 |
| Op2_10 | Can DO zero noncompliance be achieved everywhere with the largest (dominant) WWTPs in Main Basin and those near the most difficult noncompliance location at BNR 3/3/3? | Very small WWTPs ^b and WWTPs in the Straits of Juan de Fuca and Georgia, Admiralty Inlet, and Hood Canal | Three WWTPs within or near Sinclair Inlet set at BNR 3/3/3. All dominant Main Basin WWTPs ^c at BNR 3/3/3. All other WWTPs at 8/5/3 |

^a Biological nitrogen removal (BNR) levels are specified in terms of cool (Nov – Mar)/warm (Apr – Jun, Oct)/hot (Jul – Sep) months.

^b Very small wastewater treatment plants (WWTPs) are those discharging less than 10 kg TN/day or less than 6 kg DIN/day on a maximum monthly basis for model year 2014.

^c Dominant Main Basin WWTPs include Brightwater, South King, Tacoma Central and West Point.

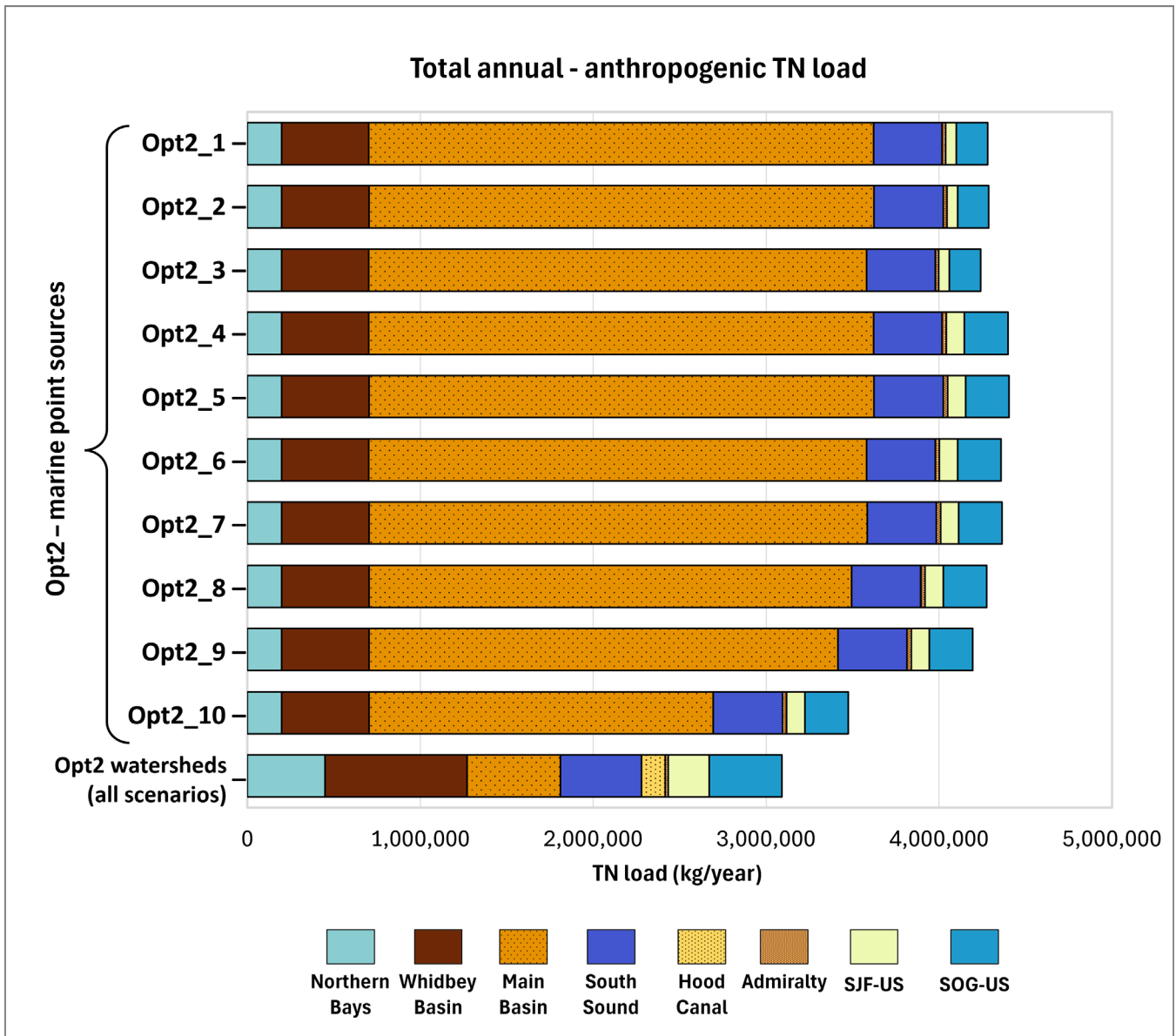


Figure ES-1. Annual anthropogenic total nitrogen (TN) watershed and marine point source loads entering different basins for each refined Opt2 scenario.

Watershed loads are the same across all scenarios and therefore represented by a single bar.

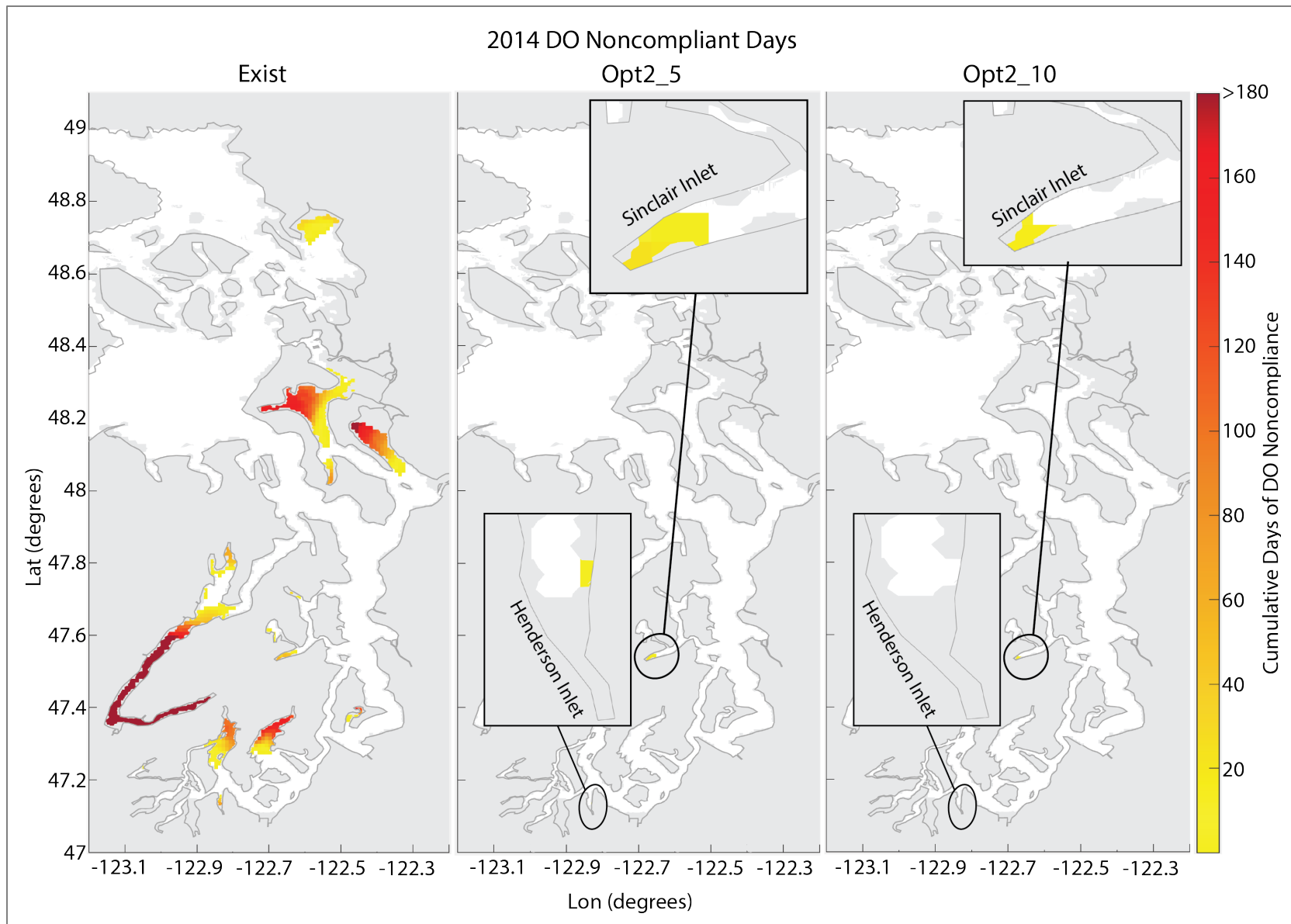


Figure ES-2. Cumulative days of DO noncompliance for 2014 existing (left), Opt2_5 (center), and Opt2_10 (right).

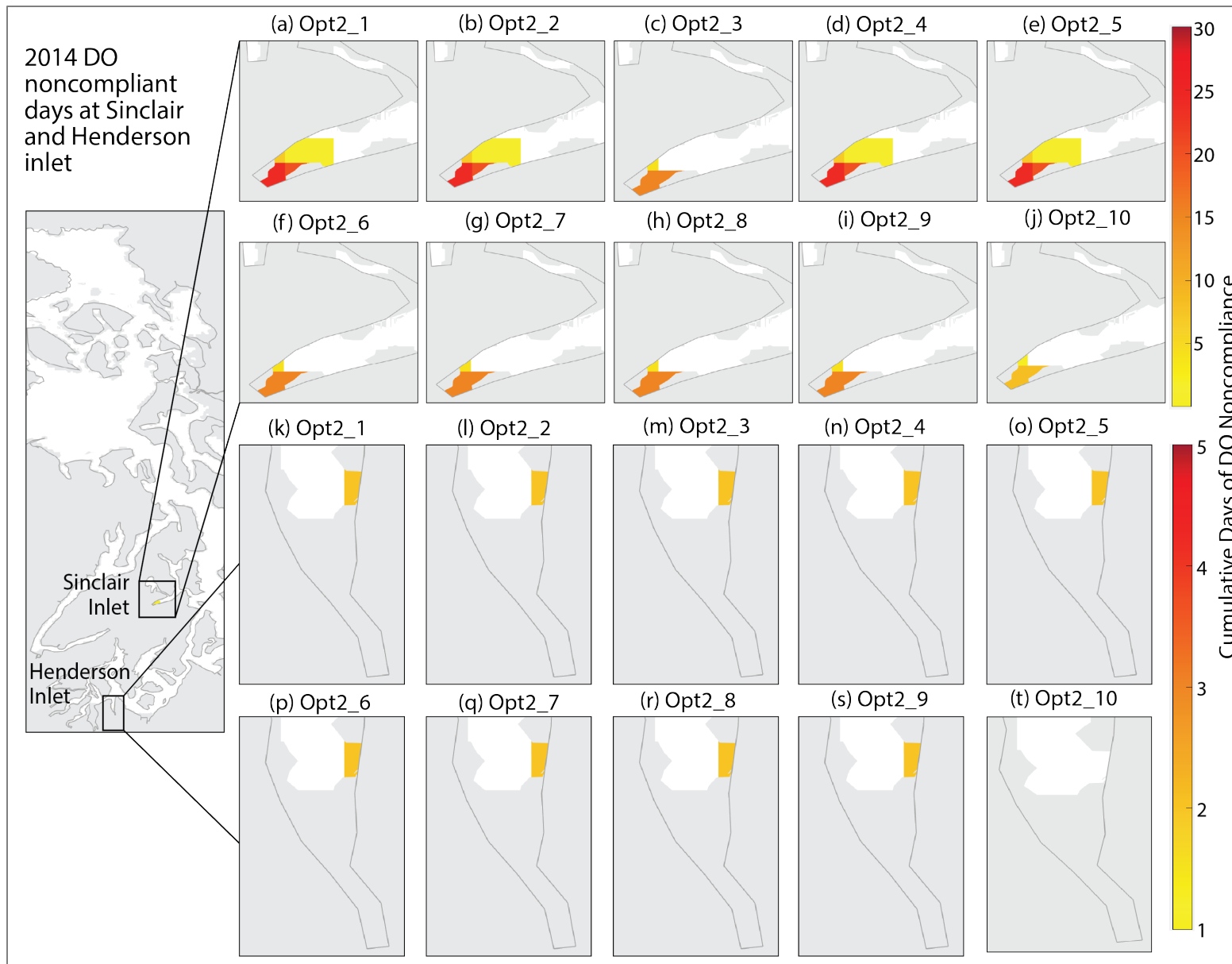


Figure ES-3. Cumulative days of DO noncompliance for all 10 refined Opt2 scenarios in Sinclair and Henderson Inlets.

Table ES-2. Dissolved Oxygen (DO) noncompliance^a and anthropogenic total nitrogen (TN) loads under existing conditions and for each of the refined ten Opt2 model scenarios for 2014.

| Opt2 scenario | Anthropogenic TN load (thousands of kg/year) | Percent reduction in anthropogenic TN load relative to existing | Total days of noncompliance | Total area of noncompliance (km²) | Maximum magnitude of DO noncompliance (mg/L) | Percent of area with zero noncompliance (relative to 2014 existing noncompliant area) |
|----------------------|---|--|------------------------------------|---|---|--|
| Existing | 21,300 | 0% | 80,279 | 467 | -1.1 | 0.00% |
| Opt2_1 | 7,370 | 65.4% | 57 | 2.50 | -0.1 | 99.5% |
| Opt2_2 | 7,380 | 65.4% | 58 | 2.50 | -0.1 | 99.5% |
| Opt2_3 | 7,330 | 65.6% | 36 | 0.93 | -0.1 | 99.8% |
| Opt2_4 | 7,490 | 64.8% | 58 | 2.50 | -0.1 | 99.5% |
| Opt2_5 | 7,500 | 64.8% | 58 | 2.50 | -0.1 | 99.5% |
| Opt2_6 | 7,450 | 65.0% | 36 | 0.93 | -0.1 | 99.8% |
| Opt2_7 | 7,460 | 65.0% | 36 | 0.93 | -0.1 | 99.8% |
| Opt2_8 | 7,370 | 65.4% | 36 | 0.93 | -0.1 | 99.8% |
| Opt2_9 | 7,290 | 65.8% | 35 | 0.93 | -0.1 | 99.8% |
| Opt2_10 | 6,570 | 69.2% | 18 | 0.83 | -0.1 | 99.8% |

^a Noncompliance excludes masked areas (e.g., Budd Inlet).

Introduction

The Washington State Department of Ecology (Ecology) is conducting the Puget Sound Nutrient Source Reduction Project (PSNSRP) to address water quality concerns in Puget Sound. This collaborative process aims to reduce local and regional anthropogenic nutrients from point and nonpoint sources to meet dissolved oxygen (DO) water quality standards. For the remainder of this report, the term “anthropogenic” will refer to local and regional human loads or human influence.

Several factors affect oxygen levels in Puget Sound. These include the depth and shape of the seafloor (bathymetry), water circulation, meteorological conditions, transfer of gases and nutrients to and from the sediment bed, and the flow of water from the Pacific Ocean. Additionally, regional and local nutrient inputs from watersheds and marine point sources play a role. Some of these factors are natural, for example, coastal upwelling near the Strait of Juan de Fuca can bring low DO and nutrient-rich waters onto the continental shelf, influencing Puget Sound oxygen levels (Landry and Hickey 1989). Other factors are anthropogenic, such as excess nutrient loading from human sources, which can further stimulate algal growth in Puget Sound waters (Bernhard and Peele 1997; Newton et al. 1998; Aura Nova et al. 1998; Newton and Van Voorhis 2002). When these algae die, the resulting organic matter decomposes, consuming DO, prompting shifts in the ecosystem’s ability to support aquatic life—a process termed eutrophication (Howarth et al. 2011; Diaz and Rosenberg 2008; Glibert et al. 2005).

Embayments and shallow inlets in Puget Sound are vulnerable to seasonally lower dissolved oxygen levels (Ahmed et al. 2019; Khangaonkar et al. 2018; Roberts et al. 2014b) and eutrophication (Thom et al. 1988; Mackas and Harrison 1997; Newton and Reynolds 2002), due to reduced flushing (Ahmed et al. 2017; Khangaonkar et al. 2012; Sutherland et al. 2011). Shallow finger inlets in Puget Sound are often stratified (Moore et al. 2008), which means that they can experience reduced vertical mixing.

Multiple studies of Puget Sound embayments and terminal inlets have reported poor flushing, stratification, and/or limited circulation. Among them are studies in Sinclair Inlet (Lincoln and Collias 1975; Albertson et al. 1995; Newton et al. 2002), Saratoga Passage (Lincoln and Collias 1970; Newton et al. 2002), Lynch Cove, Dabob Bay, Port Susan (Barnes and Collias 1958), as well as Hood Canal, Budd Inlet, Commencement Bay, and Penn Cove (Newton et al. 2002).

The complexity of the bathymetry, geometry, and variability in regional and local scale drivers necessitates the use of a three-dimensional hydrodynamic and biogeochemical mechanistic model to adequately simulate DO in Puget Sound waters. A mechanistic model also allows us to specifically isolate the impact of anthropogenic nutrients from local and regional sources on DO from all these other factors.

The Salish Sea Model (SSM) simulates the complex physical, chemical, and biological patterns in the Salish Sea (Khangaonkar et al. 2018; Khangaonkar et al. 2021a, 2021b; Khangaonkar and Yun 2023). The SSM model domain includes all of Puget Sound, plus the Strait of Georgia (SOG) and the Strait of Juan de Fuca (SJF). The model uses an unstructured computational grid to define the complex shoreline and bathymetry of Puget Sound (Figure 1).

The SSM consists of a hydrodynamic model coupled with a water quality model. The hydrodynamic model, Finite Volume Community Ocean Model (FVCOM, Chen et al. 2006), was originally developed at the University of Massachusetts in collaboration with the Woods Hole Oceanographic Institute. The water quality model, FVCOM-ICM (Kim and Khangaonkar 2012; Khangaonkar et al. 2012, 2018, 2019, and 2021b), is an adaptation of a biogeochemical model, CE-QUAL-ICM (Cerco and Cole 1993, 1994).

This work uses the SSM to quantify DO improvements resulting from different regional anthropogenic nutrient reduction scenarios. The model includes flow and nutrient inputs from watersheds and marine point source outfalls (WWTPs and industrial facilities) that discharge directly to the Salish Sea.

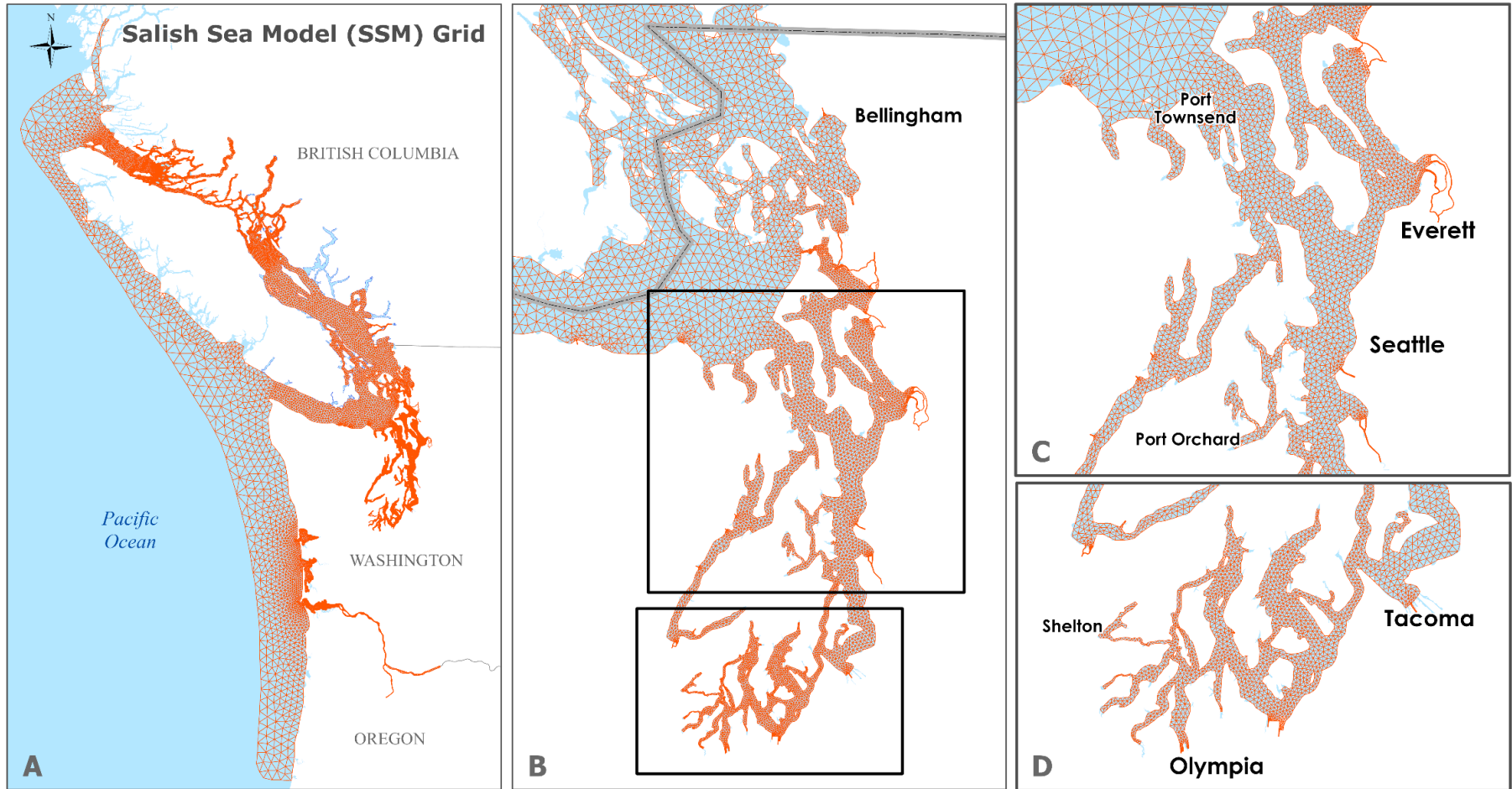


Figure 1. The Salish Sea Model domain and intermediate scale model grid (A) in Greater Puget Sound (B), northern Puget Sound (C), and South Sound (D).

Ahmed et al. (2019, 2021) contain results from two earlier modeling efforts (the Bounding Scenarios Report and the Optimization Phase 1 or Opt1 memo³) as reflected in Figure 2. This work, Optimization Scenarios Phase 2 (Opt2), constitutes the most recent SSM-related effort for the Puget Sound Nutrient Reduction Plan (Nutrient Reduction Plan), Ecology’s initial water clean-up plan for Puget Sound (Ecology 2025). The Nutrient Reduction Plan is an essential component of Ecology’s broader PSNSRP.

The focus here is on reporting Phase 2 Optimization Scenarios (also previously referred to as Optimization Year 2) developed by Ecology in collaboration with stakeholders. Aside from presenting the latest model scenario results, this report and its appendices also contain details about recently updated model input files, reference condition scenario, updates to a newer model version at the same intermediate scale/spatial resolution as before, as well as a comprehensive model evaluation and other related and relevant results.

Scientific peer review has occurred from the initial phases of model conceptualization through development and application. In 2008, a technical advisory committee composed of scientists from local, state, and federal agencies and universities shaped the attributes and model selection for this effort. In 2010, EPA commissioned an independent third-party review of the intermediate scale model (Tetrattech 2010). Multiple articles in the scientific literature, reports, and quality assurance project plans were peer reviewed and published, listed in McCarthy et al. (2018). Following that, Ahmed et al. (2019) was also peer reviewed and published.

For Optimization Phase 2 (Opt2), Carl Cerco has been our overall scientific reviewer since 2022. Carl Cerco is the developer of CE-QUAL-ICM, a mechanistic model that has been notably and successfully used in Chesapeake Bay and other estuaries to understand the impact of nutrient reductions on water quality improvements. He is the author of biogeochemical modeling papers published broadly in scientific literature of interest nationally and internationally. Additionally, as we show in the acknowledgement section of this report, several regionally focused scientists reviewed specific sections of this work pertinent to each of their specialty areas.

³ Or also previously referred to as Optimization Year 1. This change in terminology from “Year 1” and “Year 2” to “Phase 1” and “Phase 2” was made because the original terminology did not capture phases of this work that spanned longer than one year.

| Salish Sea Modeling Work Supporting the Puget Sound Nutrient Source Reduction Project | | |
|--|---|---|
| (1) Bounding Scenarios | (2) Optimization Scenarios | |
| Volume 1: Model Updates and Bounding Scenarios Report (Ahmed et al., 2019) | Optimization Scenarios (Opt1), Technical Memorandum (2021) | Optimization Scenarios (Opt2), Volume 2 Report (this report) |
| Model Scenarios (2006, 2008, 2014): <ol style="list-style-type: none"> 1. Impact of all anthropogenic sources 2. Impact of marine point sources 3. Improvement with BNR at all municipal WWTPs 4. Improvement with BNR at large WWTPs 5. Improvement with BNR at mid-size WWTPs | Phase 1 Scenarios (2006, 2014): <ol style="list-style-type: none"> 1. Watershed reductions by region 2. WWTP reductions by region 3. Annual vs. seasonal WWTP reductions 4. Future growth scenarios 5. Watershed and WWTP reductions | Phase 2 Scenarios (2014): <ol style="list-style-type: none"> 1. Initial set: Exploration of watershed and WWTP reduction frameworks by basin. 2. Refined set: Optimization of WWTP reduction frameworks by basin. |

Figure 2. Components of the Salish Sea Modeling effort to support the Puget Sound Nutrient Source Reduction Project.

Each stage of the project involved model runs and nutrient loading scenarios run for different years (as specified in parentheses in the bottom row).

Project Description

SSM work supporting the PSNSRP is composed of several phases built upon model development work that began in 2008. Between 2008 and 2019, Pacific Northwest National Laboratory developed the model in collaboration with Ecology (with funding from the EPA). Since then, in support of the PSNSRP, Ecology has made refinements, checked calibration, evaluated performance, and run all PSNSRP scenarios.

We produced a Quality Assurance Project Plan (QAPP) for the applications portion of the modeling effort (McCarthy et al. 2018). This QAPP puts the previous QAPPs and development work in context. We then conducted extensive testing and evaluation with independent observational data not used in the calibration process. We also acquired continuous nitrate-nitrite data at the mouths of major rivers discharging to Puget Sound, collaborated on a project to obtain water column respiration measurements, and encouraged the acquisition of additional sediment flux data. We used all these independent data sets to evaluate the model.

The first volume of PSNSRP modeling work was published in the Bounding Scenarios Report (BSR), which evaluated the impact of Washington State anthropogenic nutrient sources from watersheds and marine point sources (Ahmed et al. 2019). The results of this first modeling report indicated that human sources of nutrients (nitrogen and organic carbon) are cumulatively influencing predicted DO noncompliances in multiple embayments and inlets. The BSR described intra-basin transport that can influence predicted noncompliances. It also showed the possibility of improvements in DO levels from the hypothetical implementation of advanced biological nitrogen removal (BNR) at United States (U.S.) wastewater treatment plants (WWTPs) that discharge to the Salish Sea.

The second volume of PSNSRP modeling work consisted of Optimization Phase 1 (Opt1) scenarios, Ahmed et al. (2021). Opt1 scenarios were used to further evaluate the relative influences of load reductions from watershed and marine point source loads on DO noncompliance. The BSR and the Opt1 conclusions reflected that a combination of nutrient reductions from both marine WWTPs and watersheds is needed to meet water quality standards.

The present work is the third volume of modeling work supporting the PSNSRP and is published as the Model Updates and Optimization Phase 2 Scenarios (Opt2). This work builds on earlier efforts and delves deeper into understanding how temporal and spatial nutrient reductions can help us meet DO water quality standards. Opt2 work also includes enhancements that resulted in measurable model improvements, further characterization of the performance of the intermediate scale SSM model, and support for earlier findings about how human nutrient inputs make low DO conditions worse in the bottom waters of poorly flushed terminal inlets and embayments. We accomplished model improvements and a comprehensive comparative analysis of biogeochemical predictions with recently obtained observational data sets. This report contains detailed analyses in the appendices and summaries of the results.

Opt2 scenario results are grouped into eight basins (Northern Bays, Whidbey Basin, Main Basin, South Sound, Hood Canal, Admiralty Inlet, U.S. portion of the Strait of Juan de Fuca, and the

U.S. portion of the Strait of Georgia) which are further described, along with their input loads, in the Methods section. Results are also aggregated to “WA waters of the Salish Sea,” which is equivalent to the total combined area of all eight basins.

Opt2 encompassed many model scenarios that were needed to support the Nutrient Reduction Plan (Ecology 2025), which will guide further actions. These scenarios involved reductions in anthropogenic watershed nutrient loads, paired with reductions in WWTPs to reflect different levels of BNR, paired with actual flows from 2014. Different scenarios involved variations in BNR levels for different facilities and seasons. The Methods contain a full description of characterization and assumptions made when setting up each scenario and the associated loads.

The key questions regarding the scenarios centered around the influence of the magnitude of WWTP load discharges, how the location of these discharges impacts DO concentrations within the modeling domain, and the sensitivity of the system when altering cool-month nitrogen concentrations for the nine WWTPs that treat flows from combined sewer systems. Sinclair Inlet became a geographic area of interest for SSM scenario refinements because predicted DO depletions at the head of the inlet were consistently greater than the 0.2 mg/L human use allowance (defined in the glossary), and three WWTPs discharge in its vicinity.

This report contains the refined set of Opt2 scenarios and the questions they were designed to address. All refined Opt2 scenarios include significant reductions in watershed loads (53% – 90% reduction in total nitrogen and organic carbon anthropogenic loads, depending on the basin) compared to the existing scenario. These watershed reductions are the same for each of the refined Opt2 scenarios. However, they are paired with a different WWTP framework, which involves different combinations of seasonal BNR treatment applied to U.S. WWTPs, while holding industrial facility loads at existing 2014 levels.

The Results detail DO noncompliances calculated for Opt2 refined scenarios. SSM output includes a year-long hourly time series of DO predictions at all model grid-cell-layers. The largest predicted noncompliance magnitude for each 303(d) assessment unit (defined in the glossary) is used to create plan view maps, tables, and plots. The term “noncompliance” used in this report refers to computed DO deficits greater in magnitude than the human use allowance (0.2 mg/L) or out of compliance with the biologically based numeric criteria, whichever is applicable.

Here, we highlight the important definitional distinction between the *natural* and the *reference* condition scenarios. The latter only excludes local and regional human influence within WA borders, and the former excludes all human influence, including that beyond WA borders. This report contains approaches that may apply to reference and natural conditions to document them. However, as in BSR and Opt1, this report is restricted to noncompliance computations with the local and regional reference condition (relevant to the human use allowance).

Appendix C in Ecology (2025) describes the provisions adopted in 2024 (but that have not yet gone through EPA review) pertinent to natural conditions for marine DO. A performance-based approach in the recently adopted provisions focuses on the *natural* condition, in which any human influence is removed.

Methods

The Quality Assurance Project Plan (McCarthy et al. 2018) provides an overview of the modeling system and its history related to PSNSRP. It also contains information on methodologies used for model boundaries and inflows, set-up, data needs, modeling assumptions in the applications phase, data quality and analysis, and assessment methods, while allowing for future improvements.

Large-scale climatological, meteorological, and hydrological drivers produce substantial variabilities in Puget Sound water quality, so while seasonal patterns are evident, each year brings its own key features. We ran the model in a hindcast mode for four different years (2000, 2006, 2008, and 2014) to examine interannual variability. However, we ran the PSNSRP loading reduction scenarios only for 2014 in Opt2 (see subsection “Opt2-Scenarios”).

We ran the hydrodynamic model decoupled from the water quality runs and obtained hourly simulations. The modeling and processing framework, including vertical and horizontal structure of the model and grids, boundary conditions, and meteorological inputs, has been described previously (Ahmed et al. 2019 and 2021). We accomplished multiple updates and enhancements described below and in the appendices, which resulted in further model prediction improvements.

The rest of this section focuses on updates made to the modeling framework since the publication of Ahmed et. al. 2021. This section also details the methodology used to develop Opt2 scenarios.

Model initialization and parameterization

A key change to model initialization that we instituted, after conversations with our reviewer Carl Cerco, is to run each model year ten consecutive times to create the input to the run used for analysis, so the eleventh model run consists of the last run, which is the one used. This allows for the sediment fluxes derived from the labile particulate organic carbon fraction to stabilize. Appendix A contains details about this update.

With support from the UW Salish Sea Modeling Center (SSMC), we investigated the use of updated code for the hydrodynamic (FVCOM2.7d) as well as the biogeochemical portions of the model (from ICM2 to ICM4). While we are not changing the model spatial resolution, we are using updated intermediate-scale model code for Opt2 scenarios. Details about the updated model code, parameterizations, model skill, and additional sensitivity analyses performed are found in Appendix A.

Most of the parameter set used in Ahmed et al. 2019 and Khangaonkar et al. (2018) remains unchanged. The change in model initialization mentioned above and using an updated version of the FVCOM-ICM code prompted a review of key parameters such as settling velocities. These updates are also documented in Appendix A.

Watershed updates

During the earlier phases of the work, we recognized that further improvements, particularly in the watershed load inventory, were feasible and potentially useful to optimize model performance. Ahmed et al. 2019 suggested review and improvements to watershed loadings. Ahmed et al. 2021 described improvements primarily to organic carbon and temperature watershed regressions and Canadian river inflows. In the current work, we further refined watershed inputs to SSM. This refinement set us up to conduct the Opt2 scenarios with enhancements to both the water quality input loads and the spatial distribution of freshwater inputs.

Watershed improvements include an increase of about 20% in the number of freshwater input points into the model, from 161 to 193 inflow points. We disaggregated inflows that combined large watersheds into inflows for smaller watersheds. For example, one of the basins where the change is notable is the Northern Bays, which previously was modeled via freshwater inflows at three locations from the Nooksack, Samish/Bell South, and Whatcom/Bell North watersheds. In the updated watershed input files, these three inflows are now subdivided into ten smaller drainage basins so that smaller streams, such as Silver Creek and Squalicum Creek, discharge into separate model nodes.

We located and compiled additional flow and concentration data, often from local entities with quality-assured measurement programs. We used that data to develop separate regressions for the newly disaggregated inflows and to supplement data for other freshwater time series. In certain cases, we are using synthetic gage data. Furthermore, we updated previously used regressions to improve their performance. Details about all these updates are found in Appendix B1. Appendix B1 also contains information about how we evaluated the skill of the watershed regressions.

Loads from the watersheds changed because of the improvements described above. Appendix B2 contains an analysis of the changes to the watershed loadings due to the updates. Appendix B3 contains time series plots of flow and water quality for all watersheds entering the SSM domain.

On a parallel track, Ecology's Freshwater Monitoring Unit (FMU) recently commenced continuous nitrate-nitrite monitoring at stations located near major river mouths discharging into marine waters of the WA Salish Sea. We compared these data sets, which are completely independent, continuous data, though not contemporaneous, to our estimates developed from watershed regressions used as SSM inputs. Appendix B4 contains details from that comparison.

Open boundary

Water quality at the open boundary with the Pacific Ocean was established using data from the Canadian Department of Fisheries and Oceans (DFO) and outputs from the Hybrid Coordinate Ocean Model (HYCOM). Open boundary conditions were set up using similar procedures to those in our Opt1 report (Ahmed et al. 2021).

As in the Opt1 work (Ahmed et al. 2021), we reduced the temporal resolution of HYCOM outputs from 3-hour to daily intervals, as temperature and salinity variations were gradual, showing noticeable changes over longer periods but minimal fluctuations within a given day. We did not use HYCOM for model year 2008 due to several days of instability near the Washington coast that produced incorrect HYCOM output. As a result, for 2008, we used the same open boundary conditions as in the BSR, which consisted of interpolated DFO data. Except for 2008, we used HYCOM outputs for temperature and salinity, and applied piecewise regressions based on salinity to predict DO, dissolved inorganic carbon (DIC), alkalinity, and nitrate (Ahmed et al. 2021). In our Opt1 report, we found that these predictions were reasonable in their representation of water quality profiles when compared against several years of DFO data. A more detailed overview of our open boundary conditions can be found in Appendix B5.

Marine point source updates

We found opportunities to refine some marine point source inputs. We identified and filled data gaps to improve input time series for WWTPs and industrial point sources, the two types of permitted discharges that represent marine point sources in SSM.

We filled outstanding data gaps. For example, we previously did not have estimates of organic nitrogen discharged from refineries, but have now located pertinent data. In addition, we consulted with permit managers regarding further review of point source time series.

As described in the BSR, data for marine point sources under Washington State jurisdiction were obtained primarily from data reported to Ecology's Water Quality Permitting and Reporting Information System (PARIS). Data for federally regulated facilities were obtained from EPA Region X. We examined all regressions derived from discharge monitoring reports. We consulted with permit managers when we found data outliers to confirm they were not due to a data entry error. We used monthly means instead of regressions with a low correlation coefficient (R) or unreasonable normalized root mean squared error (NRMSE) to fill data gaps.

Appendix C1 describes these updates to the marine point source inventory and resulting load changes, while Appendix C2 contains marine point source time series plots of flow and water quality.

Other methods

To understand model skill, we compute various statistical metrics with paired discrete observations in marine waters. Appendix D contains equations for the following statistical metrics used in computations and defined in the glossary: correlation coefficient (R), bias, root mean square error (RMSE), centered (or unbiased) RMSE_c, Willmott skill score, relative error (RE), mean absolute error (MAE), normalized bias, normalized RMSE (NRMSE), centered and normalized RMSE (NRMSE_c or uNRMSE), model efficiency (MEF), and normalized standard deviation (N_{sd}). We employ scatterplots, time-depth plots, time series, and vertical profiles to review model performance. Appendices E, F, G, and H contain plots comparing paired available

observed and simulated data and the corresponding statistical skill metrics for 2000, 2006, 2008, and 2014 data sets, respectively.

We also evaluated model skill using data from mesocosm observations for sediment fluxes (Appendix I), productivity (Appendix J), and water column respiration (Appendix K). Each of these appendices describes approaches used.

Appendix L describes the approach used to develop initial hypothetical scenarios using watershed and wastewater treatment plant reduction frameworks. Noncompliance calculations for these scenarios, as well as the refined and existing scenarios, were performed using the algorithm detailed in Opt 1 (Appendix F in Ahmed et al. 2021).

The compliance grids we are employing here are not the model grids, but the 303(d) assessment units that are used for determining the health of Washington's waters in our statewide Water Quality Assessment. We averaged daily minimum DO for each model grid layer contained within the assessment units using a volume weighted average approach; this methodology is explained in Appendix D. The model includes 16,012 grid cells that vary in diameter from 130 to 250 meters in the inlets and bays to 800 meters in the main basin of Puget Sound, up to 3000 meters in the Strait of Juan de Fuca, and up to 15 Km at the open boundary near the continental shelf. The 303(d) assessment units are about 1130 m long and 790 m wide.

We produced a comparative analysis of residence times between basins (see Appendix M) in the Greater Puget Sound. In this study, residence and flushing are defined in terms of the length of time it takes for an initial dye concentration to be reduced to approximately 37% of its initial concentration. However, residence time is a local measure of the length of time that a particular water parcel remains within a water body, while flushing time is an integrative measure of the time required to replace the entire volume of water within a water body.

Longer residence times promote stagnation and buildup of pollutant concentrations, increase primary productivity and depletion of nutrients, increase nitrification (oxidation of ammonia to nitrate, which depletes oxygen), increase settling of particulate organic matter (e.g., dead algae), and increase decomposition of organic carbon (which depletes oxygen). We conducted a virtual dye study (i.e., a hypothetical dye concentration introduced into the model domain) for each basin for each of the four years modeled (2000, 2006, 2008, and 2014). Appendix M presents the procedure for the virtual dye study and calculation of residence and flushing times.

SSM limitations reiterated in the Overview of Model Limitations section and discussed previously (McCarthy et al. 2018; Ahmed et al. 2019, 2021) require that we mask model output at intertidal and some shallow subtidal locations. We are not using model output generated within intertidal and some shallow subtidal areas for noncompliance calculations. We reviewed our masking approach and made updates as specified in Appendix D. Aside from masked areas nearshore, we are also masking the entire area of Budd Inlet because it is addressed in a separate EPA-approved TMDL, Ecology (2022). At the Budd Inlet open boundary, Ecology (2022) established an aggregate load allocation for external sources (termed the "bubble allocation"). In this study, we evaluated whether one of the refined selected scenarios, updated with Budd

Inlet TMDL loads and waste loads, met the bubble allocation. The procedure for calculating the landward loads at the Budd Inlet open boundary is discussed in Appendix O.

Existing and reference loads

The SSM requires boundary condition input files that represent all watershed and marine point source inputs entering the model domain. We created input files to represent existing and reference conditions for the years 2000, 2006, 2008, and 2014 to evaluate and compare model skill and DO noncompliance for multiple years.

- Existing conditions for years 2000, 2006, 2008, and 2014 reflect all the updates made to watershed regressions and marine point source input estimates described in earlier sections of this report, as well as in Appendices B and C.
- Reference conditions for each of these years represent nutrient inputs from watershed and marine point sources estimated in the absence of local and regional anthropogenic influence. Under reference conditions, the location of marine point sources and watershed inflows remains unchanged, as do the magnitude of flows associated with these inputs.

The only difference between the existing and reference conditions is that the nitrogen and organic carbon nutrient concentrations are lower in the reference condition. Appendix D contains details and further describes how these reference conditions were estimated. Anthropogenic loads are calculated as the difference between existing and reference loads for each respective year.

Input loads and model results, including DO noncompliance plots and analyses, are grouped into eight basins: Northern Bays, Whidbey Basin, Main Basin, South Sound, Hood Canal, Admiralty Inlet, U.S. portion of the Strait of Juan de Fuca (SJF-US), U.S. portion of the Strait of Georgia (SOG-US). Loads and results are also aggregated to “WA waters of the Salish Sea”, which is equivalent to the total combined area of all eight basins. These eight basins are illustrated in Figure 3.

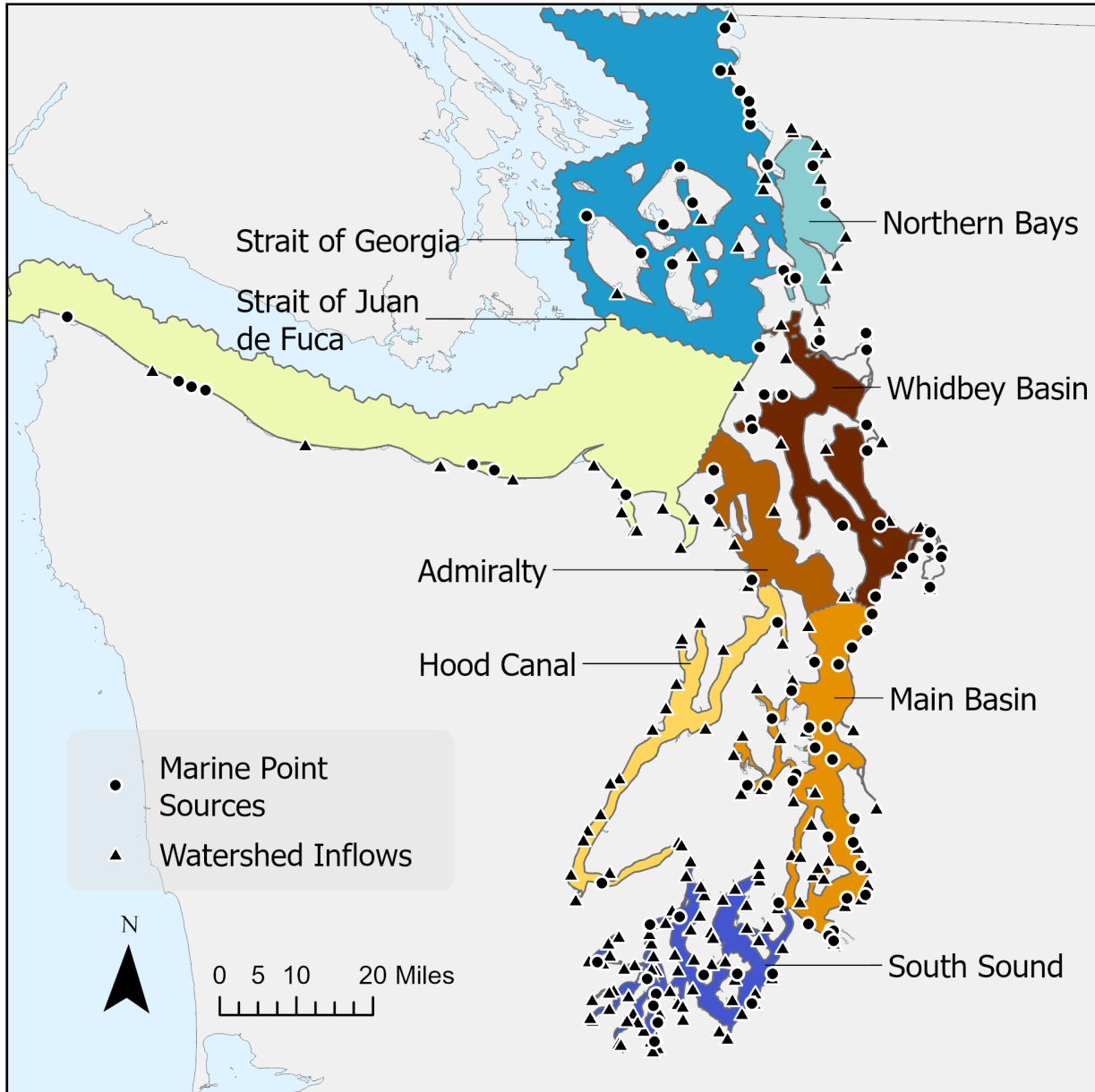


Figure 3. Map showing the location of the eight basins that are used to group input loads and model results, along with the location of watershed and marine point source inputs.

Table 1 presents average annual flows, as well as annual average existing, reference, and anthropogenic TN and TOC loads from watersheds and marine point sources across all four years as total magnitudes entering WA waters of the Salish Sea.

The years 2006 and 2014 have a similar magnitude of average annual watershed flows entering WA waters of the Salish Sea, and these flows are higher relative to the years 2000 and 2008. The magnitude of watershed loads follows the same pattern as flows, with higher TN and TOC loads in the years 2006 and 2014 relative to the other two years, pointing to the fact that interannual differences in watershed loads are predominantly driven by flow magnitudes. However, for marine point sources, flows are higher in 2000 and 2006 relative to 2008 and

2014. Similarly, TN loads from marine point sources are also higher for those same two years, while TOC loads are highest in 2000, similar in 2006 and 2008, and lowest in 2014.

Table 1 also compares the relative percent contribution of marine point source loads and watershed loads to the total anthropogenic load. For TN, marine point sources contribute 63% – 73% while watershed sources contribute the remaining 27% – 37% of the anthropogenic load. For TOC loads, marine point sources contribute 8% – 32% while watershed sources contribute the remaining 68% – 91% of the anthropogenic load.

Figures 4 and 5 both compare flow and the anthropogenic component of TN and TOC loads entering WA waters of the Salish Sea across all four years. Figure 4 distinguishes between marine point source loads versus watershed loads, aggregated to WA waters of the Salish Sea, while Figure 5 illustrates the combined marine point source and watershed flows and loads entering different basins.

The overall magnitude of flows entering WA waters of the Salish Sea is lower in 2000 and 2008, and higher in 2006 and 2014. Anthropogenic TN and TOC load magnitudes follow a similar pattern, reflecting the fact that the years with more freshwater flow also result in higher nutrient loads. This is more pronounced for anthropogenic TOC loads, since most of this TOC load comes from watersheds, which are also the dominant source of flows. Interestingly, 2006 had lower average annual flows than 2014 but higher TN loads — this is primarily due to TN loads from two of the largest WWTP facilities (West Point and South King) having a higher TN load in 2006 (relative to 2014) due to a major flood event in November of that year.

While Figure 5 does not distinguish relative load contributions between watersheds and WWTPs, Main Basin receives the largest magnitude of anthropogenic marine point source TN loads, since this is where some of the largest Puget Sound WWTPs (that serve the larger Seattle metro area) discharge their effluent to. Whidbey Basin receives the largest magnitude of anthropogenic TOC loads, which again reflects that most of the TOC loads are from watersheds, and Whidbey is the basin with the largest watershed flows since this is where three of the largest Puget Sound rivers discharge to (Skagit, Snohomish, and Stillaguamish Rivers).

Table 1. Average annual daily flows and average annual daily total nitrogen (TN) and total organic carbon (TOC) marine point source and watershed loads^a entering WA waters of the Salish Sea for each of the four modeled years.

| Average annual flow or load | Source | 2000 | 2006 | 2008 | 2014 |
|-----------------------------|----------------------------------|----------------|----------------|----------------|----------------|
| Flows (cms) | Marine point sources | 19.1 | 20.1 | 17.7 | 18.1 |
| | Watersheds | 1,370 | 1,810 | 1,560 | 1,950 |
| | Total | 1,390 | 1,830 | 1,580 | 1,970 |
| TN loads (kg/day) | Marine point sources — existing | 37,400 | 38,400 | 36,200 | 36,900 |
| | Marine point sources — reference | 256 | 286 | 244 | 254 |
| | Marine point — anthro. | 37,100 | 38,100 | 36,000 | 36,600 |
| | Watersheds — existing | 28,800 | 43,600 | 32,400 | 44,700 |
| | Watersheds — reference | 15,000 | 22,000 | 16,900 | 23,300 |
| | Watersheds — anthro. | 13,800 | 21,600 | 15,500 | 21,400 |
| | Total — existing | 66,200 | 82,000 | 68,600 | 81,600 |
| | Total — reference | 15,300 | 22,300 | 17,100 | 23,600 |
| | Total — anthro. | 50,900 | 59,700 | 51,500 | 58,000 |
| Anthro. TN load (%) | Marine point sources | 73% | 64% | 70% | 63% |
| | Watersheds | 27% | 36% | 30% | 37% |
| TOC loads (kg/day) | Marine point sources — existing | 21,900 | 17,200 | 17,200 | 14,700 |
| | Marine point sources — reference | 3,330 | 3,690 | 3,020 | 3,170 |
| | Marine point sources — anthro. | 18,600 | 13,500 | 14,200 | 11,500 |
| | Watersheds — existing | 174,000 | 316,000 | 223,000 | 322,000 |
| | Watersheds — reference | 134,000 | 198,000 | 150,000 | 198,000 |
| | Watersheds — anthro. | 40,000 | 118,000 | 73,000 | 124,000 |
| | Total — existing | 196,000 | 333,000 | 240,000 | 337,000 |
| | Total — reference | 137,000 | 202,000 | 153,000 | 201,000 |
| | Total — anthro. | 59,000 | 131,000 | 87,000 | 136,000 |
| Anthro. TOC load (%) | Marine point sources | 32% | 10% | 16% | 8.5% |
| | Watersheds | 68% | 90% | 84% | 91% |

^a All values are rounded to three significant figures

cms = cubic meters per second

anthro. = anthropogenic

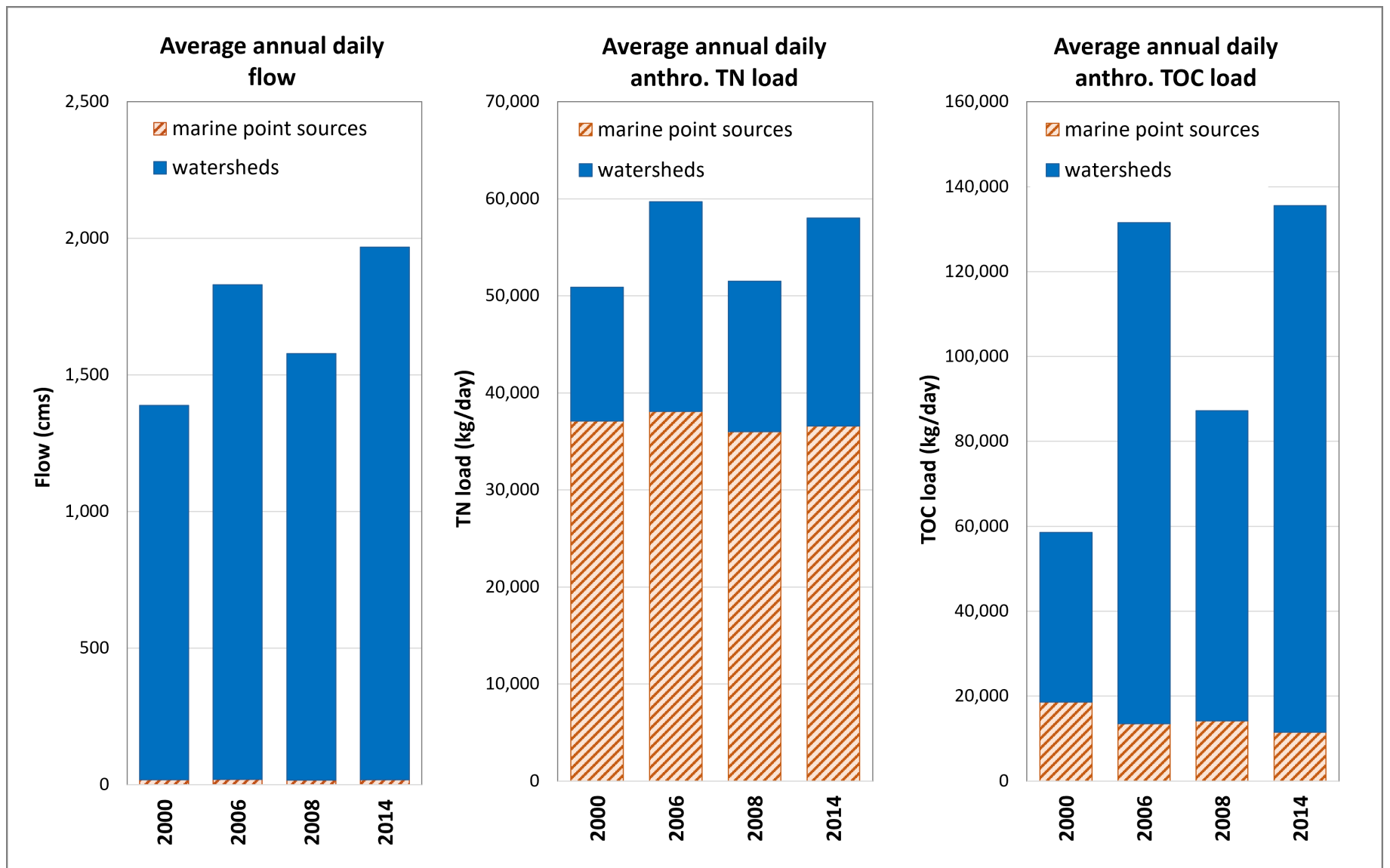


Figure 4. Bar plots showing average annual daily flows as well as average annual daily anthropogenic (anthro.) total nitrogen (TN) and total organic carbon (TOC) loads entering WA waters of the Salish Sea in 2000, 2006, 2008, and 2014.

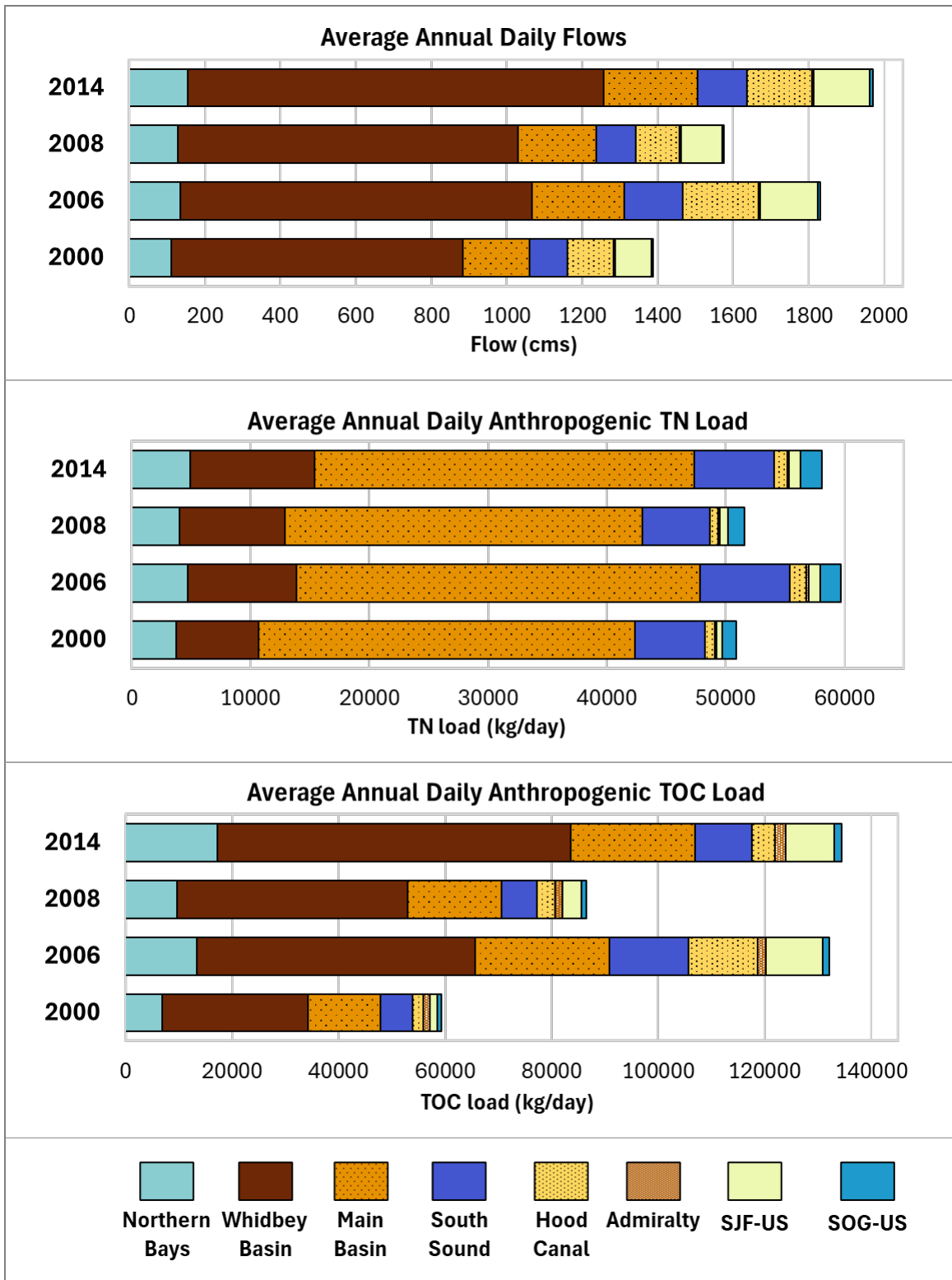


Figure 5. Bar plots showing average annual daily flows and average annual daily anthropogenic nitrogen loads (TN) and total organic carbon loads (TOC) entering different basins in 2000, 2006, 2008, and 2014 from both watersheds and marine point sources. Magnitude of inputs to Admiralty and SOG-US inputs are relatively small, and are not visible in all three plots.

Figures 6 and 7 compare time series for daily anthropogenic TN and TOC loads from all watershed and marine point sources entering WA waters of the Salish Sea. These plots show similar patterns, with 2000 being the low flow year, resulting in low daily TN and TOC loads relative to the other years. The plots illustrate how watershed loads entering the SSM domain vary daily while marine point sources only vary monthly, which is an artifact of how the concentrations and flows for these two different inputs are specified in the model input files based on the temporal frequency of available data and the inherent variability of these inflows. Anthropogenic TN marine point source loads are more constant, while watershed loads are highly variable with a seasonal pattern where loads are lower in the warmer months relative to marine point source loads. The primary driver for this seasonal pattern in watershed loads is watershed flows, which are low during drier months.

Marine point source anthropogenic TN loads are generally greater in magnitude than watershed anthropogenic TN loads, and watershed anthropogenic TOC loads are generally greater than marine point source anthropogenic TOC loads. However, during the late summer and early fall, anthropogenic watershed and marine point source TOC loads are similar in magnitude.

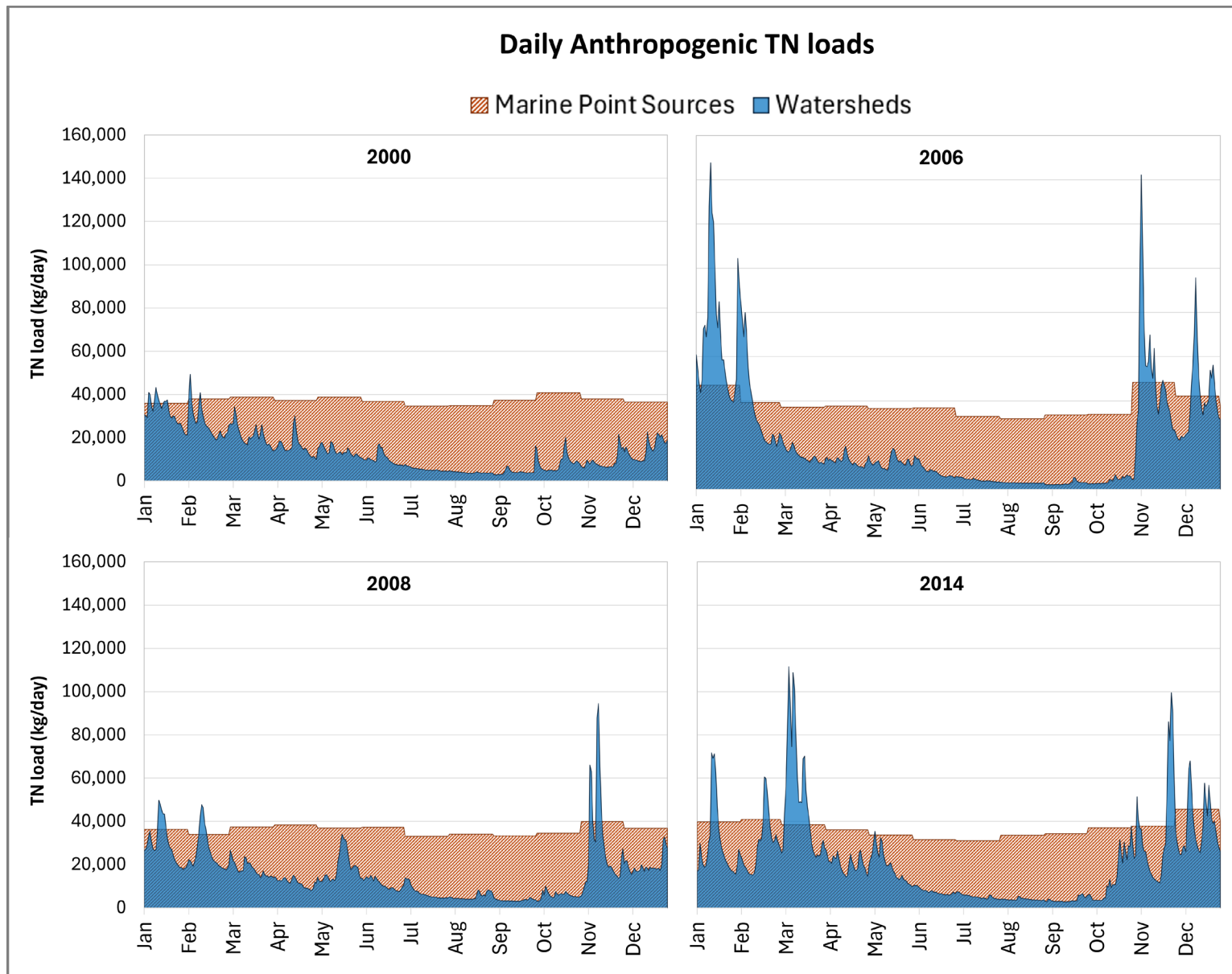


Figure 6. Daily anthropogenic total nitrogen (TN) loads entering WA waters of the Salish Sea in 2000, 2006, 2008, and 2014.

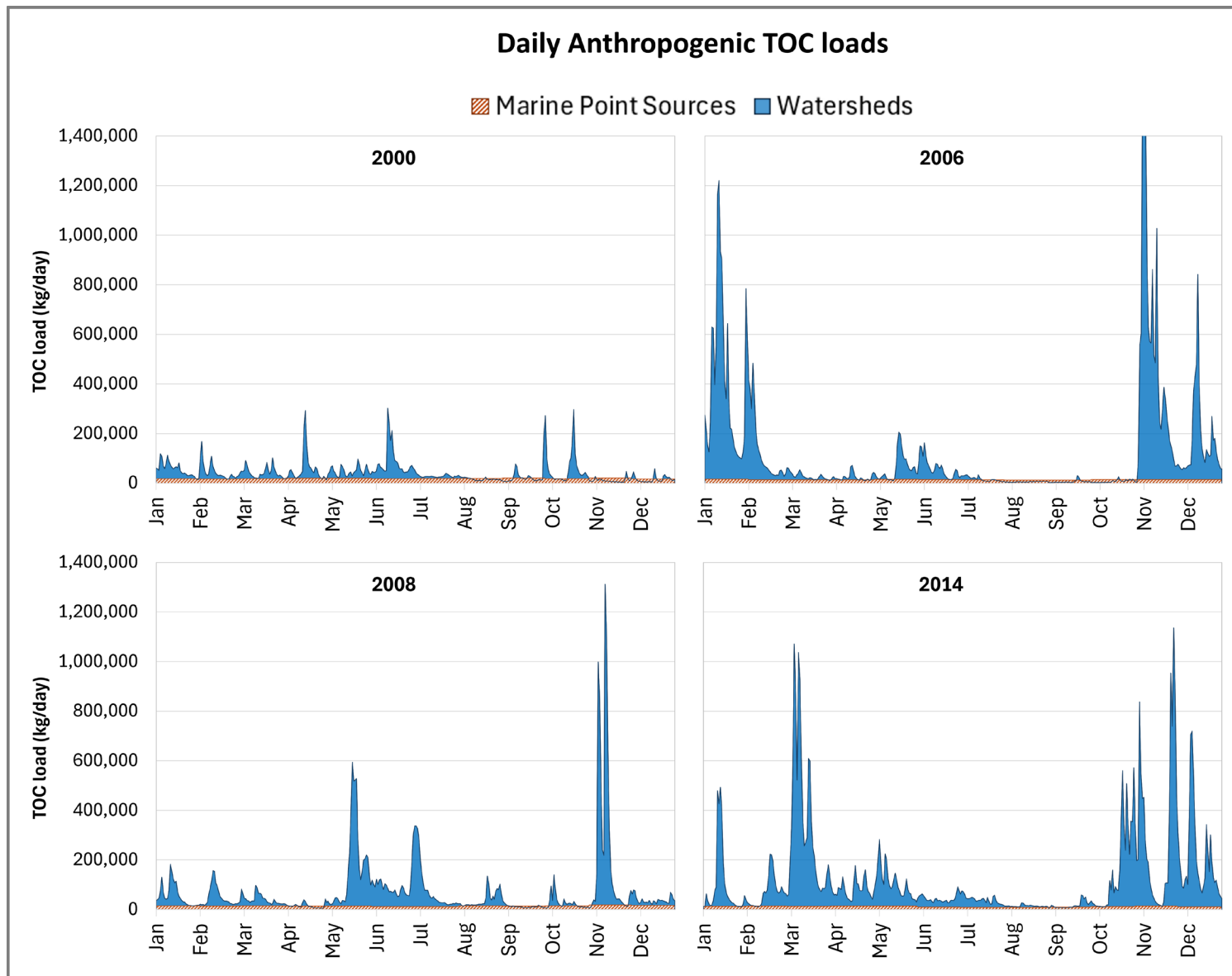


Figure 7. Daily anthropogenic total organic carbon loads entering WA waters of the Salish Sea in 2000, 2006, 2008, and 2014. Marine point source TOC loads are much smaller than watershed TOC loads and are not very visible in the plot.

Opt2 scenarios

After running the model under existing and reference conditions for the years 2000, 2006, 2008, and 2014 and evaluating model outputs for DO noncompliance (as discussed in the Results and Discussion section), we then developed Opt2 model scenarios, as follows.

Step 1. Select a single year for all subsequent model scenarios:

Even though four years were modeled under existing and reference conditions, due to computational and resource constraints, a single year, 2014, was selected for the modeling of Opt2 Scenarios. Ecology selected 2014 as the model year for Opt2 PSNSRP load variations scenarios because it is a more recent year that includes the Brightwater facility (a newer WWTP that discharges to Main Basin that came online in September 2011). Additionally, previous analysis had shown that 2014 was an average year in terms of residence time for the Central Basin (PSEMP 2016). However, in this phase of the work, we found that overall, at the Puget Sound scale, 2014 is the year with the fastest winter flushing time within the set of years considered (Appendix M).

Step 2. Run an initial set of model scenarios and evaluate them for DO noncompliance:

All initial scenarios involved pairing different watershed frameworks with different wastewater frameworks to identify the optimal combination of reductions that could be further refined. Each “framework” involves different reductions in anthropogenic TN and TOC mass loads from WWTPs and watersheds. These initial scenarios are described in Appendix L.

This process identified initial Scenario H1_C as the optimal scenario, because it resulted in similar levels of noncompliance as other initial scenarios without having to reduce anthropogenic loads in watersheds entering the Straits (i.e., with less effort). Scenario H1_C represented the pairing of Watershed Framework H1 with WWTP Framework C. Scenario H1_C involved the following:

- Greater percent reductions in watersheds that have larger existing anthropogenic loads.
- Greater percent reductions in watersheds entering Northern Bays, Whidbey Basin, Main Basin, and South Sound.
- Setting loads for watersheds entering the Straits (SJF-US and SOG-US) to existing 2014 loads.
- All U.S. WWTPs’ effluent DIN concentrations set to BNR of 3 mg/L, 5 mg/L, and 8 mg/L in hot, warm, and cool months, respectively.

Step 3. Run a set of ten more refined model scenarios:

Scenario H1_C, from Step 2, was the starting point for further refinement of scenarios. As illustrated in Figure 8, Scenario H1_C still showed remaining DO noncompliance in some inlets and inner bays of Puget Sound — namely, in Lynch Cove within Hood Canal, and Henderson and Carr Inlets in South Sound, and Sinclair Inlet and Liberty Bay in Main Basin.

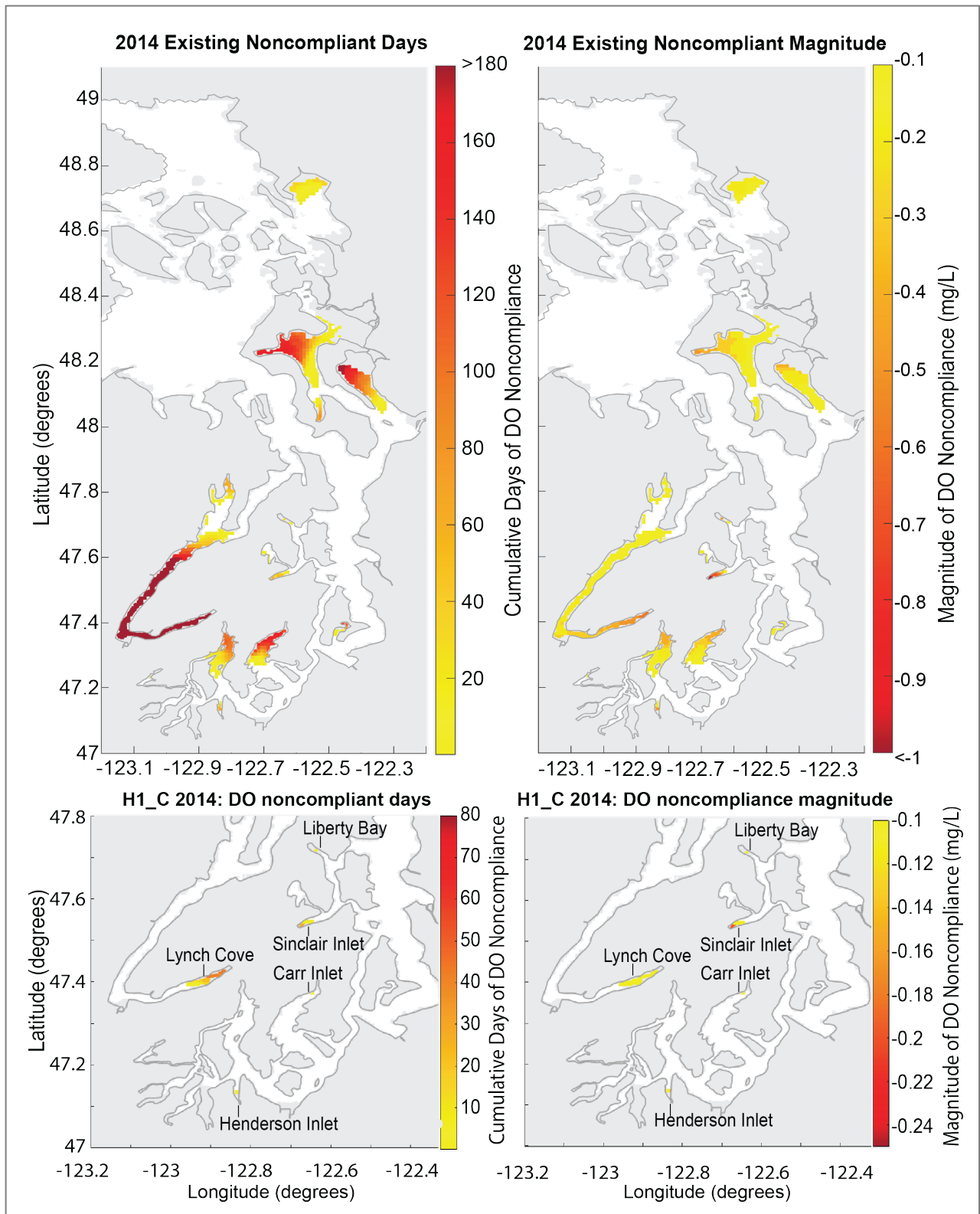


Figure 8. Plan view maps showing dissolved oxygen (DO) noncompliance days (left) and DO noncompliance magnitude (right) under existing 2014 conditions (top) and under Opt2 Scenario H1_C (bottom).

The bottom panel has a different scale to highlight remaining noncompliances that are lower in magnitude.

Development of the refined set of Opt2 scenarios involved further varying loads relative to Scenario H1_C via the following steps:

1. Selecting a single watershed framework — one that further refines anthropogenic load reductions relative to Watershed Framework H1
2. Pairing this new watershed framework with multiple WWTP frameworks to create 10 scenarios — these WWTP Frameworks used WWTP Framework C as a starting point, but then further varied BNR treatment levels at different facilities and during different seasons.
3. Identifying refined scenarios that can be used to develop nutrient reduction targets in the Nutrient Reduction Plan (Ecology 2025).

The following sections describe these steps.

Selecting a single watershed framework

A single watershed framework was developed to represent the “refined watershed framework” to pair with all 10 refined Opt2 scenarios. This framework was a variation of the H1 watershed framework and was informed by the DO noncompliance results in Figure 8. It involved the same level of anthropogenic nutrient reductions as H1 in all watersheds except those discharging to recalcitrant areas (areas where DO noncompliance persists, i.e., in Lynch Cove, Henderson, Carr, and Sinclair Inlets, and Liberty Bay). In these areas, anthropogenic watershed nutrient concentrations were reduced by 90% (flows remained the same). These percent reductions were applied equally across all forms of nitrogen and organic carbon. Watershed reductions associated with this framework are summarized in Table 2. Figure 9 compares the annual loads associated with this watershed framework, by basin, to existing 2014 anthropogenic loads.

Table 2. Description of the refined watershed framework and associated annual anthropogenic (anthro.) loads^a used for all refined Opt2 scenarios.

| Basin | Reductions applied to watershed anthropogenic TN and TOC loads | Annual anthro. TN load under existing conditions (thousands of kg/year) | Annual anthro. TN load with refined watershed framework (thousands of kg/year) | Basin-wide percent reduction in anthro. TN load ^b | Annual anthro. TOC load under existing conditions (thousands of kg/year) | Annual anthro. TOC load with refined watershed framework (thousands of kg/year) | Basin-wide percent reduction in anthro. TOC load ^b |
|----------------------|--|---|--|--|--|---|---|
| Northern Bays | 67.6% ("large" rivers) 61.2% (all other rivers) | 1,330 | 450 | 66.2% | 6,120 | 2,020 | 67.0% |
| Whidbey Basin | 67.6% ("large" rivers) 61.2% (all other rivers) | 2,460 | 820 | 66.7% | 24,200 | 8,600 | 64.5% |
| Main Basin | 90% (rivers near Sinclair Inlet and Liberty Bay) 67.6% ("large" rivers) 61.2% (all other rivers) | 1,690 | 540 | 68.0% | 6,000 | 1,900 | 68.3% |
| South Sound | 90% rivers near Henderson and Carr Inlets 61.2% (all other rivers) | 1,260 | 469 | 62.8% | 3,760 | 1,420 | 62.2% |
| Hood Canal | 90% rivers near Lynch Cove 53.4% (all other rivers) | 407 | 137 | 66.3% | 1,580 | 610 | 61.4% |
| Admiralty | 53.4% (all other rivers) | 37.3 | 17.4 | 53.4% | 210 | 98.0 | 53.3% |
| SJF-US | No reductions | 238 | 238 | 0.0% | 3,240 | 3,240 | 0.0% |
| SOG-US | No reductions | 419 | 419 | 0.0% | 370 | 370 | 0.0% |

^a All loads are rounded to three significant digits.

^b These percentages were calculated on rounded numbers.

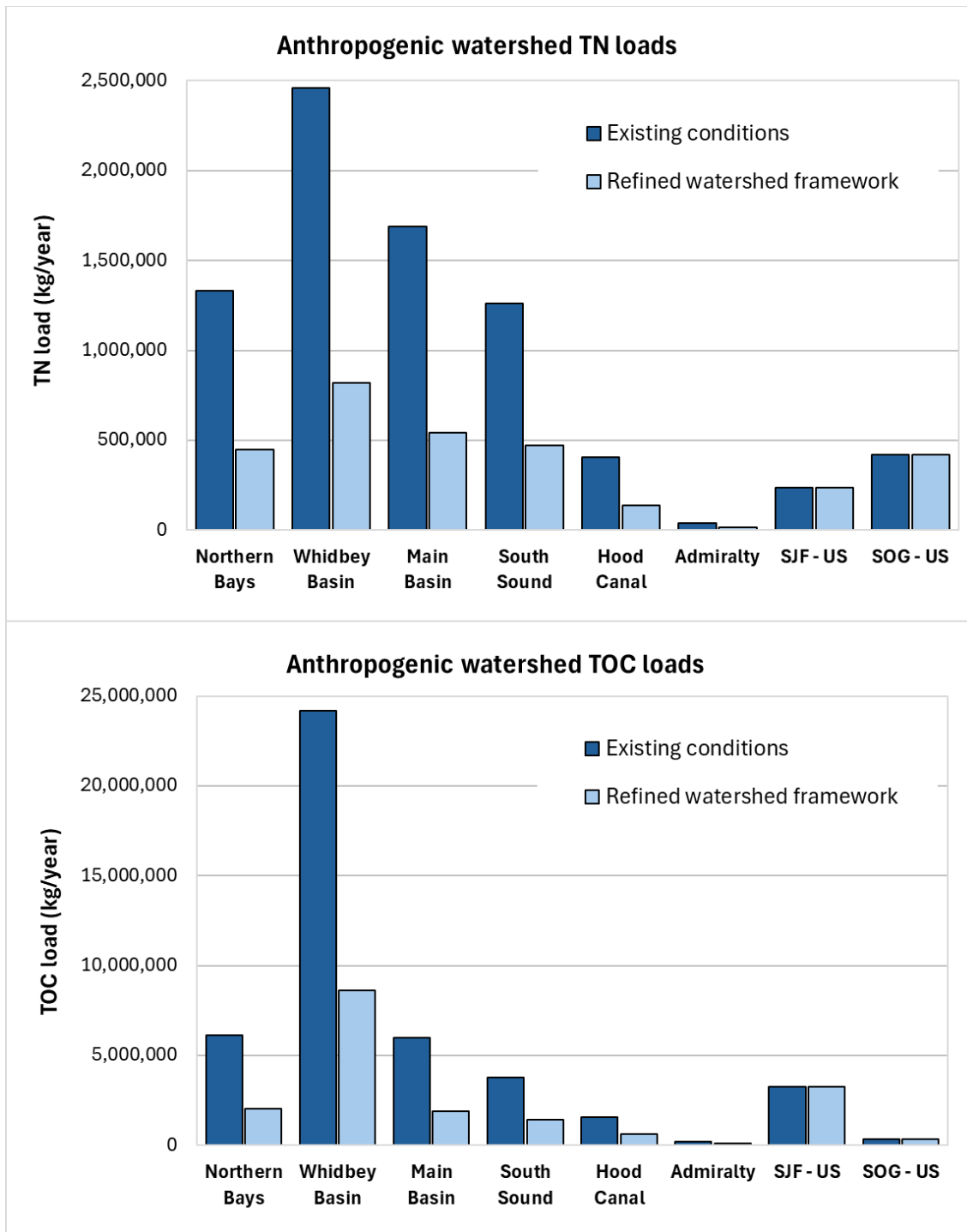


Figure 9. Annual anthropogenic watershed total nitrogen (TN, top) and total organic carbon (TOC, bottom) loads, by basin under existing 2014 conditions and the refined watershed framework for all Opt2 scenarios.

WWTP frameworks

The selected watershed framework was then paired with ten different WWTP frameworks to create the refined set of Opt2 scenarios. WWTP reductions involved applying different levels of biological nitrogen removal (BNR) treatment during different seasons across groups of WWTPs. These BNR levels were applied by setting WWTP effluent dissolved inorganic nitrogen (DIN) concentrations to 3 mg/L, 5 mg/L, and 8 mg/L⁴ relative to existing 2014 DIN concentrations. These levels were based on a study that consisted of a technical and economic evaluation of nutrient removal at WWTPs that involved BNR levels of 3 to 8 mg/L of DIN (Tetra Tech 2011). Within this report, these three BNR levels are often expressed in shorthand as BNR3, BNR5, and BNR8 to represent effluent DIN concentrations of 3 mg/L, 5 mg/L, and 8 mg/L, respectively. Industrial facility loads remained at existing 2014 loads under all these WWTP frameworks (for reference, there are 10 industrial facilities in WA waters of the Salish Sea, which contribute about 1.7% of the total TN load and 25% of the total TOC load from all U.S. marine point sources in 2014).

The different WWTP frameworks represent different levels of BNR treatment, which were varied based on the following:

- **Season** — since DO is seasonally lower during hotter months in vulnerable inlets, we explored varying the levels of BNR applied in different seasons, with generally higher levels of nutrient removal from effluent during the more critical hot months (July – September) relative to warm months (April – June and October) and cool months (November – March).
- **Location of effluent discharge** — in some frameworks, a higher level of nutrient removal from effluent was tested for facilities discharging to or near areas with persistent DO noncompliance, specifically Sinclair Inlet. Some frameworks also explored the impact of no additional treatment for those facilities discharging to basins that are either relatively well-flushed (Admiralty, SJF, and SOG) or located in basins where WWTPs’ discharges are small (Hood Canal).
- **Size of WWTP** — we explored the impact of implementing higher levels of treatment at dominant WWTPs⁵ located in Main Basin, as well as the impact of no additional treatment at very small WWTPs (i.e., by holding loads for these facilities to existing 2014 levels). The size of the WWTP was determined based on the magnitude of its existing 2014 nitrogen loads.
- **Type of WWTP** — among the dominant WWTPs in Main Basin, West Point is a facility treating combined sewers. Facilities that treat flows from combined sewer systems have a more challenging time treating wastewater during the cool season when stormwater runoff often creates high variability flows and influent pollutant concentrations. We explored the relative impact of West Point’s facility’s effluent by creating a scenario that limited BNR treatment during the cool season to 8 mg/L⁶.

Table 3 presents the refined set of Opt2 scenarios and the questions they were designed to address, as well as the BNR levels applied to different facilities under each scenario.

⁴ All BNR levels included an effluent limit of 8 mg/L of carbonaceous biological oxygen demand (CBOD₅)

⁵ See Glossary for definition of “dominant WWTPs”

⁶ There are other combined sewer facilities in addition to West Point, and limiting their cool month BNR levels to 8 mg/L was tested in WWTP Framework E, discussed in Appendix L.

Table 3. Refined Opt2 WWTP frameworks (each paired with a single watershed framework).

| Scenario ID | Question that it addresses | WWTPs at existing 2014 loads | WWTP BNR levels ^a |
|-------------|--|---|---|
| Opt2_1 | What is the effect of BNR 8/5/3 at all WWTPs on noncompliance? | None | All WWTPs at 8/5/3 |
| Opt2_2 | How does setting very small WWTPs at existing 2014 loads affect noncompliance? | Very small WWTPs ^b | All other WWTPs at 8/5/3 |
| Opt2_3 | How does increasing BNR treatment for those WWTPs discharging within or near Sinclair Inlet affect noncompliance? | None | Three WWTPs within or near Sinclair Inlet set at BNR 3/3/3. All other WWTPs at 8/5/3 |
| Opt2_4 | How does setting WWTPs discharging into the Straits of Juan de Fuca and Georgia, Admiralty Inlet, and Hood Canal, at existing 2014 loads, affect noncompliance? | WWTPs in Straits of Juan de Fuca and Georgia, Admiralty Inlet, and Hood Canal | All other WWTPs at BNR 8/5/3 |
| Opt2_5 | What is the combined effect on noncompliance of 1) setting very small WWTPs and 2) setting WWTPs discharging into the Straits of Juan de Fuca and Georgia, Admiralty Inlet, and Hood Canal at existing 2014 loads? | Very small WWTPs ^b and WWTPs in Straits of Juan de Fuca and Georgia, Admiralty Inlet, and Hood Canal | All other WWTPs at BNR 8/5/3 |
| Opt2_6 | What is the combined effect on noncompliance of 1) setting WWTPs discharging into Straits of Juan de Fuca and Georgia, Admiralty Inlet, and Hood Canal at existing 2014 loads and 2) increasing BNR treatment for those WWTPs discharging within or near Sinclair Inlet? | WWTPs in Straits of Juan de Fuca and Georgia, Admiralty Inlet, and Hood Canal | Three WWTPs within or near Sinclair Inlet set at BNR 3/3/3. All other WWTPs at BNR 8/5/3 |
| Opt2_7 | What is the combined effect of 1) setting very small WWTPs at existing 2014 loads, 2) setting WWTPs discharging into Straits of Juan de Fuca and Georgia, Admiralty Inlet, and Hood Canal at existing 2014 loads, and 3) increasing BNR treatment for those WWTPs discharging within or near Sinclair Inlet? | Very small WWTPs ^b and WWTPs in the Straits of Juan de Fuca and Georgia, Admiralty Inlet, and Hood Canal | Three WWTPs within or near Sinclair Inlet set at BNR 3/3/3. All other WWTPs at BNR 8/5/3 |
| Opt2_8 | Can DO zero noncompliance be achieved everywhere with largest (dominant) WWTPs in the Main Basin at BNR 8/3/3 and those in the vicinity of Sinclair Inlet at BNR 3/3/3, but West Point (a dominant facility treating combined sewers) at 8/5/3? | Very small WWTPs ^b and WWTPs in Straits of Juan de Fuca and Georgia, Admiralty Inlet, and Hood Canal | Three WWTPs within or near Sinclair Inlet set at BNR 3/3/3. All dominant Main Basin WWTPs ^c at BNR 8/3/3 (except West Point set at 8/5/3). All other WWTPs at 8/5/3) |

| Scenario ID | Question that it addresses | WWTPs at existing 2014 loads | WWTP BNR levels ^a |
|-------------|---|--|--|
| Opt2_9 | Can DO zero noncompliance be achieved everywhere with largest (dominant) WWTPs in the Main Basin at BNR 8/3/3 and those in the vicinity of Sinclair Inlet at BNR 3/3/3? | Very small WWTPs ^b and WWTPs in Straits of Juan de Fuca and Georgia, Admiralty Inlet and Hood Canal | Three WWTPs within or near Sinclair Inlet set at BNR 3/3/3. All dominant Main Basin WWTPs ^c at BNR 8/3/3. All other WWTPs at 8/5/3 |
| Opt2_10 | Can DO zero noncompliance be achieved everywhere with largest (dominant) WWTPs in the Main Basin and those in the vicinity of the most difficult noncompliance location at BNR 3/3/3? | Very small WWTPs ^b and WWTPs in Straits of Juan de Fuca and Georgia, Admiralty Inlet and Hood Canal | Three WWTPs within or near Sinclair Inlet set at BNR 3/3/3. All dominant Main Basin WWTPs ^c at BNR 3/3/3. All other WWTPs at 8/5/3 |

^a BNR levels are specified in terms of cool (Nov – Mar)/warm (Apr – Jun, Oct)/hot (Jul – Sep) months.

^b Very small WWTPs are defined as those discharging less than 10 kg TN/day or less than 6 kg DIN/day on a maximum monthly basis for model year 2014.

^c Dominant Main Basin WWTPs include Brightwater, South King, Tacoma Central, and West Point.

Opt2 scenario loads

This section presents the nutrient loads associated with all 10 refined Opt2 scenarios listed in Table 3. Nutrient loads for each scenario only change the anthropogenic component of the loads, since reference loads are held constant across scenarios.

Figure 10 compares anthropogenic TN loads entering different basins under each refined Opt2 scenario, from watersheds and marine point sources. All of the Opt2 scenarios use the same watershed anthropogenic TN loading. This figure shows that marine point source loads vary only slightly among scenarios, which is due to small variations in the DIN fraction of total nitrogen achieved when different BNR treatment levels are applied to WWTP facilities in each scenario. DO noncompliance computations from scenarios are discussed in the Results section of this report.

Tables 4 and 5 compare annual watershed and marine point source anthropogenic TN and TOC loads, respectively, for each refined Opt2 scenario entering each basin. Both Tables 4 and 5 show that basin marine point source loads are the same across Opt2 scenarios four through 10 for those basins that are held at existing loads (Hood Canal, Admiralty, SJF-US, and SOG-US).

Tables 6 and 7 compare the magnitude and percent reduction in watershed and marine point source annual anthropogenic TN and TOC loads, respectively, associated with each refined Opt2 modeling scenario. These loads represent the sum of all loads discharging to WA waters of the Salish Sea.

Watershed loads and percent watershed reductions, respectively, are identical across all Opt2 scenarios, since these represent the single “refined watershed framework” described earlier, which involves a 60.6% and 59.8% reduction in overall anthropogenic watershed TN and TOC loads, respectively.

Marine point source loads vary slightly between scenarios, reflecting the different WWTP frameworks, which represent varying levels of BNR treatment depending on the season, location, size, and type of WWTP. However, even with these variations in BNR treatment, the refined Opt2 scenarios do not

result in dramatically different marine point source loads or percent reductions at the scale of WA waters of the Salish Sea. Across all refined Opt2 scenarios, percent anthropogenic marine point source reductions range from 68.1% to 74.2% for TN and 17.8% to 18.3% for TOC.

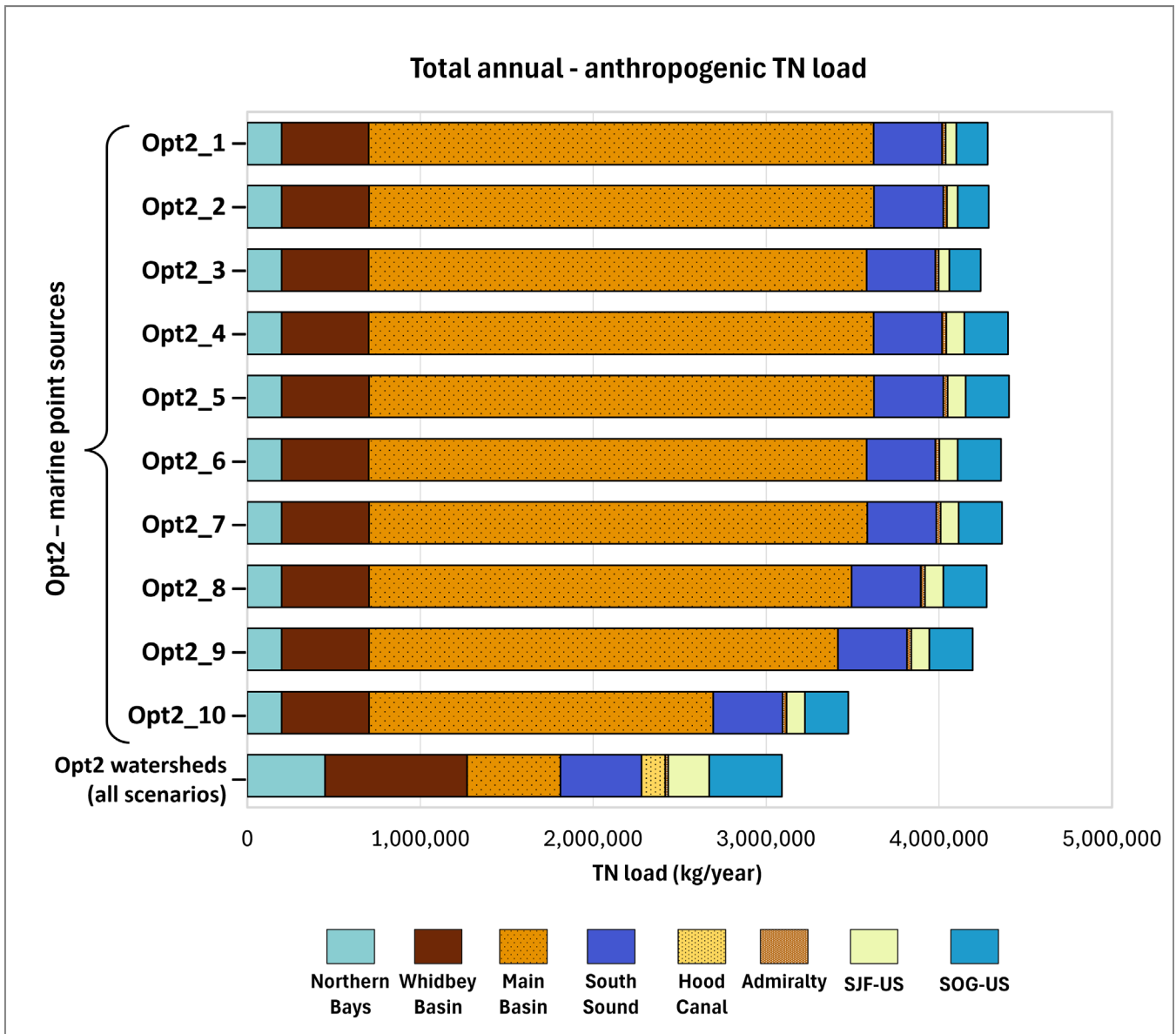


Figure 10. Annual anthropogenic total nitrogen (TN) watershed and marine point source loads entering different basins for each refined Opt2 scenario.

Watershed loads are the same across all scenarios and therefore represented by a single bar.

Table 4. Annual anthropogenic (anthro.) total nitrogen (TN) loads^a entering different basins for each refined Opt2 model scenario for the year 2014.

| Opt2 scenario | Northern Bays anthro. TN load (thousands of kg/year) | Whidbey Basin anthro. TN load (thousands of kg/year) | Main Basin anthro. TN load (thousands of kg/year) | South Sound anthro. TN load (thousands of kg/year) | Hood Canal anthro. TN load (thousands of kg/year) | Admiralty anthro. TN load (thousands of kg/year) | SJF-US anthro. TN load (thousands of kg/year) | SOG-US anthro. TN load (thousands of kg/year) |
|-----------------------------------|--|--|---|--|---|--|---|---|
| Existing - watersheds | 1,330 | 2,460 | 1,690 | 1,260 | 407 | 37.3 | 238 | 419 |
| Opt2 (all scenarios) - watersheds | 450 | 820 | 540 | 469 | 137 | 17.4 | 238 | 419 |
| Existing - marine point sources | 474 | 1,380 | 10,000 | 1,180 | 0.371 | 24.1 | 105 | 251 |
| Opt2_1 - marine point sources | 199 | 502 | 2,920 | 396 | 0.282 | 20.5 | 62 | 180 |
| Opt2_2 - marine point sources | 199 | 505 | 2,920 | 400 | 0.371 | 20.5 | 62 | 180 |
| Opt2_3 - marine point sources | 199 | 502 | 2,880 | 396 | 0.282 | 20.5 | 62 | 180 |
| Opt2_4 - marine point sources | 199 | 502 | 2,920 | 396 | 0.371 | 24.1 | 105 | 251 |
| Opt2_5 - marine point sources | 199 | 505 | 2,920 | 400 | 0.371 | 24.1 | 105 | 251 |
| Opt2_6 - marine point sources | 199 | 502 | 2,880 | 396 | 0.371 | 24.1 | 105 | 251 |
| Opt2_7 - marine point sources | 199 | 505 | 2,880 | 400 | 0.371 | 24.1 | 105 | 251 |
| Opt2_8 - marine point sources | 199 | 505 | 2,790 | 400 | 0.371 | 24.1 | 105 | 251 |
| Opt2_9 - marine point sources | 199 | 505 | 2,710 | 400 | 0.371 | 24.1 | 105 | 251 |
| Opt2_10 - marine point sources | 199 | 505 | 1,990 | 400 | 0 | 24.1 | 105 | 251 |

^a Basin loads are calculated by first calculating total monthly loads (rounded to three significant digits), and then summing them up to the annual load, which is again rounded to three significant digits.

Table 5. Annual anthropogenic (anthro.) total organic carbon (TOC) loads^a entering different basins for each refined Opt2 model scenario for the year 2014.

| Opt2 scenario | Northern Bays anthro. TOC load (thousands of kg/year) | Whidbey Basin anthro. TOC load (thousands of kg/year) | Main Basin anthro. TOC load (thousands of kg/year) | South Sound anthro. TOC load (thousands of kg/year) | Hood Canal anthro. TOC load (thousands of kg/year) | Admiralty anthro. TOC load (thousands of kg/year) | SJF-US anthro. TOC load (thousands of kg/year) | SOG-US anthro. TOC load (thousands of kg/year) |
|-----------------------------------|---|---|--|---|--|---|--|--|
| Existing - watersheds | 6,120 | 24,200 | 6,000 | 3,760 | 1,580 | 210 | 3,240 | 370 |
| Opt2 (all scenarios) - watersheds | 2,020 | 8,600 | 1,900 | 1,420 | 610 | 98.0 | 3,240 | 370 |
| Existing - marine point sources | 228 | 392 | 2,540 | 221 | 0.129 | 534 | 140 | 163 |
| Opt2_1 - marine point sources | 192 | 301 | 1,970 | 171 | 0.127 | 534 | 135 | 146 |
| Opt2_2 - marine point sources | 192 | 301 | 1,970 | 171 | 0.129 | 534 | 135 | 146 |
| Opt2_3 - marine point sources | 192 | 301 | 1,970 | 171 | 0.127 | 534 | 135 | 146 |
| Opt2_4 - marine point sources | 192 | 301 | 1,970 | 171 | 0.129 | 534 | 140 | 163 |
| Opt2_5 - marine point sources | 192 | 301 | 1,970 | 171 | 0.129 | 534 | 140 | 163 |
| Opt2_6 - marine point sources | 192 | 301 | 1,970 | 171 | 0.129 | 534 | 140 | 163 |
| Opt2_7 - marine point sources | 192 | 301 | 1,970 | 171 | 0.129 | 534 | 140 | 163 |
| Opt2_8 - marine point sources | 192 | 301 | 1,970 | 171 | 0.129 | 534 | 140 | 163 |
| Opt2_9 - marine point sources | 192 | 301 | 1,970 | 171 | 0.129 | 534 | 140 | 163 |
| Opt2_10 - marine point sources | 192 | 301 | 1,970 | 171 | 0.129 | 534 | 140 | 163 |

^a Basin loads are calculated by first calculating total monthly loads (rounded to three significant digits) and then summing them up to the annual load, which is again rounded to three significant digits.

Table 6. Annual loads^a and percent load reductions in total nitrogen (TN) to WA waters of the Salish Sea associated with each refined Opt2 scenario for the year 2014.

| Opt2 scenario | Total TN load (thousands of kg/year) | Watershed TN load (thousands of kg/year) | Marine point source TN load (thousands of kg/year) | Total anthro. TN load (thousands of kg/year) | Watershed anthro. TN load (thousands of kg/year) | Marine point source anthro. TN load (thousands of kg/year) | Total % reduction in anthro. TN loads | Percent reduction in watershed anthro. TN loads | Percent reduction in point source anthro. TN loads |
|----------------------|---|---|---|---|---|---|--|--|---|
| Reference | 8,630 | 8,537 | 92.9 | 0 | 0 | 0 | 100% | 100% | 100% |
| Existing | 29,930 | 16,380 | 13,550 | 21,300 | 7,843 | 13,460 | 0% | 0% | 0% |
| Opt2_1 | 16,000 | 11,630 | 4,374 | 7,370 | 3,093 | 4,281 | 65.4% | 60.6% | 68.2% |
| Opt2_2 | 16,010 | 11,630 | 4,381 | 7,380 | 3,093 | 4,288 | 65.4% | 60.6% | 68.1% |
| Opt2_3 | 15,960 | 11,630 | 4,334 | 7,330 | 3,093 | 4,241 | 65.6% | 60.6% | 68.5% |
| Opt2_4 | 16,120 | 11,630 | 4,492 | 7,490 | 3,093 | 4,399 | 64.8% | 60.6% | 67.3% |
| Opt2_5 | 16,130 | 11,630 | 4,499 | 7,500 | 3,093 | 4,406 | 64.8% | 60.6% | 67.3% |
| Opt2_6 | 16,080 | 11,630 | 4,452 | 7,450 | 3,093 | 4,359 | 65.0% | 60.6% | 67.6% |
| Opt2_7 | 16,090 | 11,630 | 4,459 | 7,460 | 3,093 | 4,366 | 65.0% | 60.6% | 67.6% |
| Opt2_8 | 16,000 | 11,630 | 4,369 | 7,370 | 3,093 | 4,276 | 65.4% | 60.6% | 68.2% |
| Opt2_9 | 15,920 | 11,630 | 4,289 | 7,290 | 3,093 | 4,196 | 65.8% | 60.6% | 68.8% |
| Opt2_10 | 15,200 | 11,630 | 3,569 | 6,570 | 3,093 | 3,476 | 69.2% | 60.6% | 74.2% |

^a These are the sum of basin loads, rounded to four significant digits.

Table 7. Annual loads^a and percent load reductions in total organic carbon (TOC) to WA waters of the Salish Sea associated with each refined Opt2 scenario for the year 2014.

| Opt2 scenario | Total TOC load (thousands of kg/year) | Watershed TOC load (thousands of kg/year) | Marine point source TOC load (thousands of kg/year) | Total anthro. TOC load (thousands of kg/year) | Watershed anthro. TOC load (thousands of kg/year) | Marine point source anthro. TOC load (thousands of kg/year) | Total % reduction in anthro. TOC loads | Percent reduction in watershed anthro. TOC loads | Percent reduction in point source anthro. TOC loads |
|----------------------|--|--|--|--|--|--|---|---|--|
| Reference | 73,700 | 72,540 | 1,160 | 0 | 0 | 0 | 100% | 100% | 100% |
| Existing | 123,400 | 118,000 | 5,376 | 49,700 | 45,460 | 4,216 | 0% | 0% | 0% |
| Opt2_1 | 95,410 | 90,800 | 4,607 | 21,710 | 18,260 | 3,447 | 56.3% | 59.8% | 18.2% |
| Opt2_2 | 95,410 | 90,800 | 4,607 | 21,710 | 18,260 | 3,447 | 56.3% | 59.8% | 18.2% |
| Opt2_3 | 95,410 | 90,800 | 4,607 | 21,710 | 18,260 | 3,447 | 56.3% | 59.8% | 18.2% |
| Opt2_4 | 95,430 | 90,800 | 4,629 | 21,730 | 18,260 | 3,469 | 56.3% | 59.8% | 17.7% |
| Opt2_5 | 95,430 | 90,800 | 4,629 | 21,730 | 18,260 | 3,469 | 56.3% | 59.8% | 17.7% |
| Opt2_6 | 95,430 | 90,800 | 4,629 | 21,730 | 18,260 | 3,469 | 56.3% | 59.8% | 17.7% |
| Opt2_7 | 95,430 | 90,800 | 4,629 | 21,730 | 18,260 | 3,469 | 56.3% | 59.8% | 17.7% |
| Opt2_8 | 95,430 | 90,800 | 4,629 | 21,730 | 18,260 | 3,469 | 56.3% | 59.8% | 17.7% |
| Opt2_9 | 95,430 | 90,800 | 4,629 | 21,730 | 18,260 | 3,469 | 56.3% | 59.8% | 17.7% |
| Opt2_10 | 95,430 | 90,800 | 4,629 | 21,730 | 18,260 | 3,469 | 56.3% | 59.8% | 17.7% |

^a These are the sum of basin loads, rounded to four significant digits.

Results and Discussion

Performance of updated model

The SSM produces predictions of hydrodynamic and water quality characteristics throughout the Salish Sea. The version of SSM we are using has 16,012 nodes and ten vertical layers, with higher spatial resolution (smaller node grid elements) in Puget Sound. Model grid cell diameters vary from about 130 to 250 meters in the inlets and bays to 800 meters in the main basin of Puget Sound, up to 3000 meters in the Strait of Juan de Fuca, and up to 15 Km at the open boundary near the continental shelf. The purpose of this section is to synthesize our findings with respect to model skill within the large spatial domain of the model and over the four model years (2000, 2006, 2008, and 2014) that we ran the model in a hindcast mode.

Overall approach

Model performance evaluation has occurred throughout the model development and application phases, including in Ahmed et al. (2019, 2021), plus multiple papers and reports as listed in McCarthy et al. (2018). In Opt2, we conducted a thorough model performance evaluation that included statistical skill metrics, diverse visualizations of predictions and observations plotted over time and space, multiple comparative analyses between predictions and independent mesocosm observations of key drivers, and analyses that segregate different portions of the water column.

Appendix D contains information relevant to interpreting model performance results, such as model skill statistics and formulas, observational data sources, and maps showing monitoring locations, including a guide on how to understand time-depth plots.

We reviewed performance for the following water column parameters that SSM predicts: temperature, salinity, DO, chlorophyll-a, nitrate-nitrite, photosynthetically active radiation (PAR), and ammonium ion. Appendices E, F, G, and H contain scatter, time series, time-depth, and profile plots and statistics for the complete data set of marine monitoring stations available for each parameter for each of the years modeled (2000, 2006, 2008, and 2014). These appendices also contain scatterplots and model skill statistics at the surface, middle, and bottom waters for all stations with DO observations and segregated by the station type — open water or embayment. Also included in each of these appendices are scatter and time series comparison plots of predicted and observed water surface elevations.

We also conducted comparative analyses with independent data sets that have recently become available to understand model performance in reproducing gas exchanges to and from the sediments, water column microbial respiration, and phytoplankton production. A summary of each of these analyses follows, with details presented in Appendices I, J, and K.

Watershed flow and water quality regressions

Background

To characterize freshwater constituent inputs into SSM, we used regression models to estimate daily-scale water quality from discrete monthly data. These regressions relate constituent concentrations to flow patterns and time of year, based on methods established by Cohn et al. (1989, 1992) and adapted by Mohamedali et al. (2011). We developed regression models for 12 distinct water quality parameters, including temperature, DO, pH, ammonium-ammonia, nitrate-nitrite, TPN, DTPN, orthophosphate, total phosphorus, DTP, DOC, and TOC. Out of 193 SSM watersheds, 76 had sufficient data to establish regressions. For these 76 watersheds, most had data for 9 or 10 of the 12 water quality parameters, resulting in a total of 750 regression models. A more detailed description of the regression methods is provided in Appendix B1: Water Quality Regressions.

Regression performance was evaluated for all 12 parameters by comparing constituent predictions against discrete monthly data (see “Regression performance on discrete data” for a brief overview or Appendix B1 for more detail). For nitrate-nitrite, an entirely independent data set separate from the one used to train the regression models was used for additional validation. The additional performance evaluation for nitrate-nitrite was conducted for four watersheds (Nooksack, Puyallup, Skagit, and Snohomish) with coincident monitoring locations to those used in our regressions. A brief overview of nitrate-nitrite performance for these four watersheds is discussed in the “Inorganic nitrogen regression performance on continuous data” section, and a more detailed discussion is provided in Appendix B4.

Regression performance on discrete data

Regression performance was determined primarily using Normalized Root Mean Square Error (NRMSE), R-Squared, and, to a lesser extent, normalized bias. Near-perfect model performance would be characterized by an R-squared value approaching 1, indicating a strong correlation between predicted and observed values, and an NRMSE close to zero, reflecting minimal total error. An NRMSE of 1 or greater signals a less representative estimate than the mean of observations (Jolliff et al. 2009; USECos Team 2008). We employed a conservative NRMSE threshold of 0.894, instead of 1, to segregate between acceptable and unacceptable model performance. This threshold was based on an internal review of an extensive number of time series performance plots, which indicated a breakdown in performance above an NRMSE of 0.894.

In total, we fit 750 regression models for SSM watersheds, with 11% exhibiting an NRMSE exceeding 0.894. For most variables, with the exception of ammonium, pH, and total phosphorus, regressions exhibited good performance with R-squared values ranging from 0.6 (total organic carbon) to 0.87 (temperature). NRMSE statistics followed an almost identical trend to R-squared, with ammonium, pH, and total phosphorus regressions performing adequately, though with lower skill (NRMSE ranged from 0.67 to 0.61) than other parameters. DOC, dissolved total phosphorus, DO, DTPN, and temperature regressions performed really well

with NRMSE ranging from 0.53 to 0.35, respectively (Figure 11). Ammonium-ammonia tended to perform the worst relative to other parameters, with an average NRMSE of 0.672 and average R-squared of 0.52 (Figure 11).

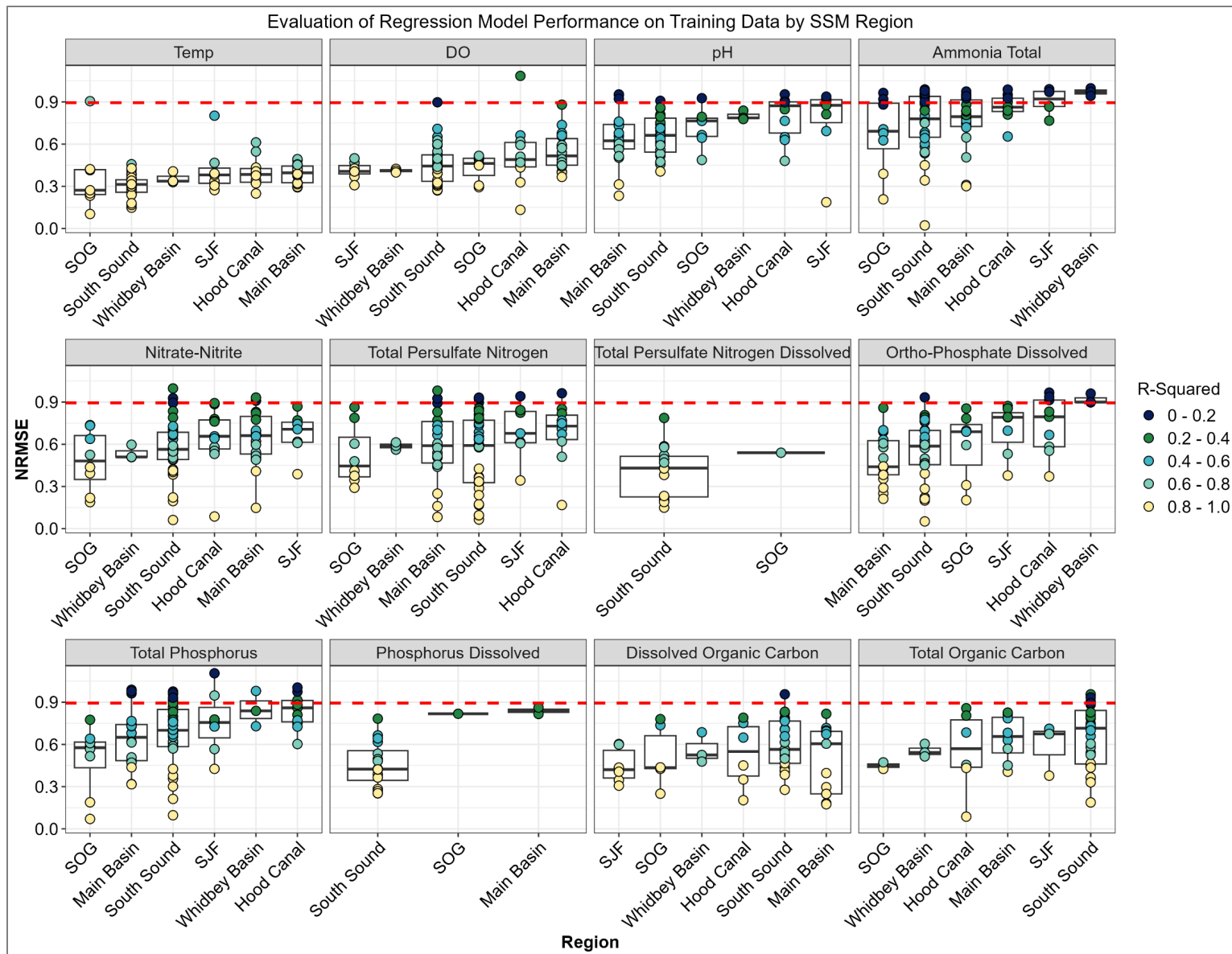


Figure 11. Diagnostic plots of model performance on the training data set for all variables for watersheds in different SSM basins.

Inorganic nitrogen regression performance on continuous data

In addition to the discrete data used for regression validation previously discussed, regression performance for nitrate-nitrite was also evaluated using Ecology's Freshwater Monitoring Unit's continuous Submersible Ultraviolet Nitrate Analyzers (SUNA) observations near the mouth of major Puget Sound watersheds. These SUNA locations are the same locations where discrete monthly monitoring data used to fit the regressions were collected, but the SUNA observations are entirely independent data for testing that were not used for training the regressions.

Evaluation locations included Nooksack, Puyallup, Skagit, and Snohomish Rivers. For these four rivers, we compared regression-predicted nitrate-nitrite concentrations and loads with SUNA observations. At these rivers, continuous flow data and SUNA nitrate-nitrite data sets we obtained span from either July or August 2023 to October 2024, with the exception of the Puyallup, where data spanned from November 2023 to October 2024.

Nitrate-nitrite regression performance was good for all four of the watersheds assessed. Regression predictions in all four watersheds are less variable on a daily time scale than SUNA measurements. This is likely due to the resolution of the data used to fit the regressions, which consisted of discrete monthly observations and daily average flows corresponding to the day of measurement. As shown in Figure 12, nitrate-nitrite regression predictions explained 72% (Snohomish) to 86% (Nooksack) of the variance in the observed data based on R-squared values and had NRMSE values ranging from 0.4 (Nooksack) to 0.55 (Snohomish). The combination of low NRMSE values and high R-squared values indicates that the regressions are adequately representing nitrate-nitrite in these four watersheds. Overall, the regressions appear to be capturing general seasonal trends well but struggle with short-term sporadic events.

Regression performance was also assessed for different flow conditions using 24 years of gage data (1999 – 2023) for each of the four watersheds. We evaluated performance for high flow conditions (90th percentile or greater flows), low flow conditions (10th percentile or lower flows), and normal flow conditions (everything else). Regression performance was found to be good for all flow conditions at all locations except low flow conditions at Snohomish and Skagit. We found that Snohomish nitrate-nitrite regression was fit on monthly data that, on average, had higher values and a greater range (minimum to maximum) of values than the continuous SUNA data. This seems to explain the overpredictions occurring during low flow conditions in Snohomish from September 1st to October 1st in 2023 and 2024 (Figure 11). Similarly, the regression for Skagit was trained on data with a much higher minimum value than the continuous SUNA data, but had a lower average and maximum. This is consistent with Skagit predictions in Figure 11, which alternate from overpredicting to underpredicting during low flow conditions between September 1st and November 1st, 2023, and mid-September and October 1st, 2024.

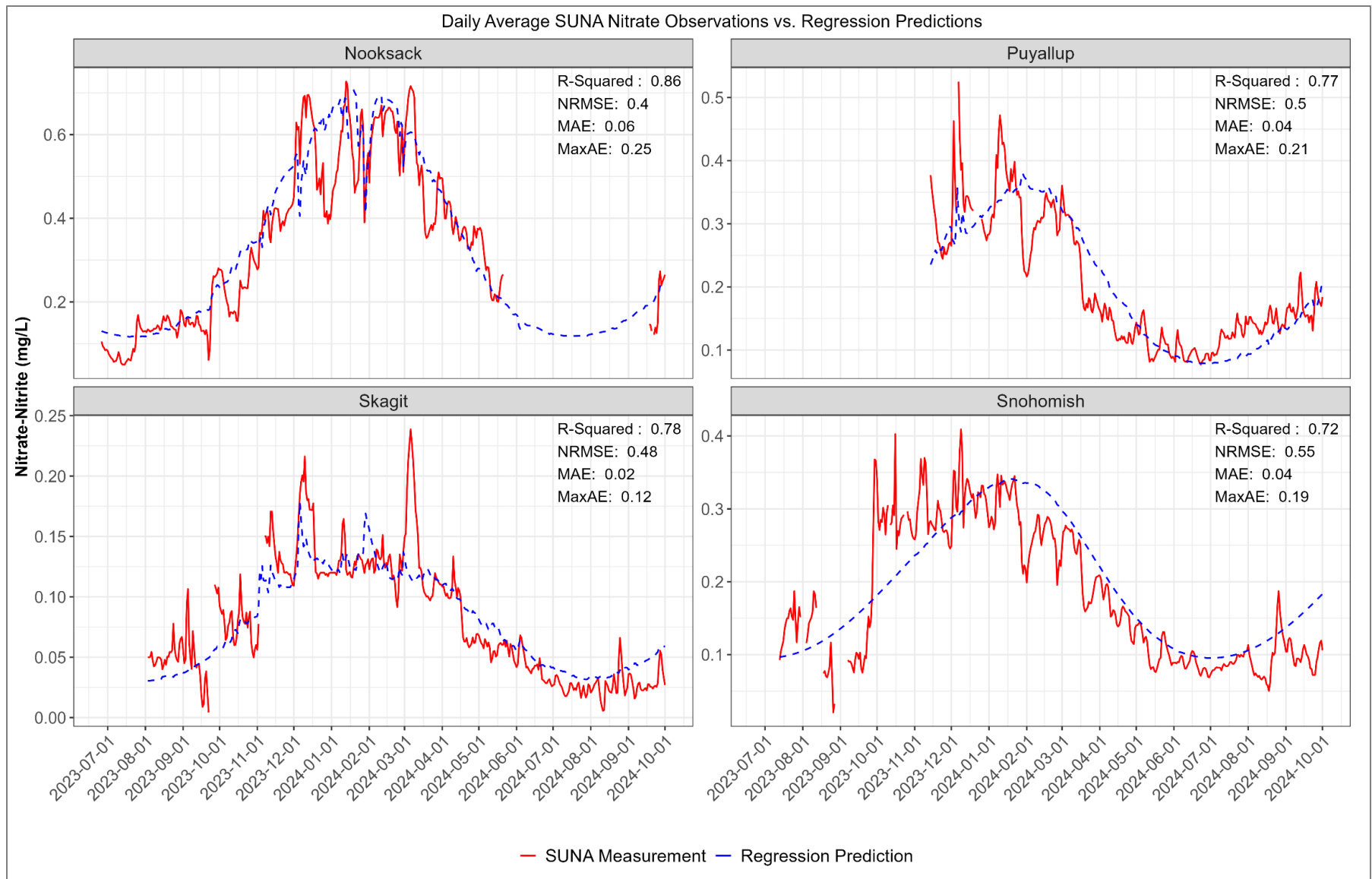


Figure 12. Comparison of continuous SUNA nitrate-nitrite data with regression predictions at four major Puget Sound watersheds.

We also compared regression-predicted and SUNA observed monthly average nitrate-nitrite loads to determine how well predicted values captured seasonal patterns. For all watersheds, except for Snohomish, the same gage flow data were used for both predicted and observed loads. Predicted and observed loads were similar for most months, with notable discrepancies in June – July for Nooksack, February, April, and July for Puyallup, July for Skagit, and September to October for Snohomish (Figure 13). Performance was strong across all flow regimes for Nooksack and Puyallup, although Puyallup performed slightly worse during high flow, while Skagit and Snohomish showed larger discrepancies during low flow periods, consistent with the concentration analysis. For a more detailed overview of the regression evaluation, see Appendices B1 and B4.

Hydrodynamics

For this study, we used a relatively newer version of FVCOM (FVCOM2.7d) than the one used in Ahmed et al. (2019, 2021). This newer version enables the use of distributed bottom friction as employed by Khangaonkar et al. (2021a). As discussed in Appendix A, we compared constant and spatially variable bottom friction using FVCOM2.7d, and the distributed bottom friction gave better estimates of observed water surface elevation. As discussed in Appendix B, in addition to watershed inflow updates, we also changed open boundary tidal constituents using an updated Eastern North Pacific (ENPAC 2015) database (Szpilka et al. 2018).

Given the updated version of the hydrodynamic model used in this study, including variable bottom friction, updated tidal constituents at the open boundary, and the updated watershed inputs to the model, we checked calibration against observed water surface elevations and tidal currents. Observed water surface elevation data are available at seven NOAA stations for the years 2000, 2006, 2008, and 2014 (Figure 14).

Results comparing predicted and observed water surface elevations are presented in Appendices E, F, G, and H for years 2000, 2006, 2008, and 2014, respectively. Results show that there was an improvement in predicting observed water surface elevations compared to Ahmed et al. (2019) by an average RMSE of 5% in 2006 and 2008 and 2% in 2014 (year 2000 was not modeled by Ahmed et al. (2019), so there was no equivalent comparison). All RMSEs in 2014 for water surface elevations were below 50 cm. All RMSEs in 2006 and 2008 for water surface elevations were at or below 50 cm. Figure 15 shows a typical scatterplot and time series plot at NOAA's Seattle station.



Figure 14. NOAA water surface elevation observation stations.

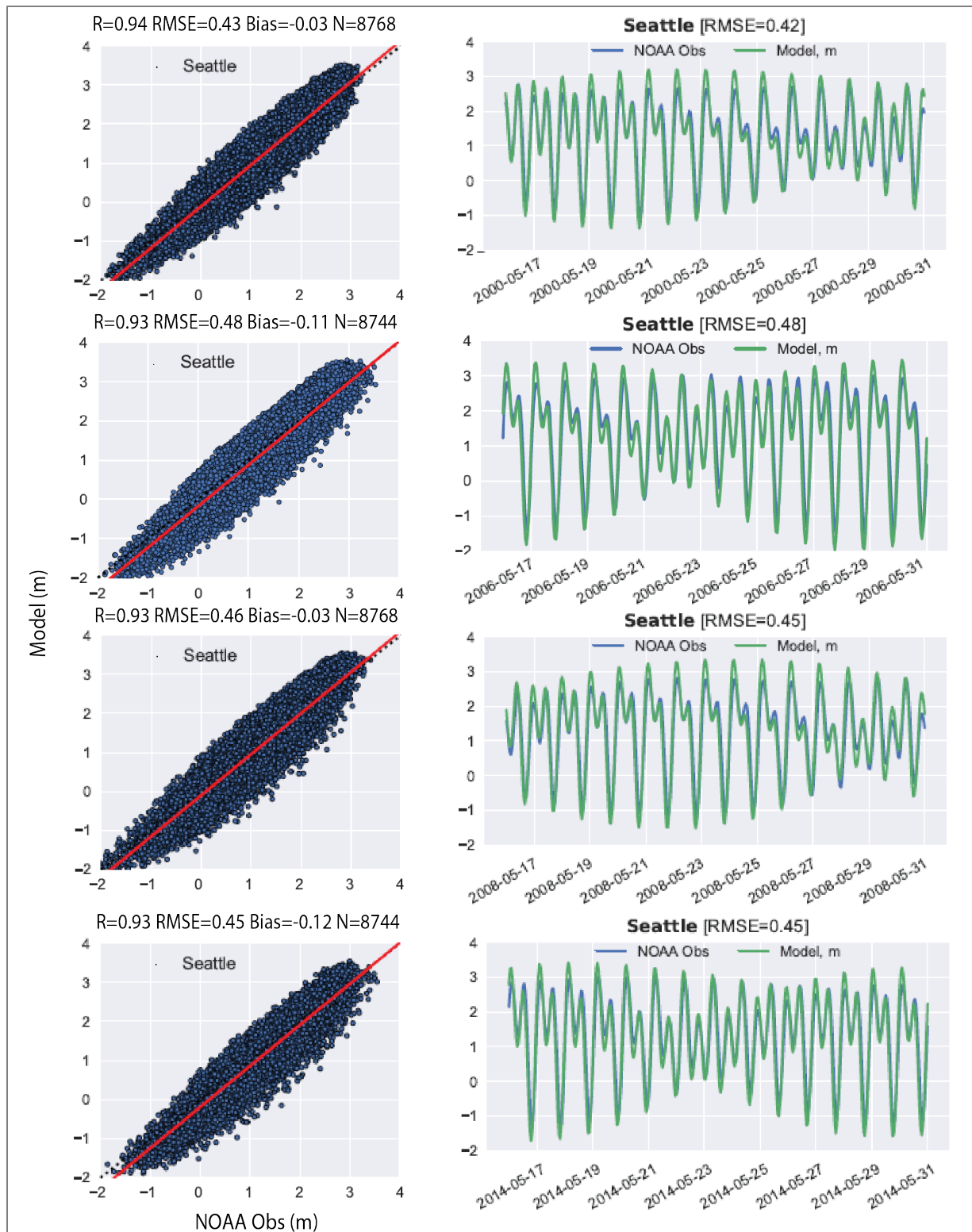


Figure 15. Model predictions and observed data for water surface elevations.

Left panel, typical scatterplots for 2000, 2006, 2008, and 2014. Red lines are regression lines, while dotted lines are 1:1 lines. Right panel, time series for the selected time interval in 2000, 2006, 2008, and 2014.

We also compared predicted and observed tidal currents. Two stations were available with observed current data for the year 2006 only (Roberts et al. 2014a, see Figure 16 below). Predicted current velocities were compared with observed data at these two stations. Results are presented in Appendix F. The average RMSE in predicted current velocity in this study was 26% better than those reported in Ahmed et al. (2019). Figure 17 shows the depth-averaged time series plot of predicted and observed eastward (U, cm/s) and northward (V, cm/s) currents at Dana and Pickering Passages.



Figure 16. Location of stations where currents were measured in 2006.

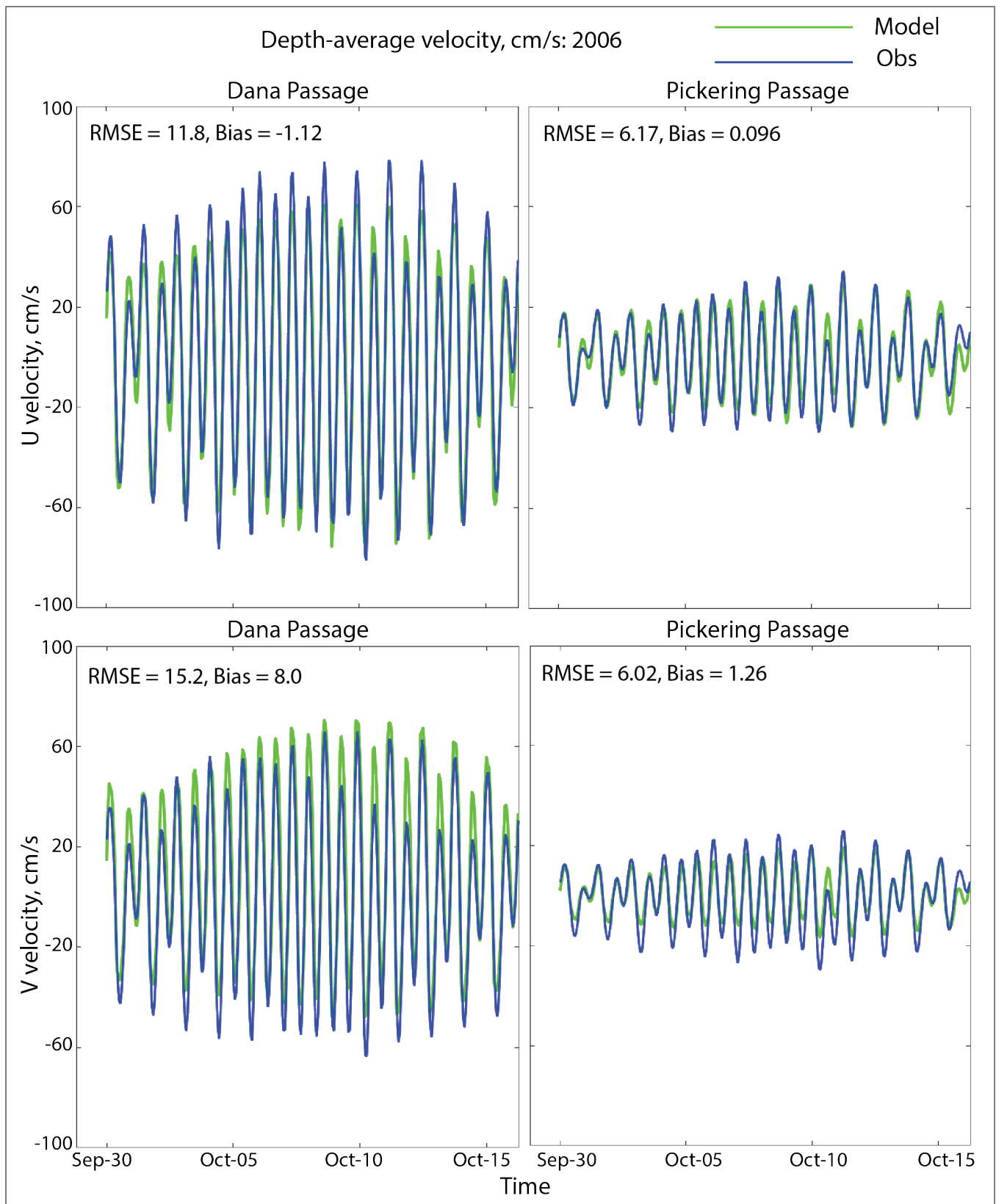


Figure 17. Eastward (U velocity, top panel) and northward (V velocity, bottom panel) depth-averaged current comparison between model prediction and observed data for Dana Passage (right panel) and Pickering Passage (left panel).

Water quality

Model performance water quality objectives for SSM applications, described in the QAPP (McCarthy et al. 2018), were met. We applied quantitative and qualitative methods to determine model skill and to determine how well the model approximates the real system. We used statistics for goodness-of-fit as well as visual comparison of predicted and observed time series and depth profiles. We calculated eleven different statistical skill metrics, including typical comparative goodness-of-fit metrics such as bias, correlation coefficient, and RMSE. Appendix D contains equations for statistical metrics used in computations.

Qualitative review of water quality performance

Recent Salish Sea modeling studies point to variations in residence times and flushing rates at various locations within Puget Sound (MacCready et al. 2021; Premathilake and Khangaonkar 2022; this work, Appendix M), which are modulated by oceanic, Puget Sound estuarine scale, basin scale, and local dynamics. SSM is responsive to processes at each of these scales (Khangaonkar et al. 2011, 2017, 2018), and so we expect to see predicted SSM temporal trends reflective of trends from continuous water quality observations, which capture the effects of drivers at multiple scales.

Northwest Environmental Moorings (NWEM), a group affiliated with the University of Washington (UW), uses the Oceanic Remote Chemical Analyzer (ORCA) autonomous moored profiling systems to produce real-time continuous data streams of multiple water quality variables. These data are valuable because they provide water quality trends at selected locations over broader time periods and can therefore contribute insights into processes and timescales that play a role in local DO dynamics. The data are provided with a disclaimer that states that the data have been automatically processed and not validated, so the data are preliminary. Our SSM applications QAPP (McCarthy et al. 2018) precludes us from using unvalidated or preliminary data in a quantitative sense, but we can use it for qualitative comparisons.

Figure 18 shows DO surface and bottom layer predictions compared to available NWEM observations for 2014 at four embayment locations. These observations are completely independent of the data used for SSM calibration.

Visual comparison of trends at these four embayment stations located in Carr Inlet, Hood Canal (Hoodsport and Twanoh), and Dabob Bay shows congruence in patterns and overall magnitudes between modeled and observed data. Surface layers, particularly at Carr Inlet, produce highly variable DO concentrations often in response to finer-scale biological and physical events, which the model cannot reproduce. Algal blooms can create large diel fluctuations, at times resulting in supersaturated DO conditions at the surface. The model does not reach the DO observational peaks and lows at the surface, but SSM predictions fall well within the range of surface DO observations.

The model captured variations in observed data for bottom layers well at all locations except Twanoh in the fall of 2014, when predictions trended higher, and observations trended towards

lower DO. In areas of reduced advective transport and horizontal diffusion, vertical mixing, which promotes oxygenation, can be limited below the pycnocline (Peña et al. 2010). Predicted temperature was about one degree Celsius higher than observed at Twanoh during that period, which can result from the model overshooting vertical mixing in mid-September and allowing warmer water and higher DO concentrations from an upper layer to mix with bottom waters sooner than when DO levels started increasing towards the end of October.

Overall, this qualitative comparison with independent, high-resolution temporal observational data provides evidence that SSM predictions realistically simulate DO trends at these locations.

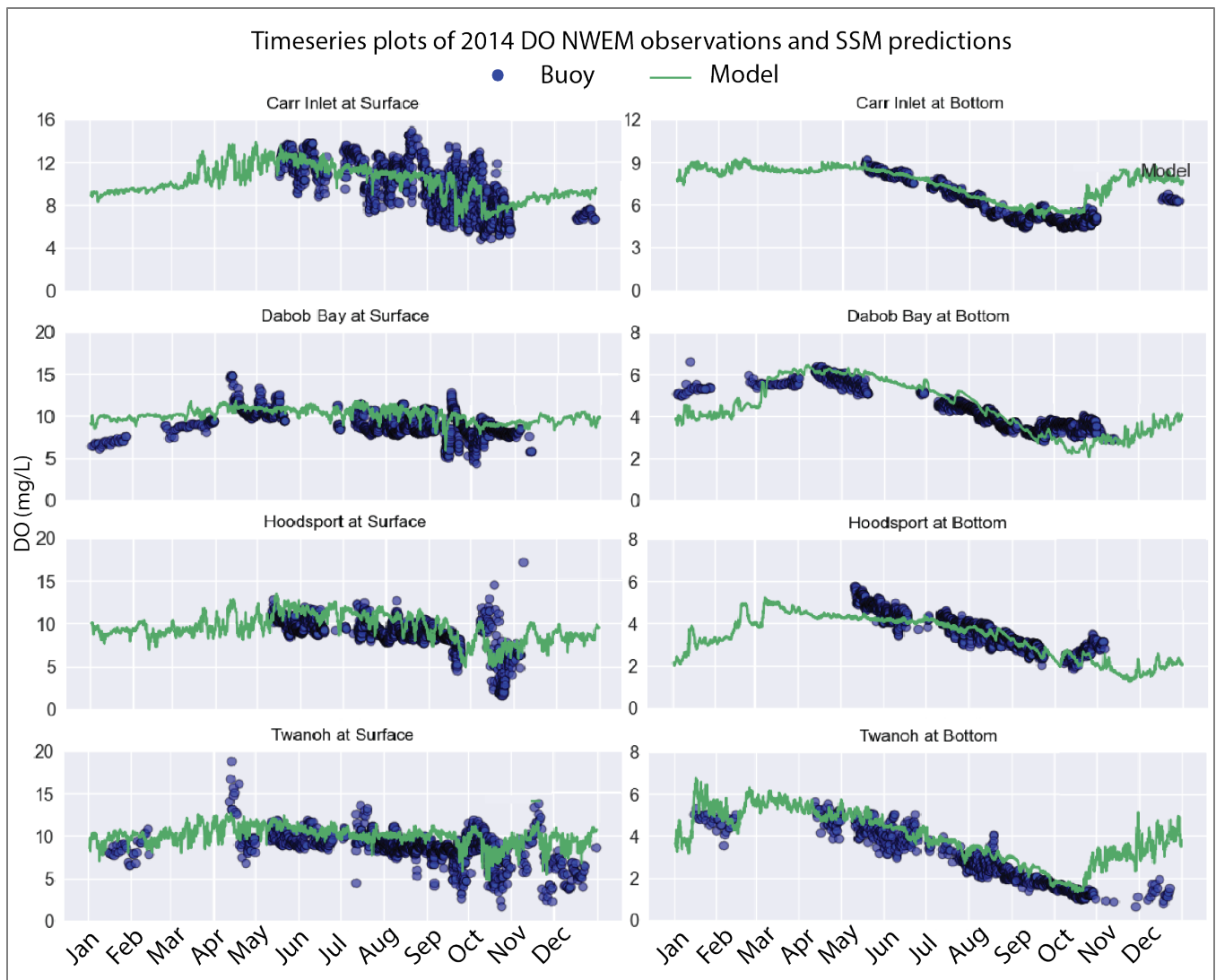


Figure 18. Time series plots of 2014 dissolved oxygen (DO) surface and bottom NWEM observations and SSM predictions.
 NWEM observations are collected via moored profiling systems.

Quantitative review of water quality performance

Appendices E-H contain comprehensive visualizations of predicted versus quality-assured observed data (for the years 2000, 2006, 2008, and 2014, respectively), including scatterplots for predicted water quality parameters, time-depth plots, time series for each station and parameter for the top and bottom layers, and vertical depth profiles for each parameter. These plots also include corresponding goodness of fit statistics. In addition, we segregated DO data into surface, middle, and bottom waters to understand model performance differences between vertical layers. We also segregated stations into inlets and open channel locations to ascertain whether there are differences in model performance between these station types. Time series and profile plots at selected sites are presented below for 2014, which will be the year used as the basis for the PSNRP (Ecology 2025).

Time series plots

Figures 19, 20, and 21 show time series plots for temperature, salinity, and DO for observed and predicted data at the surface and bottom layers for 2014 at selected stations in South Puget Sound (Ecology station DNA001 in Dana Passage), Central Puget Sound (King County station KSBP01), Hood Canal (Ecology station HCB003), Admiralty Inlet (Ecology station ADM001), and Bellingham Bay (Ecology station BLL009). For station BLL009, layer 3 (near surface) and layer 8 (middle) were used as these layers had the most data. Specific error statistics for each station are also included in the plots. Time series plots for all stations for the years 2006, 2008, and 2014 are presented in Appendices E through H, respectively.

In general, model performance, as measured by RMSE, is better for the bottom layer relative to the surface layer. The distinct temperature, salinity, and DO difference between the surface and bottom layer is well predicted by the model, particularly at stations HCB003 and KSBP01. The observed hypoxia at HCB003 is also simulated by the model.

Profile plots

Figures 22, 23 and 24 show observed and predicted profile plots for temperature, salinity, and oxygen for 2014 at selected stations in South Puget Sound (Ecology station DNA001 in Dana Passage), Central Puget Sound (King County Station KSBP01), Hood Canal (Ecology station HCB003), Admiralty Inlet (Ecology station ADM003), and Bellingham Bay (Ecology station BLL009). Specific error statistics for each station are included for each of the profile plots. These figures also show that the model does a good job of simulating the thermocline, halocline, and oxycline at the respective stations. Station HCB003, in Hood Canal, has a relatively pronounced stratification compared to other stations. Profile plots for all stations and for the years 2000, 2006, 2008, and 2014 are presented in Appendices E through H, respectively.

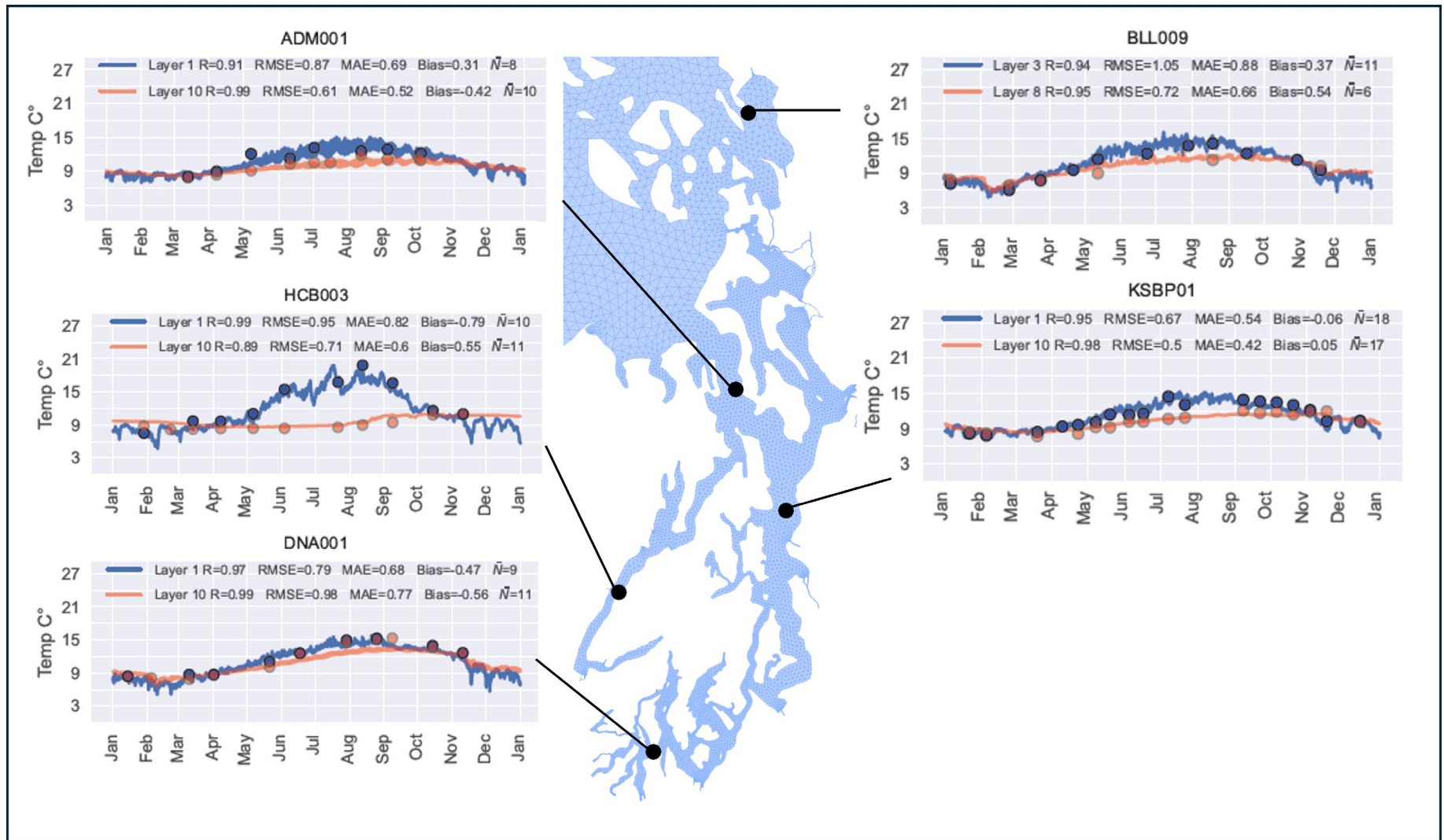


Figure 19. Time series plots for temperature (°C) at the surface (blue) and bottom (red) at selected stations for 2014. Circles show observations. For station BLL009, layer 3 (near surface) and layer 8 (middle) were used as these layers had the most data. Stations: Admiralty Inlet (Ecology station ADM003), Bellingham Bay (Ecology station BLL009), Hood Canal (Ecology station HCB003), Central Puget Sound (King County Station KSBP01), and South Puget Sound (Ecology station D001 in Dana Passage).

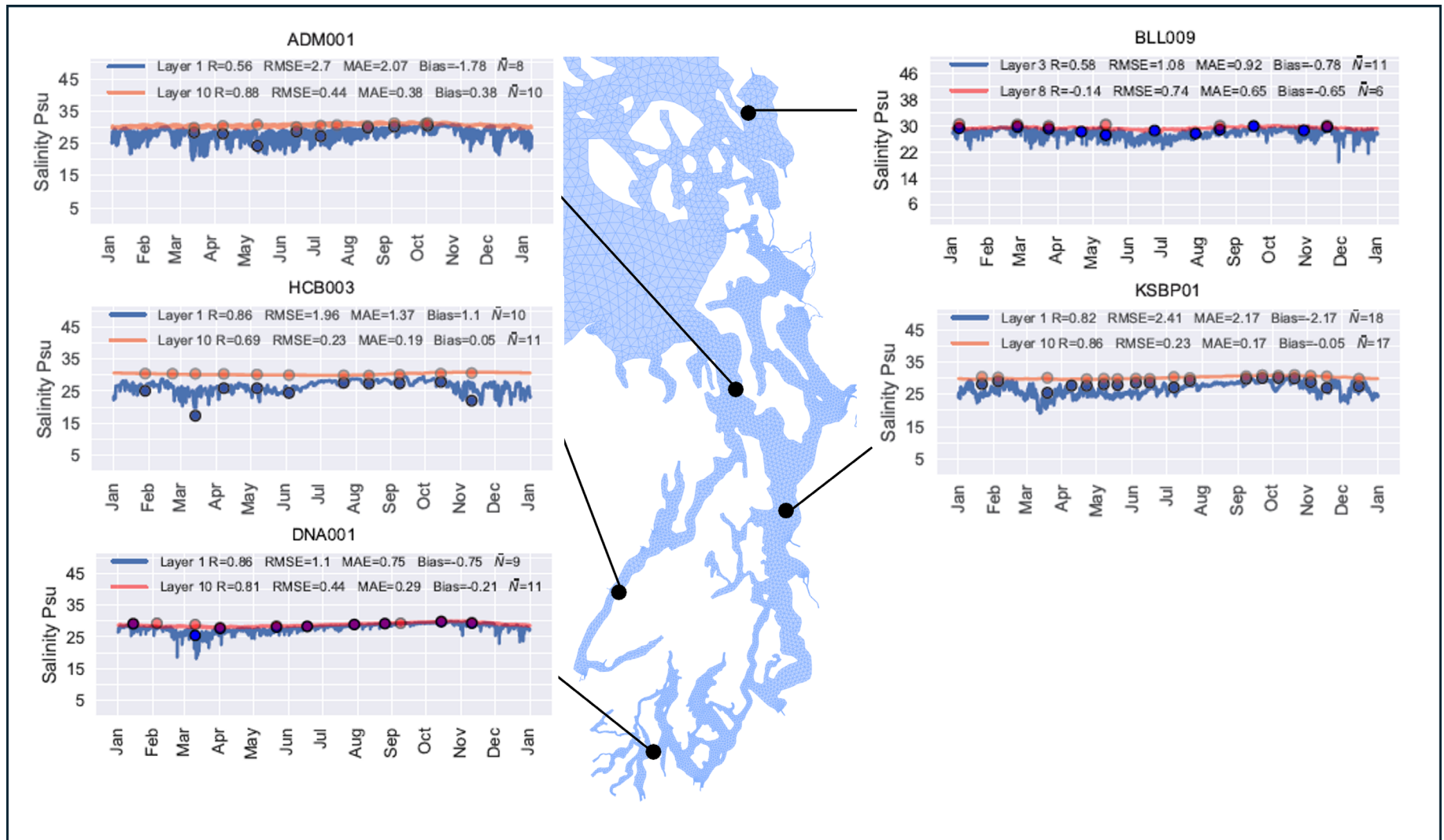


Figure 20. Time series plots for salinity (psu) at the surface (blue) and bottom (red) at selected stations for 2014.

Circles show observations. For station BLL009, layer 3 (near surface) and layer 8 (middle) were used as these layers had the most data. Stations: Admiralty Inlet (Ecology station ADM003), Bellingham Bay (Ecology station BLL009), Hood Canal (Ecology station HCB003), Central Puget Sound (King County Station KSBP01), and South Puget Sound (Ecology station D001 in Dana Passage).

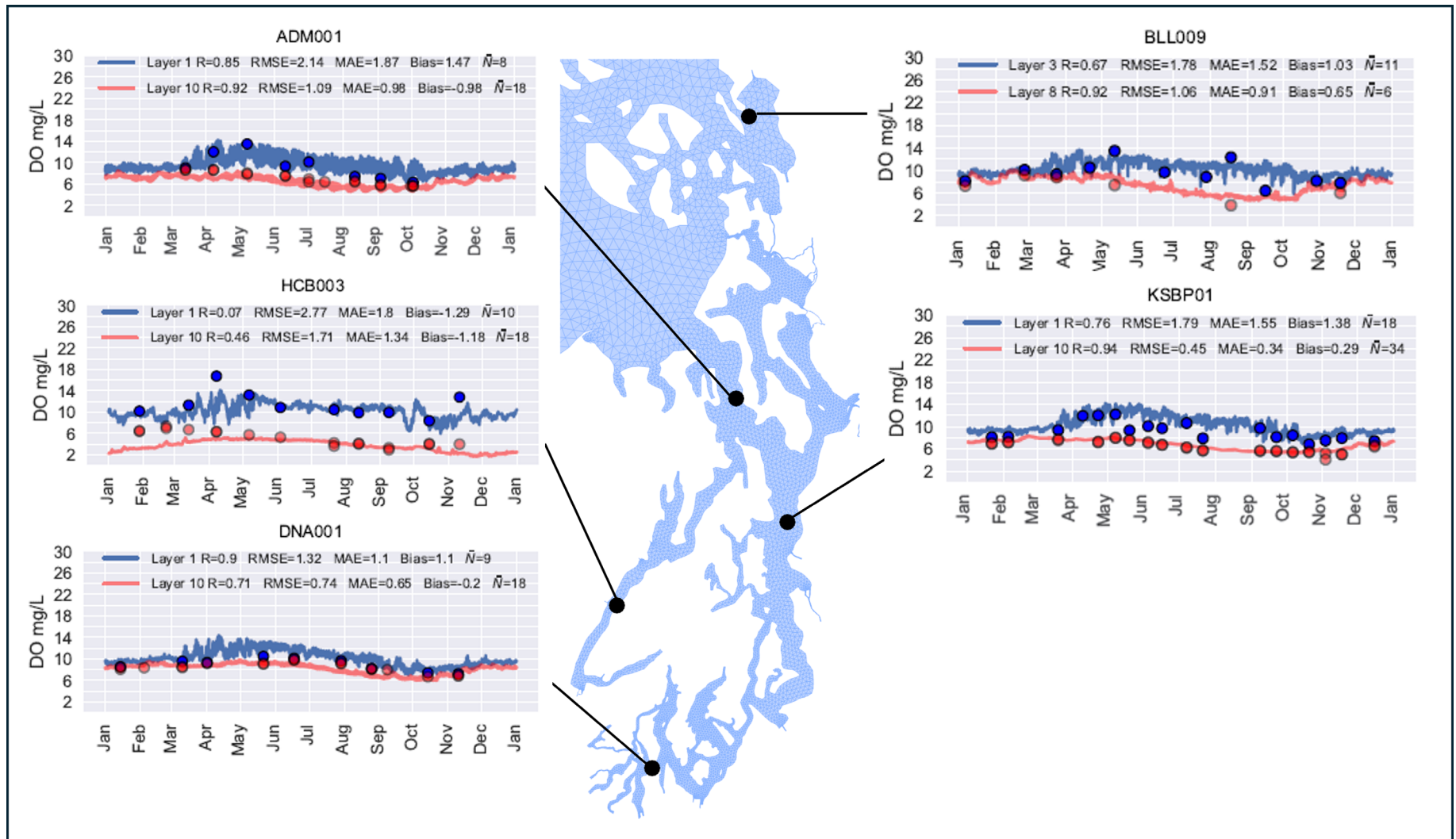


Figure 21. Time series plots for dissolved oxygen (DO, mg/L) at the surface (blue) and bottom (red) at selected stations for 2014. Circles show observations. For station BLL009, layer 3 (near surface) and layer 8 (middle) were used as these layers had the most data. Stations: Admiralty Inlet (Ecology station ADM003), Bellingham Bay (Ecology station BLL009), Hood Canal (Ecology station HCB003), Central Puget Sound (King County Station KSBP01), and South Puget Sound (Ecology station D001 in Dana Passage).

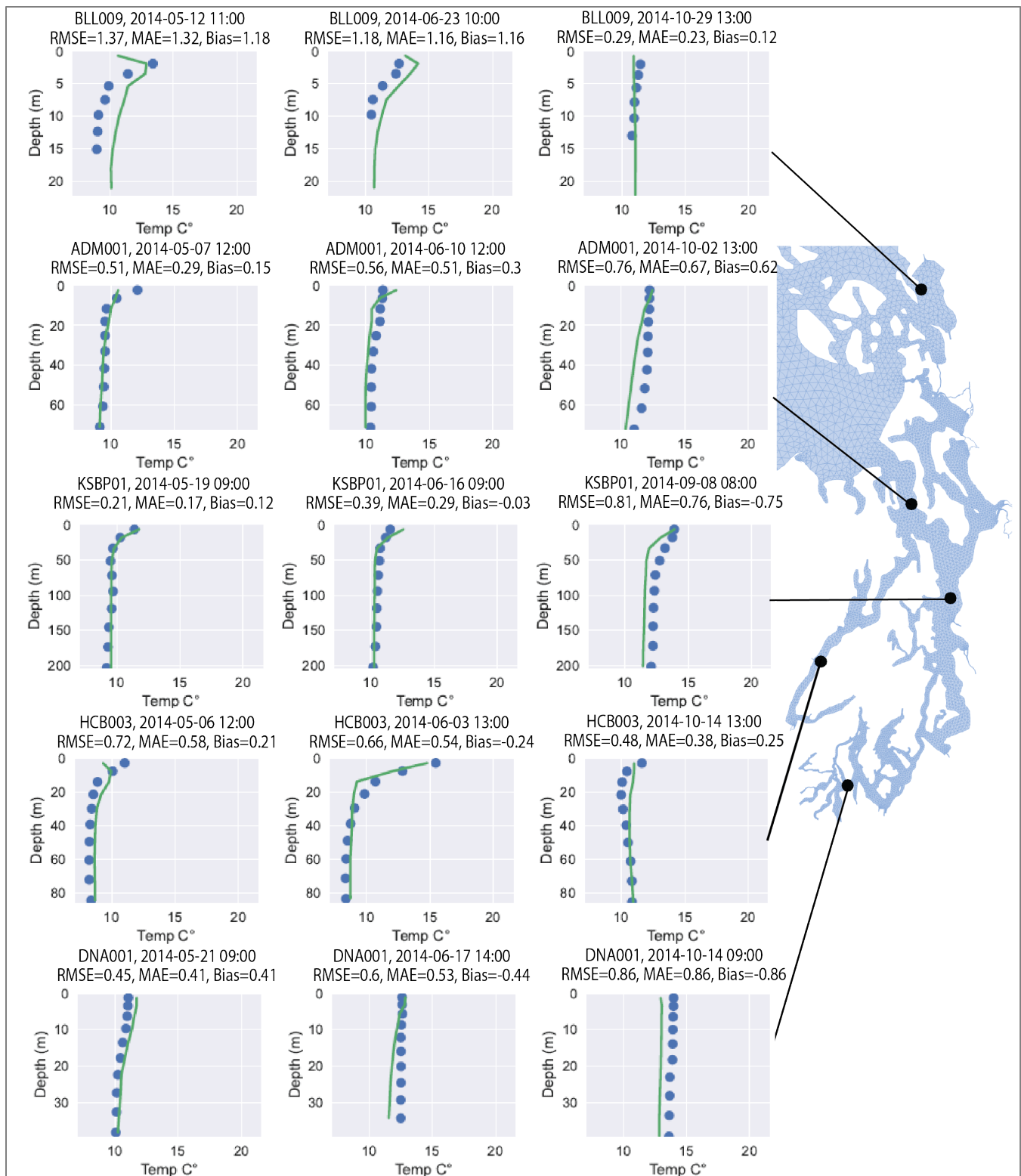


Figure 22. Year 2014 temperature profiles (°C) at selected stations for spring (left column), summer (center column), and fall (right column) conditions.

Circles show observations. Top row: Bellingham Bay (Ecology station BLL009). Second row: Admiralty Inlet (Ecology station ADM003). Third row: Central Puget Sound (King County Station KSBP01). Fourth row: Hood Canal (Ecology station HCB003). Fifth row: South Puget Sound (Ecology station D001 in Dana Passage).

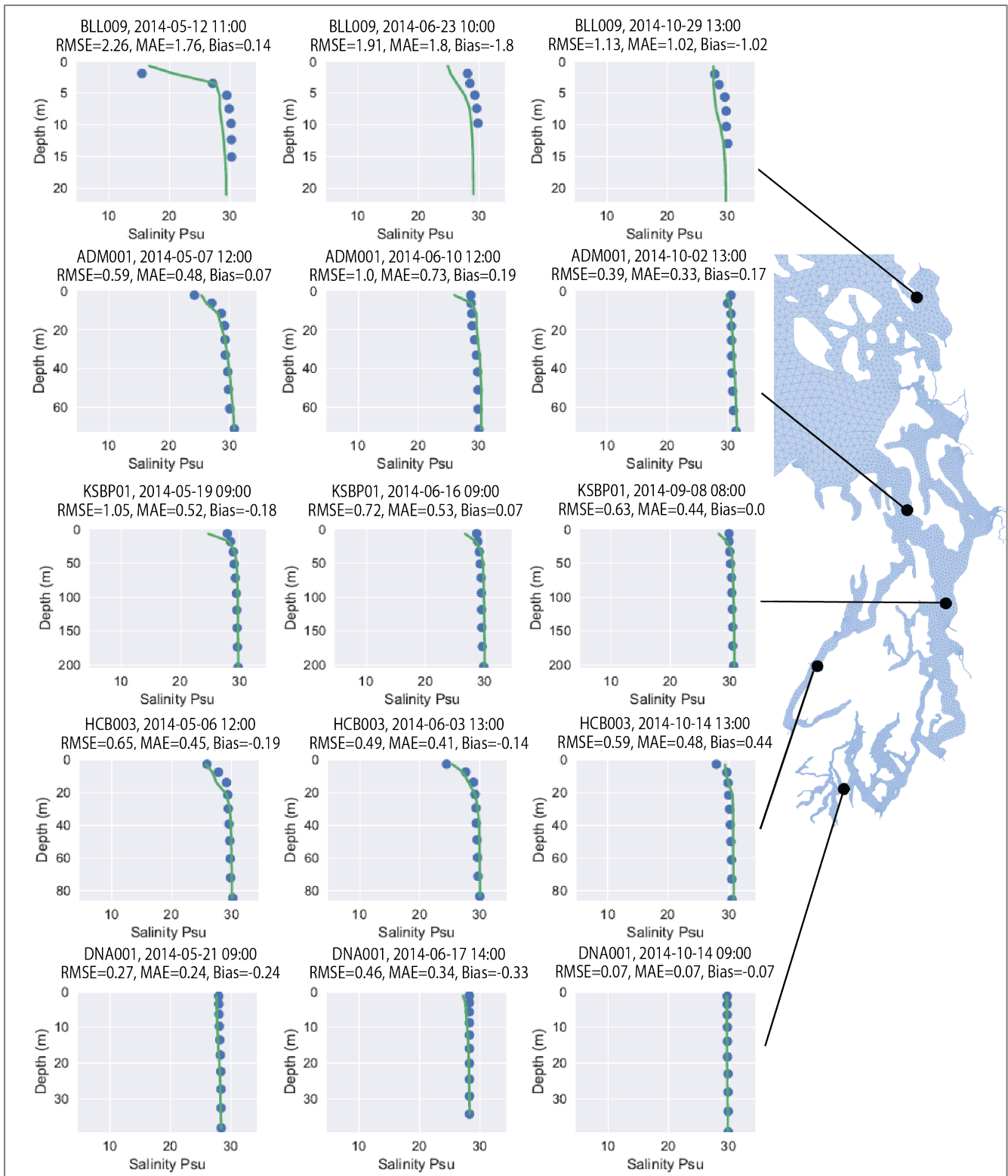


Figure 23. Year 2014 salinity profiles at selected stations for spring (left column), summer (center column), and fall (right column) conditions. Circles show observations. Top row: Bellingham Bay (Ecology station BLL009). Second row: Admiralty Inlet (Ecology station ADM003). Third row: Central Puget Sound (King County Station KSBP01). Fourth row: Hood Canal (Ecology station HCB003). Fifth row: South Puget Sound (Ecology station D001 in Dana Passage).

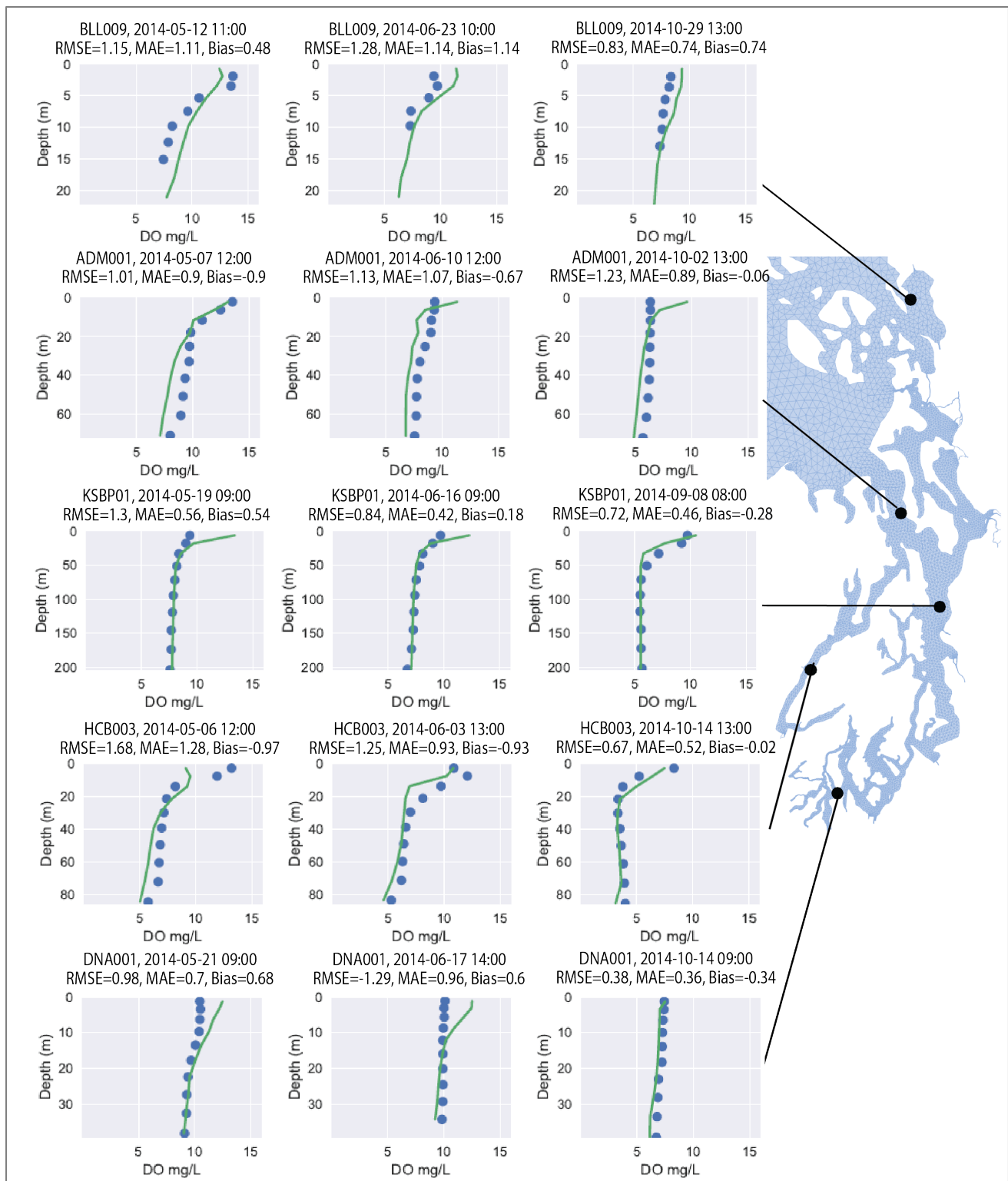


Figure 24. Year 2014 dissolved oxygen (DO, mg/L) profiles at selected stations for spring (left column), summer (center column), and fall (right column) conditions. Circles show observations. Top row: Bellingham Bay (Ecology station BLL009). Second row: Admiralty Inlet (Ecology station ADM003). Third row: Central Puget Sound (King County Station KSBP01). Fourth row: Hood Canal (Ecology station HCB003). Fifth row: South Puget Sound (Ecology station D001 in Dana Passage).

Taylor and target plots

We use Taylor (Taylor 2001) and target (Jolliff et al. 2009) diagrams to coalesce, summarize, and communicate the results of the water quality model performance evaluation. These plots are used widely in comparative analyses of mechanistic models and observational data.

Both Taylor and target diagrams illustrate the centered (or unbiased) RMSE normalized by the standard deviation of the observations. A perfect model (and no model is perfect) would have zero normalized centered RMSE. The target diagrams also show the normalized bias (bias divided by the standard deviation of the observations). Target diagrams include a unit circle. Any points inside the unit circle identify when the model is performing better as a predictor than the mean of the observational data, while points outside the unit circle are instances when using the observational data mean would have performed better than the model. In the target plot, the negative region of the x-axis is utilized to show that the model standard deviation is smaller than the observed (Jolliff et al. 2009).

On the other hand, the Taylor diagrams illustrate the correlation coefficient and the predicted standard deviation normalized by the observed standard deviation as well as the centered NRMSE. In the Taylor plot, distance from a normalized standard deviation curve of one indicates whether the model is under- or over-predicting the observations, whereas the distance from the horizontal axis indicates decreasing correlation with observations.

Figure 25 shows Taylor and target plots for 2014 DO predicted and observed concentrations segregated by water column layers into three bins: (1) surface represents the top four SSM vertical layers or the top 25% of the water column; (2) middle represents SSM layers 5 – 8 or the middle 46% of the water column; (3) bottom represents SSM layers 9 – 10 or the bottom 29% of the water column. The target plot shows that all three vertical layer bins fall within the unit circle, signifying that the model skill for predicting surface, middle, and bottom DO concentrations is better than using the mean of the observations. Surface layer performance, though acceptable, exhibited lower model skill than that of the middle and bottom water predictions for 2014.

Figure 26 shows Taylor and target plots of DO predicted and observed concentrations in the bottom layer for all years, segregated by station type (within an embayment or open channel stations). Figure D-1 in Appendix D includes a map showing how each station is categorized. Model skill for predicting DO in bottom layers was similar across years; however, 2008 performed the best in terms of both open channel and embayment stations. Model skill in predicting bottom DO at embayment stations and open channel stations was similar, as shown in these Taylor and target plots and in the scatterplots in Figure 27. The correlations coefficients were high (between 0.8 and 0.9) for all segregated bottom layer DO sets, the NRMSEc (uRMSE) were 0.5 or less and the normalized standard deviation, the ratio of predicted and observed standard deviations, hovered around 1—indicating that, overall, SSM skill is high when predicting bottom water DO at embayment or open channel (or open estuary) stations

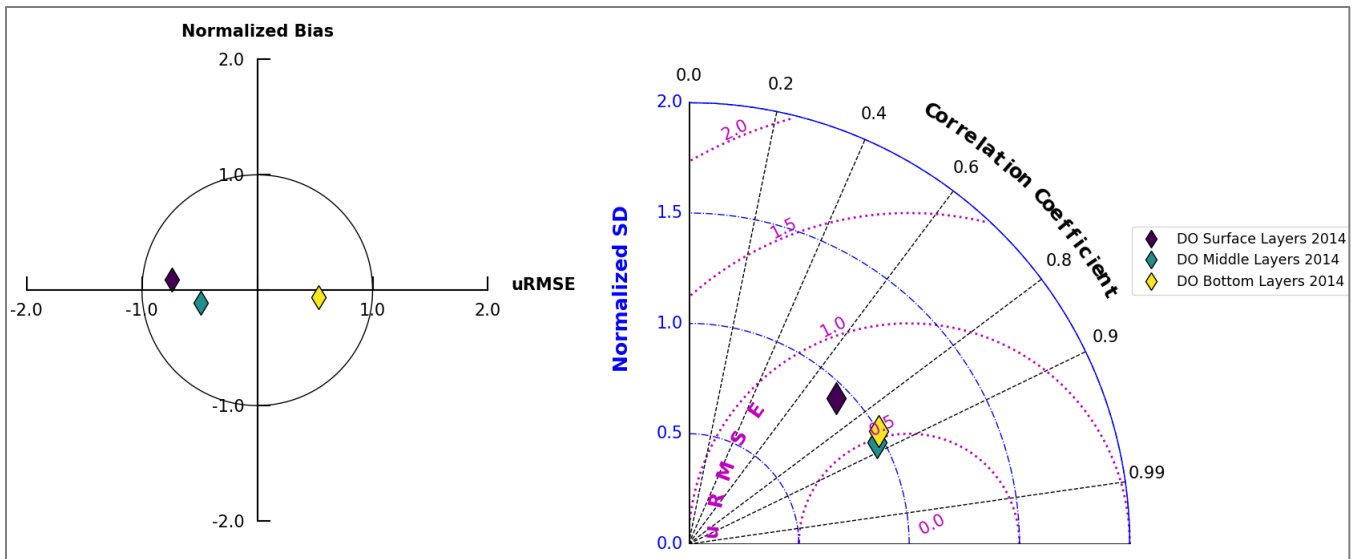


Figure 25. Taylor (right) and target (left) plots for 2014 predicted and observed dissolved oxygen (DO) concentrations.

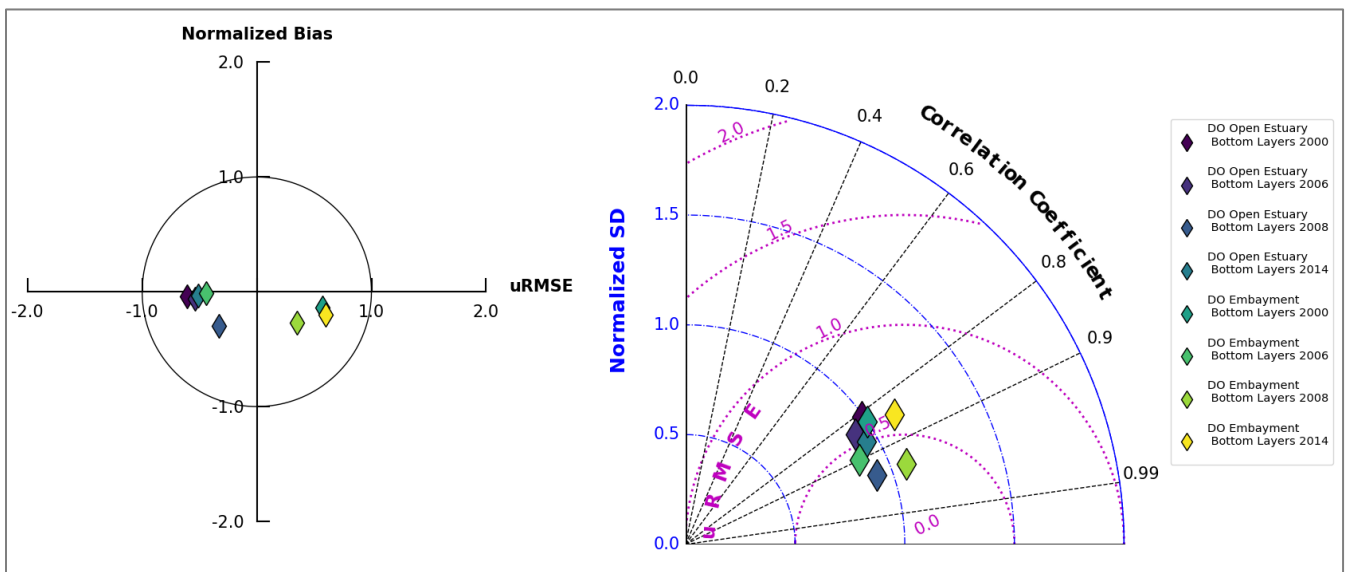


Figure 26. Taylor (right) and target (left) plots for bottom layers predicted and observed dissolved oxygen (DO) concentrations for all years (2000, 2006, 2008, and 2014) modeled. Segregated by observational station as either open estuary or embayment locations.

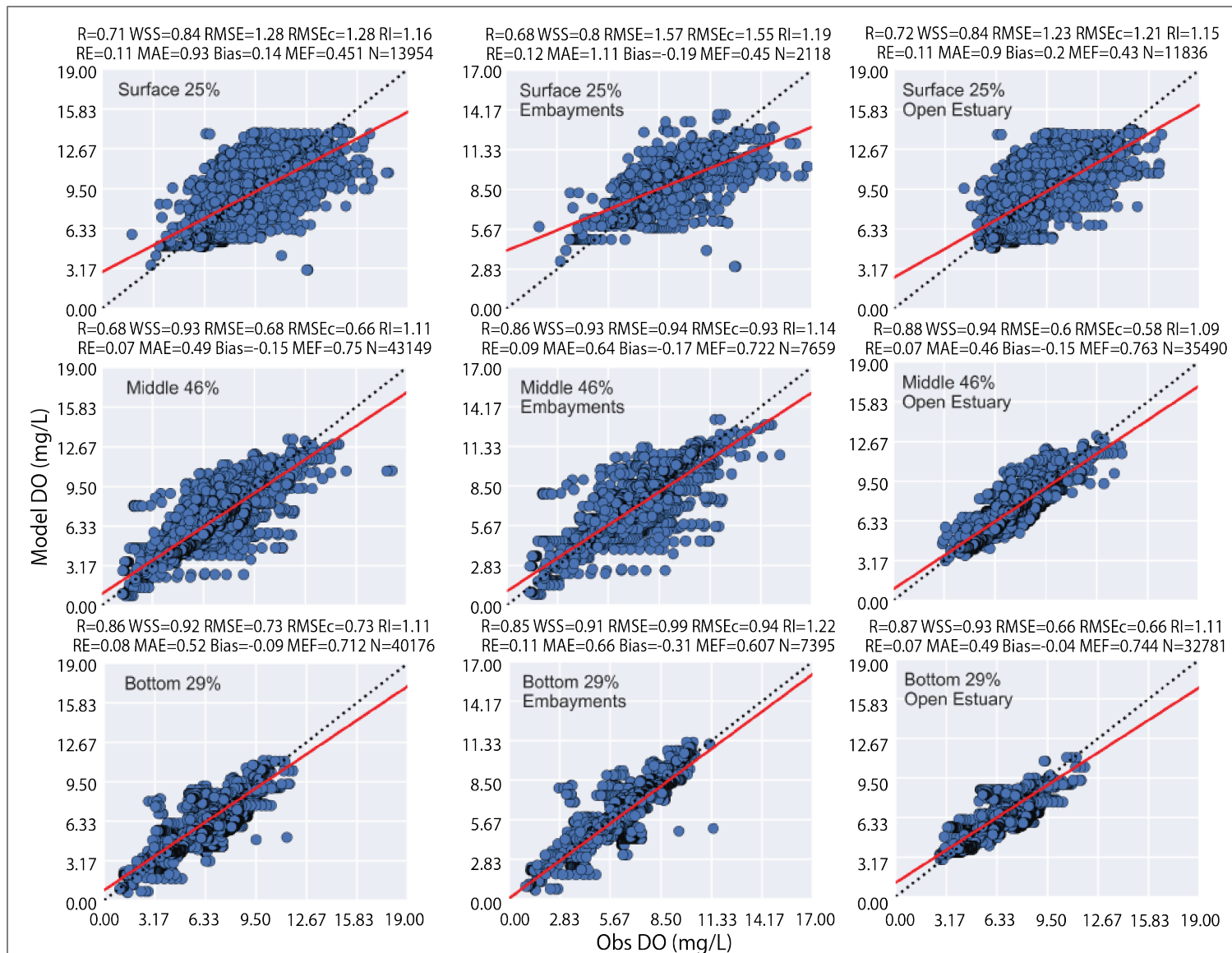


Figure 27. Dissolved oxygen (DO) scatterplots for surface, middle, and bottom layers segregated into embayments and open estuary stations in 2014.

The dotted line in the scatterplots is the 1:1 line. The red line is the regression line.

Summary of skill statistics

Tables 8 – 11 show a comparison of model skill statistics reported at different stages of the PSNSRP for each of the years that were modeled. Opt2 updates reported here resulted in higher skill in predicting DO than previous work.

Most of the data used for model skill evaluation is independent from the data used for model calibration. The first reported calibration for SSM, prior to any PSNSRP modeling, was conducted for 2006 with data from 15 Ecology monitoring locations (Khangaonkar et al. 2012), and the calibration that has served as a basis for all subsequent work was conducted with 21 stations for 2014 (Khangaonkar et al. 2018). In the BSR, Ahmed et al. (2019) checked that calibration with independent data from different years and more locations. For Opt1, Ahmed et al. (2021) identified more stations (82) for inclusion in model skill evaluation. In this work, we used the expanded set of stations from Ahmed et al. (2021).

The total number of data points reported changed as we produced each report for two reasons: we found and added more observational stations, and over the period, additional quality control and assurance of the data resulted in changes to the number of marine monitoring records in some Ecology stations. The source of the observational data for each station and the corresponding water quality parameters available are detailed in Table D-2 of Appendix D.

For all years modeled, temperature, salinity, DO, and nitrate-nitrite predictions are highly correlated with observations. For instance, in 2014, correlation coefficients between predictions and observations for these parameters fall between 0.8 and 0.9. Predictions for ammonium and chlorophyll-a exhibit lower correlation with observations. This may be due to sub-model scale biological phenomena, such as patchy algal growth increasing chlorophyll-a. In 2014, ammonium predictions show the lowest correlation coefficient (0.43), and temperature predictions exhibit the highest correlation coefficient (0.95), while chlorophyll-a and PAR correlation coefficients were 0.52 and 0.68, respectively.

For 2014, the model slightly underpredicts temperature, salinity, DO, nitrate-nitrite, and PAR and slightly overpredicts chlorophyll-a. Consequently, predicted parameters have a low absolute bias relative to the standard deviation of observations or normalized bias (0.1 or less), except for ammonium, which has a bias of 0.5 and a normalized RMSE of about 1. In summary for 2014, but this also generally applies to all years and across the different published works (BSR, Opt1 and Opt2), the model can predict temperature, DO, salinity, and nitrate/nitrite with higher skill compared to chlorophyll-a and PAR, and all those parameters with better skill than ammonium.

Table 8. Comparison of 2014 model performance for Bounding Scenarios, Opt1, and Opt2

| Report | Variable | R | WSS | RMSE | RMSE _c | RE | MAE | Bias | Sd _{obs} | N |
|--------|---|------|------|------|-------------------|------|------|-------|-------------------|--------|
| BSR | Temperature (°C) | 0.95 | -- | 0.87 | -- | -- | -- | -0.41 | -- | 88,781 |
| Opt1 | Temperature (°C) | 0.95 | 0.94 | 0.78 | 0.74 | 0.06 | 0.62 | -0.23 | -- | 97,687 |
| Opt2 | Temperature (°C) | 0.95 | 0.95 | 0.71 | 0.71 | 0.06 | 0.58 | 0.04 | 1.87 | 99,074 |
| BSR | Salinity (psu) | 0.75 | -- | 0.88 | -- | -- | -- | -0.37 | -- | 88,585 |
| Opt1 | Salinity (psu) | 0.82 | 0.87 | 0.84 | 0.71 | 0.02 | 0.51 | -0.44 | -- | 97,487 |
| Opt2 | Salinity (psu) | 0.83 | 0.90 | 0.72 | 0.72 | 0.01 | 0.39 | -0.07 | 1.13 | 98,884 |
| BSR | DO (mg/L) | 0.81 | -- | 0.96 | -- | -- | -- | -0.34 | -- | 87,284 |
| Opt1 | DO (mg/L) | 0.83 | 0.89 | 0.98 | 0.89 | 0.11 | 0.74 | -0.43 | -- | 96,152 |
| Opt2 | DO (mg/L) | 0.86 | 0.93 | 0.82 | 0.81 | 0.08 | 0.57 | -0.08 | 1.54 | 97,566 |
| BSR | Chl-a (µg/L) | 0.52 | -- | 3.48 | -- | -- | -- | -0.13 | -- | 88,895 |
| Opt1 | Chl-a (µg/L) | 0.52 | 0.67 | 3.42 | 3.42 | 0.71 | 1.41 | -0.11 | -- | 87,671 |
| Opt2 | Chl-a (µg/L) | 0.52 | 0.68 | 3.27 | 3.27 | 0.71 | 1.35 | 0.03 | 3.71 | 98,932 |
| BSR | NO ₃ -NO ₃ (N-mg/L) | 0.84 | -- | 0.07 | -- | -- | -- | 0 | -- | 1,848 |
| Opt1 | NO ₃ -NO ₂ (N-mg/L) | 0.84 | 0.90 | 0.07 | 0.07 | 0.15 | 0.05 | 0 | -- | 1,934 |
| Opt2 | NO ₃ -NO ₂ (N-mg/L) | 0.83 | 0.9 | 0.07 | 0.07 | 0.15 | 0.05 | -0.01 | 0.10 | 1,916 |
| BSR | NH ₄ ⁺ (N-mg/L) | 0.32 | -- | 0.02 | -- | -- | -- | 0 | -- | 1,510 |
| Opt1 | NH ₄ ⁺ (N-mg/L) | 0.35 | 0.56 | 0.02 | 0.02 | 0.58 | 0.01 | 0 | -- | 1,595 |
| Opt2 | NH ₄ ⁺ (N-mg/L) | 0.43 | 0.60 | 0.02 | 0.02 | 0.70 | 0.02 | 0.01 | 0.02 | 1,572 |
| BSR | PAR (E-m ² /day) | -- | -- | -- | -- | -- | -- | -- | -- | -- |
| Opt1 | PAR (E-m ² /day) | 0.61 | 0.66 | 6.00 | 5.94 | 0.78 | 1.08 | -0.81 | -- | 82,178 |
| Opt2 | PAR (E-m ² /day) | 0.68 | 0.79 | 6.36 | 6.33 | 0.76 | 1.39 | -0.60 | 8.50 | 63,813 |

"--" means not calculated or reported.

Table 9. Comparison of 2008 model performance for Bounding Scenarios and Opt2.

| Report | Variable | R | WSS | RMSE | RMSE _c | RE | MAE | Bias | Sd _{obs} | N |
|--------|--|------|------|------|-------------------|------|------|-------|-------------------|---------------|
| BSR | Temperature (°C) | 0.95 | -- | 0.56 | -- | -- | -- | -0.05 | -- | 67,857 |
| Opt2 | Temperature (°C) | 0.95 | 0.97 | 0.60 | 0.57 | 0.04 | 0.40 | 0.21 | 1.67 | 76,048 |
| BSR | Salinity (psu) | 0.76 | -- | 0.81 | -- | -- | -- | 0.03 | -- | 66,958 |
| Opt2 | Salinity (psu) | 0.79 | 0.86 | 0.84 | 0.76 | 0.02 | 0.58 | 0.36 | 1.07 | 75,141 |
| BSR | DO (mg/L) | 0.85 | -- | 0.98 | -- | -- | -- | -0.53 | -- | 66,931 |
| Opt2 | DO (mg/L) | 0.88 | 0.92 | 0.93 | 0.84 | 0.10 | 0.71 | -0.41 | 1.62 | 75,117 |
| BSR | Chl-a (µg/L) | 0.49 | -- | 3.10 | -- | -- | -- | 0.33 | -- | 66,941 |
| Opt2 | Chl-a (µg/L) | 0.46 | 0.64 | 3.14 | 3.08 | 0.94 | 1.50 | 0.58 | 2.94 | 73,934 |
| BSR | NO ₃ -NO ₂ (N-mg/L) | 0.78 | -- | 0.09 | -- | -- | -- | -0.04 | -- | 1,381 |
| Opt2 | NO ₃ -NO ₂ (N-mg/L) | 0.77 | 0.85 | 0.09 | 0.09 | 0.17 | 0.06 | -0.02 | 0.11 | 1,495 |
| BSR | NH ₄ ⁺ (N-mg/L) | 0.50 | -- | 0.02 | -- | -- | -- | 0 | -- | 881 |
| Opt2 | NH ₄ ⁺ (N-mg/L) | 0.49 | 0.62 | 0.03 | 0.02 | 1.05 | 0.02 | 0.02 | 0.02 | 1,010 |
| BSR | PAR (E-m ² /day) | -- | -- | -- | -- | -- | -- | -- | -- | -- |
| Opt2 | PAR (E-m ² /day) | 0.48 | 0.64 | 7.51 | 7.48 | 1.01 | 1.86 | -0.75 | 8.20 | 29,516 |

"--" means not calculated or reported.

Table 10. Comparison of 2006 model performance for Bounding Scenarios Report, Opt1, and Opt2.

| Report | Variable | R | WSS | RMSE | RMSE _c | RE | MAE | Bias | Sd _{obs} | N |
|--------|--|------|------|------|-------------------|------|------|-------|-------------------|---------|
| BSR | Temperature (°C) | 0.95 | -- | 0.69 | -- | -- | -- | 0.39 | -- | 140,080 |
| Opt1 | Temperature (°C) | 0.95 | 0.96 | 0.69 | 0.58 | 0.05 | 0.53 | 0.38 | -- | 145,919 |
| Opt2 | Temperature (°C) | 0.95 | 0.97 | 0.56 | 0.55 | 0.04 | 0.39 | 0.11 | 1.81 | 145,602 |
| BSR | Salinity (psu) | 0.84 | -- | 0.77 | -- | -- | -- | -0.47 | -- | 138,845 |
| Opt1 | Salinity (psu) | 0.86 | 0.88 | 0.74 | 0.57 | 0.02 | 0.53 | -0.47 | -- | 144,850 |
| Opt2 | Salinity (psu) | 0.86 | 0.92 | 0.59 | 0.58 | 0.01 | 0.32 | 0.08 | 1.04 | 144,533 |
| BSR | DO (mg/L) | 0.80 | -- | 1.09 | -- | -- | -- | -0.57 | -- | 135,115 |
| Opt1 | DO (mg/L) | 0.80 | 0.85 | 1.13 | 0.94 | 0.14 | 0.92 | -0.62 | -- | 134,591 |
| Opt2 | DO (mg/L) | 0.84 | 0.92 | 0.85 | 0.85 | 0.09 | 0.61 | 0.03 | 1.50 | 141,138 |
| BSR | Chl-a (µg/L) | 0.52 | -- | 4.48 | -- | -- | -- | 0.19 | -- | 112,567 |
| Opt1 | Chl-a (µg/L) | 0.51 | 0.64 | 4.48 | 4.47 | 0.72 | 1.70 | 0.20 | -- | 110,580 |
| Opt2 | Chl-a (µg/L) | 0.49 | 0.60 | 4.62 | 4.62 | 0.72 | 1.66 | 0.06 | 5.25 | 118,363 |
| BSR | NO ₃ -NO ₂ (N-mg/L) | 0.43 | -- | 0.12 | -- | -- | -- | -0.03 | -- | 1,416 |
| Opt1 | NO ₃ -NO ₂ (N-mg/L) | 0.82 | 0.90 | 0.08 | 0.08 | 0.16 | 0.05 | 0 | -- | 2,356 |
| Opt2 | NO ₃ -NO ₂ (N-mg/L) | 0.82 | 0.89 | 0.08 | 0.07 | 0.15 | 0.05 | -0.02 | 0.11 | 2,333 |
| BSR | NH ₄ ⁺ (N-mg/L) | 0.56 | -- | 0.02 | -- | -- | -- | 0.01 | -- | 2,082 |
| Opt1 | NH ₄ ⁺ (N-mg/L) | 0.51 | 0.66 | 0.02 | 0.02 | 1.02 | 0.01 | 0.01 | -- | 3,034 |
| Opt2 | NH ₄ ⁺ (N-mg/L) | 0.51 | 0.59 | 0.02 | 0.02 | 1.50 | 0.02 | 0.02 | 0.02 | 3,006 |
| BSR | PAR (E-m ² /day) | -- | -- | -- | -- | -- | -- | -- | -- | -- |
| Opt1 | PAR (E-m ² /day) | 0.60 | 0.69 | 4.09 | 4.06 | 0.85 | 0.76 | -0.51 | -- | 47,791 |
| Opt2 | PAR (E-m ² /day) | 0.61 | 0.74 | 4.13 | 4.12 | 0.87 | 0.78 | -0.39 | 5.08 | 47,791 |

"--" means not reported.

Table 11. Model performance statistics for Opt2 year 2000.

| Variable | R | WSS | RMSE | RMSE _c | RE | MAE | Bias | Sd _{obs} | N |
|---|------|------|------|-------------------|------|------|-------|-------------------|--------|
| Temperature (°C) | 0.9 | 0.93 | 0.75 | 0.67 | 0.06 | 0.57 | 0.34 | 1.44 | 50,753 |
| Salinity (psu) | 0.75 | 0.84 | 0.86 | 0.8 | 0.02 | 0.57 | 0.31 | 1.06 | 50,753 |
| DO (mg/L) | 0.83 | 0.91 | 0.98 | 0.98 | 0.10 | 0.7 | 0.02 | 1.65 | 47,386 |
| Chl-a (µg/L) | 0.57 | 0.72 | 2.88 | 2.88 | 0.68 | 1.0 | 0.08 | 3.38 | 21,705 |
| NO ₃ -NO ₂ (N-mg/L) | 0.85 | 0.91 | 0.07 | 0.06 | 0.15 | 0.05 | 0.01 | 0.10 | 1,797 |
| NH ₄ ⁺ (N-mg/L) | 0.33 | 0.48 | 0.03 | 0.02 | 1.4 | 0.02 | 0.02 | 0.02 | 1,587 |
| PAR (E-m ² /day) | 0.88 | 0.86 | 3.88 | 3.87 | 0.58 | 0.32 | -0.24 | 6.75 | 8,480 |

Model performance for BSR and Opt1 is not included for the year 2000 since that year was not run in the BSR.

Sediment fluxes

Progressive improvement of model predictions involves continued evaluation of simulated processes, in this case, utilizing in situ or mesocosm-based observations. Fluxes to and from the sediment layer are highly relevant to water column DO and model predictions. Sediment fluxes in the SSM are modeled using the two-layer method developed by DiToro (2001).

Notably, in the case of sediment oxygen demand (SOD), limited flux measurements in our region have hindered comprehensive analysis. However, recent observations (Merritt 2017 and Rigby 2019) allow for a more complete understanding of the spatial variation in the magnitude of sediment fluxes. A key enhancement to the water quality observational data set we are using for model evaluation is the sediment flux data reported in Santana and Shull (2023) due to the broad spatial coverage of observations, though these observations occurred only in the springtime. Appendix I contains a detailed description of the comparative work between predictions and observations of sediment fluxes. We compared 2014 predictions with observations from years when data were collected.

We found good agreement between sediment oxygen demand and nitrogen flux SSM predictions and observations. Most predicted sediment oxygen demand, ammonium, and nitrate fluxes fall within 97.5 percentile confidence intervals of recently measured fluxes throughout the Puget Sound (Merritt 2017 and Santana and Shull, 2023). The general magnitude and direction of nitrogen flux predictions fall within the range of values from an extensive compilation of nitrogen flux data for Puget Sound (Sheibley and Paulson 2014) and with other observations in the Salish Sea (Belley et al. 2016).

Simulated spatial flux patterns match expected patterns based on observational records. For example, shallower locations such as those in South Sound experience higher predicted SOD rates. The spatial variability of predicted SOD is similar between years. SSM predicts sediments generally release ammonium into the water column and uptake nitrate from the water column. The annual median denitrification within sediments is close to the median springtime range that Santana and Shull (2023) calculated from the deviation of measured nitrogen to carbon ratios. SSM predicts that, in terms of annual medians, sediments in terminal inlets and bays release more ammonium to the water column than other locations in the Greater Puget Sound and uptake relatively less nitrate from the water column. In terms of nitrate uptake, Hood Canal is an exception, where it is predicted to uptake more nitrate from the water column compared to other areas.

Predicted SOD during the annual cycle shows a seasonal pattern consistent with that described in Pamatmat (1971). While predicted SOD curves generally follow labile POC curves, sharp SOD, ammonium and nitrate flux swings may be ascribed to changes in temperature, variations in DO levels, and sudden shifts in the characteristics of the bottom water layer that could be due to variable mixing and flow regimes. Predicted reference conditions exhibit relatively lower fluxes.

Phytoplankton productivity

Appendix J contains summaries and statistics of regional phytoplankton biomass and primary productivity observational data sets, as well as comparisons with model predictions. When comparing predicted and observed chlorophyll-a measurements, as a proxy for biomass, the model reproduces seasonal and spatial variations.

Overall, chlorophyll-a prediction errors for all years are well within the lower quartile of the range of observations, which is considered good performance. Upon segregating the prediction/observations pairs by measurement location, model skill among locations varied, and most stations in 2014 (37 out of 41 or about 90%) had a mean absolute error fraction below 25% of the observational range. Furthermore, SSM produces a chlorophyll-a exponential cumulative frequency distribution that is like the observed one, which means that the model generally matches chlorophyll-a values across the measured range. Mechanistic models predict values at temporal and spatial scales, which do not resolve short-term peaks and subscale patchy algal blooms. SSM underpredicted peak algal bloom events, thus underpredicting chlorophyll-a maxima at the far tail end of the observed distribution (beyond the 99.75th percentile).

We accomplished a comparative re-analysis of observed and predicted productivities using predictions that match the observations in time and space. At three stations (West Point, Possession Sound, and Admiralty Inlet) in year 2000, observational ranges overlap both predicted net and gross productivities, while observational medians are closer to predicted net than gross primary productivity medians. Additionally, we compared all stations for which we have productivity measurements for the year 2000. Productivity observations are reasonably represented by the model. The model generally matches the productivity median and peak magnitudes for observed and predicted values for the year 2000.

Microbial respiration in bottom waters

A key process in marine environments is respiration mediated by autotrophic or heterotrophic microorganisms via the breakdown and metabolism of organic material. Salish Sea simulations produced water column microbial respiration rates that show coherent spatio-temporal patterns. SSM simulations show higher respiration rates in terminal inlets and bays. SSM predictions also indicate an expected annual respiration cycle with minima in the winter and maxima in the summer.

Simulations point to algal respiration in the spring, summer, and fall months as greater than heterotrophic respiration in bottom waters. In the winter months (December through February), heterotrophic respiration is predicted to be a larger fraction. Algal respiration is predicted to consume the largest proportion of the oxygen from the total water column respiration processes in the bottom waters at most of the observational stations. Heterotrophic respiration and nitrification are also present, though in smaller proportions, at the locations studied. Appendix K contains summaries of predicted temporal and spatial respiration in the bottom layer, as well as the proportion of oxygen consumed by each of the microbial respiration processes at selected sites.

Apple and Bjornson (2019) produced a unique observational Salish Sea microbial respiration rate data set for bottom waters. We compared those observations to respiration rates obtained from SSM simulations over a four-year period that did not encompass the observations. Monthly mean observations were, on average, about 55% higher than predictions (0.09 compared to 0.04 mg O₂/L/day). This difference between predictions and observations is less than the mean percent difference between observations at the same stations conducted in different years, which is 62%. Appendix K contains details of that analysis. Predicted respiration rates are within the expected observational ranges at the sites Apple and Bjornson (2019) sampled.

Summary of performance

Even though observational data sets within WA waters of the Salish Sea reflect large spatial and temporal variabilities, SSM predictions are consistent with field observations and interpretations. SSM reproduces seasonally low DO, particularly at inlets and bays, and reproduces its temporal variability. The model skill in bottom waters exceeds the model skill in surface layers. SSM simulates embayments and open channel locations with similar skill.

Overview of model limitations

Any computational modeling system is an imperfect representation of reality. We enhanced the intermediate SSM model with improvements described above and in the appendices. Comparisons with independent data sets for SOD, phytoplankton productivity and respiration demonstrate skill in simulating biogeochemical processes.

SSM's application in a regulatory process is not unique in terms of how water quality models are used by Ecology (and other states). Mechanistic models such as SSM have been successfully used to evaluate the effect of human contributions of pollution, compare model simulations to the water quality criteria, develop pollution reduction plans, inform what kinds of limits to set for point source discharges, and manage nonpoint source pollution. The model limitations listed below do not preclude the use of the model for regulatory purposes but rather are included here to provide context.

- **The SSM's intermediate scale is appropriate for water quality predictions at locations throughout the waters of the Salish Sea, but not at some nearshore locations.** The intermediate scale grid configuration of SSM is not designed to resolve the bathymetry of mud flats, intertidal areas, and some shallow subtidal locations. Steep changes in bathymetry at these nearshore locations are not realistically represented (Ahmed et al. 2019 Appendix J). Therefore, intertidal and shallow subtidal zones, including brackish waters where river channels connect with marine waters, are masked and not used for computing noncompliance (Ahmed et al. 2021). Additionally, we found that during some colder periods, the surface layer temperature model predictions at some very shallow subtidal locations were unrealistically low. So, nodes that represent depths of 4 m or less during ebb tides are also masked, as are selected hours in the winter where predicted temperatures at other very shallow subtidal locations were negative in the surface layers.

Appendix A describes the net heat flux correction factors that may drive this limitation. Further information about the overall masking approach is found in Appendix D.

- **The SSM predictions reflect means at the model scale.** Grid cell size limits the resolution of the model outputs. The model calculates a single concentration for each grid cell, so spatial variation in water quality within a grid cell is not captured. Examples of this include: (1) Buoyancy and plume mixing dynamics for marine outfall discharges is not captured at a sub-grid scale so that immediate near-field impacts are not resolvable in SSM, and (2) Patchy algal growth at a sub-grid horizontal scale or within a vertical layer of the water column is not resolvable in SSM. It is important to note that observations may not represent the mean of a grid-cell-volume but rather represent conditions at a single location within the much greater grid-cell-volume of the model.
- **The SSM is computationally intensive to run.** We employ the Hyak (high-performance computational clusters and supporting infrastructure) at the University of Washington to run SSM. Annual hydrodynamic runs take approximately 1 day, and water quality runs approximately 3 days in this system using 80 computational cores.
- **The SSM is not calibrated for phosphorus at this time.** While phosphorus is currently simulated by the model, obtaining an adequate phosphorus calibration will likely require additional speciated data at the open boundary. Researchers have found that phosphorus species are not limiting growth in Puget Sound (Waldichuk and Gould 1954; Lincoln and Collias 1975). Instead, inorganic nitrogen species (Winter et al. 1975; Bernhard and Peele 1997; Newton et al. 1998; Aura Nova et al. 1998; Newton and Van Voorhis 2002) have been found to be important in limiting phytoplankton growth in Puget Sound. Since phosphorus limitation is not, or seldom, a consideration, lack of phosphorus calibration is not expected to change model results.

Residence and flushing times

Residence times and flushing times (see Methods section) are ways to quantify how much time water within a water body (or a part of a water body) remains before being replaced or flushed out. These calculations can inform our understanding of circulation and have implications for water quality and DO levels (see Methods section). Appendix M includes a detailed description of the difference between residence and flushing times and quantifies these for the various basins in the SSM domain as estimated with the use of virtual dye (i.e., a hypothetical dye concentration introduced into the model domain). Key results from a virtual dye study are as follows:

- Differences in approaches, boundaries, and time scale averages lead to differences in flushing time estimates between this study and other studies (Premathilake and Khangaonkar 2022; MacCready et al. 2021; and Ahmed et al. 2017). Nonetheless, the relative variation among flushing times for basins is well established from longest to shortest in this order: Hood Canal, South Sound, Whidbey Basin. For the heads of inlets studied, the longest to shortest residence times are in the following order: Lynch Cove, Case

Inlet, Carr Inlet, and Sinclair Inlet. Appendix M compares the flushing times estimated in this study with those found in the literature.

- Among the four years studied, the overall winter flushing times for the Greater Puget Sound (PSM model domain, see Appendix M) extent of the Salish Sea, in order of longest to shortest, are: 2000, 2008, 2006, and 2014. However, winter flushing times vary by individual basins and year within the Greater Puget Sound.
- Salt-balance (Burchard et al. 2018) based residence time provides useful information, but in the case of residence times for the year 2000 (PSEMP 2016), a much shorter residence time at a location in Main Basin was estimated relative to other years. However, computations from virtual dye-based residence times using SSM show that the year 2000 in the winter had the longest residence time for the central portion of Main Basin compared to other modeled years.

DO consumption in bottom layers

In a domain as extensive and variable as the Salish Sea, we expect differences in advective and diffusive mixing patterns as well as in the proportions of DO that biochemical processes consume and their corresponding spatial and temporal patterns. We selected eight locations within the domain that represent water masses within embayments and open channel locations to explore the influence of DO-consuming biochemical processes in the bottom waters of the Salish Sea. DO noncompliances typically occur in the bottom waters, so SSM layers 9 and 10, which represent the bottom 29% of the water column, are the focus of this analysis. The selected locations are shown in Figure 28 along with their depths, areas, and model node numbers.

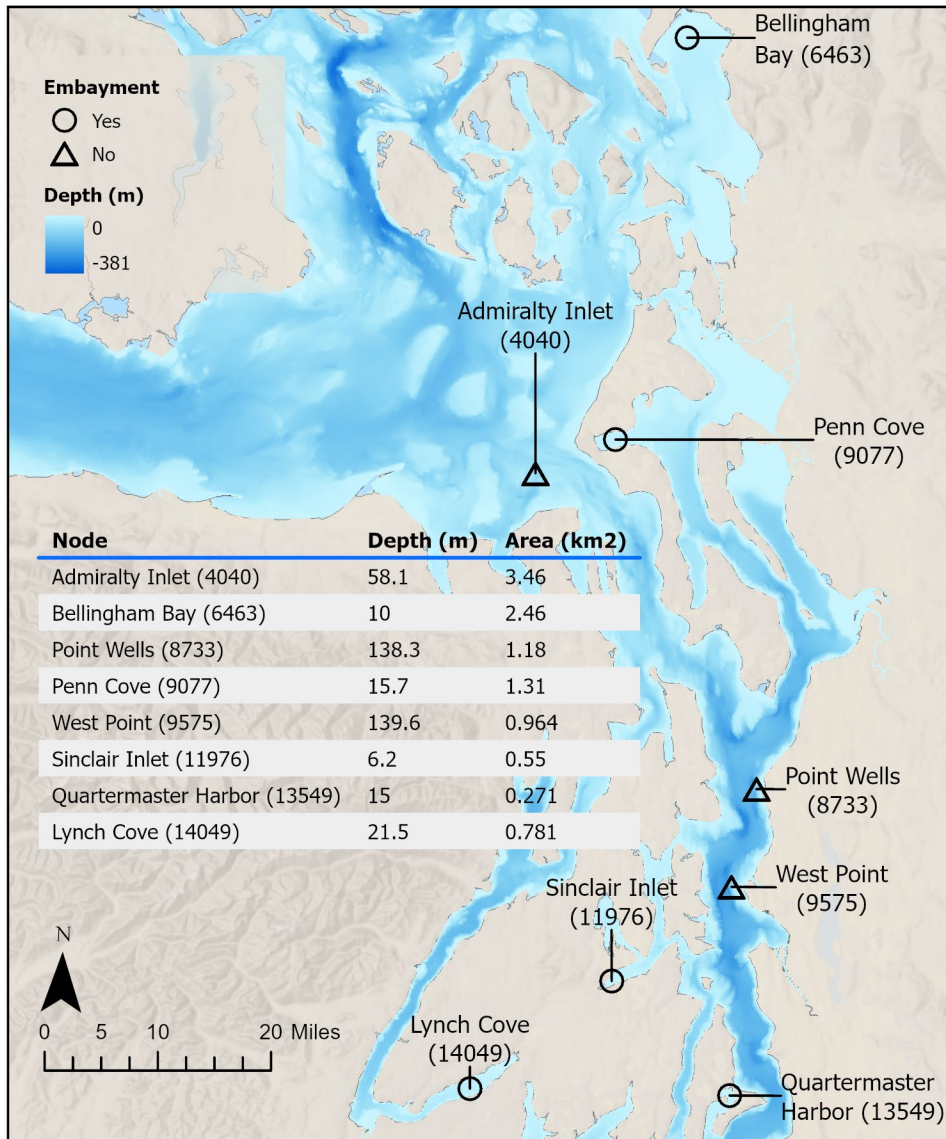


Figure 28. Map of selected locations for biochemical process DO consumption analysis.

The mid-channel locations are in Admiralty Inlet, Point Wells, and West Point. The embayment locations are in Quartermaster Harbor, Lynch Cove, Sinclair Inlet, Penn Cove, and Bellingham Bay. Figure 29 shows the DO time series averaged across the two bottom layers, in 2014, at each of these locations. At open channel locations, Point Wells and West Point, DO bottom layer concentrations are relatively smoother compared to those in Admiralty Inlet. However, all the embayment station time series have more pronounced peaks and lows than the open channel time series, with the lowest DO occurring either in late summer or early fall.

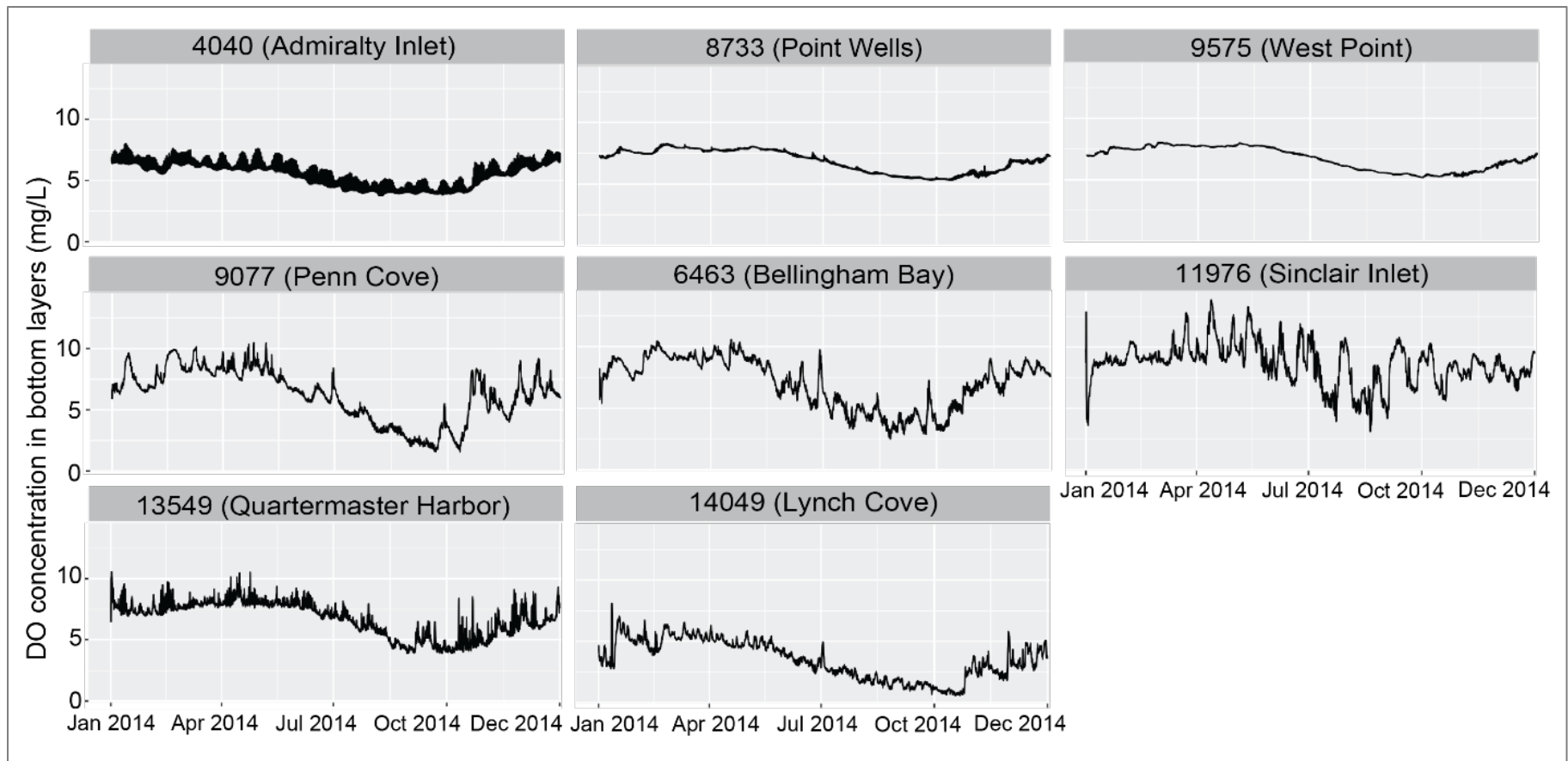


Figure 29. Time series at selected locations of average simulated dissolved oxygen (DO) concentrations at SSM bottom two layers.

DO concentrations in the bottom layers are simultaneously influenced by both biochemical and physical processes. Estuarine circulation, tidal and wind-driven mixing, vertical and horizontal diffusion and advection, and reaeration are physical processes that influence how much oxygen is available in the water column. In turn, such physical processes are influenced on a larger scale by the climatological and oceanographic cycles and at a local scale by the topobathymetric features and inflows within and near each site of interest. Within Puget Sound, embayments are generally more vulnerable to lower bottom DO levels than open channel locations.

While the complexity of the physics cannot be captured in a single metric, plotting vertical density gradients in the water column over time is one approach to visualize the combined effects of the physical processes at work at each of these selected sites. Figure 30 shows the predicted density (σ_t) throughout 2014 at each of the selected locations. The ten SSM vertical layers represent varying percentages of the water column, as shown in the legend of Figure 30 (layer 1 is the top surface layer, whereas layer 10 is the bottom layer).

The open channel locations (Admiralty Inlet (4040), Point Wells (8733), and West Point (9575)) have the least density variation throughout the year. At these locations, σ_t predictions fluctuated slightly and remained near 23 – 25 in most water column layers, indicating that the water column was generally well mixed throughout the year. However, the top three layers show consistently lower densities because of freshwater flowing into marine waters and then moving through the estuary, lack of wind mixing, or a combination of both. Freshwater outflow data for the Skagit River, the largest river discharging into Puget Sound, shows a sustained spring freshet from around early May to mid-July in 2014 ranging from about 400 to 500 cubic meters per second followed by a period of low flow until mid-October and spikes due to precipitation events for the remainder of the year (Appendix B-3).

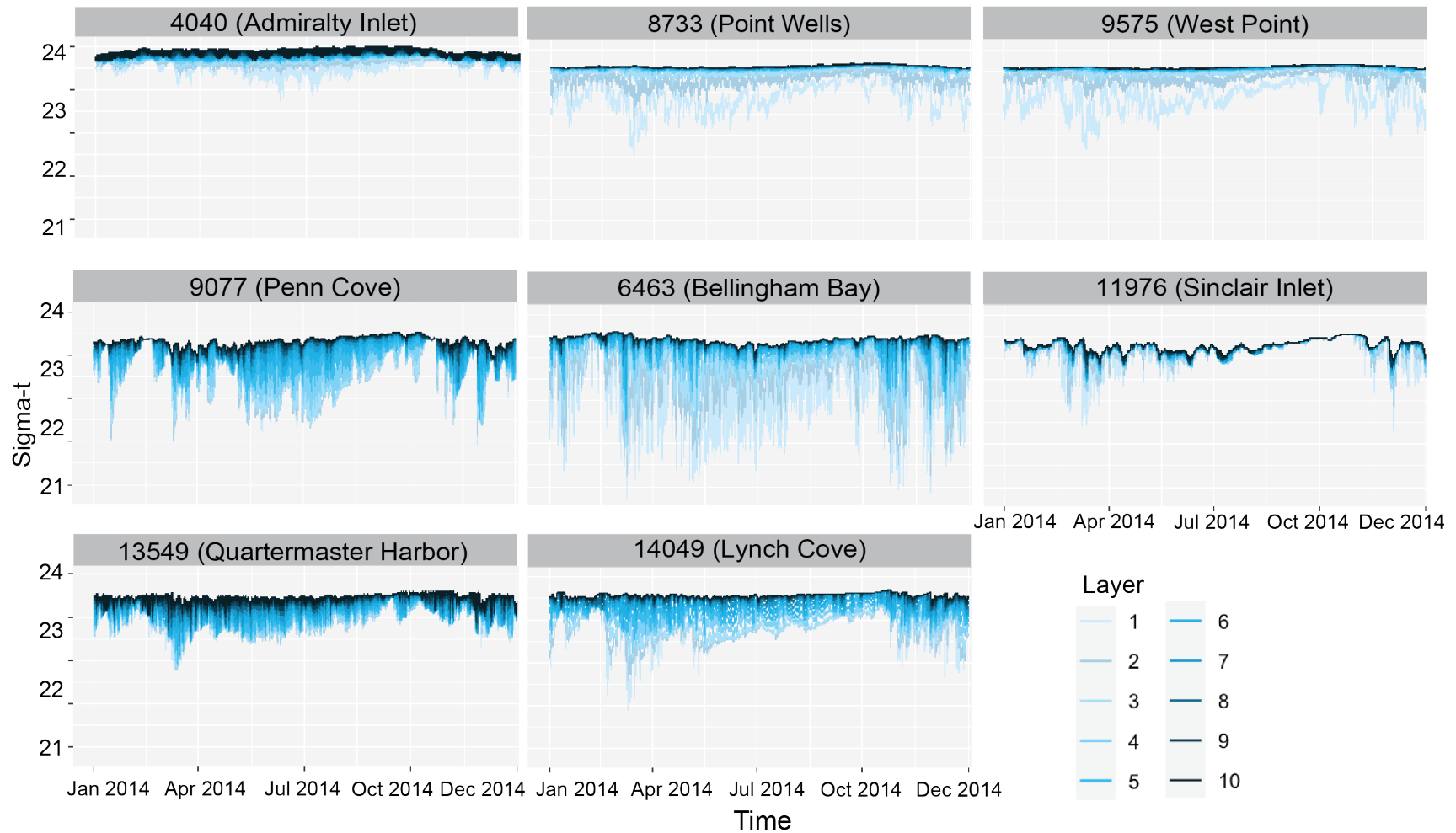


Figure 30. Sigma-t time series plots based on simulated data at selected locations.
 Layer 1 is at the top of the water column (lightest color), and layer 10 is at the bottom (darkest color).

The shallow embayment station locations show more density variability throughout the year. In the winter, when air temperatures dip and surface water temperatures also decrease, surface waters can be colder than bottom waters. Such instances are found in observational data. Puget Sound Ecosystem Monitoring Program (PSEMP) reported that surface waters were colder than bottom waters in central Puget Sound in February and November 2014 (PSEMP 2015). Ecology depth profile plots from Lynch Cove in February 2014 also show surface waters being colder than bottom layers (Appendix H). More recent sampling at King County's Penn Cove station at Coupeville Wharf, near node 9077, shows multiple instances of colder surface layers in the winter months compared to bottom layers (King County 2025). However, surface layers at some embayment locations exhibit lower salinities than at open channel locations, and, as shown in Figure 30, greater vertical density differences can occur.

In the summer, embayment stations exhibited prolonged stratification, except Sinclair Inlet (11976), where stratification occurred for shorter periods and waters were generally well mixed. Bellingham Bay exhibited much density variation in the surface layers throughout the year. The density separation and stratification in the summer months are most obvious in Penn Cove and Lynch Cove, where the top layer of the water column reached a sigma-t near 15 or less, whereas the bottom layers remained at a sigma-t near 23, resulting in stable, stratified conditions from late spring to early fall. These conditions restrict vertical mixing. DO from surface layers does not replenish DO in bottom layers during stratified conditions.

The selected embayment locations all have depths less than 30 m and so are generally within the euphotic zone. Photosynthesis, which produces DO, can occur throughout the water column at those locations. The difference between the DO produced and the DO respired by algae (referred to here as DeltaDO_Algal) represents the balance due to algal activity in these layers.

In SSM, biochemical processes which remove DO from bottom waters include: 1) algal respiration, 2) heterotrophic respiration (modeled as dissolved organic carbon mineralization), 3) nitrification, and 4) sediment oxygen demand, which represents the integration of oxygen uptake processes within the sediment bed. Water column depth coupled with stratification are key features at each location that influence the contribution of sediment bed versus water column processes to DO consumption. Although sediment oxygen demand (SOD), driven by respiration of organic matter deposited on the bottom does vary seasonally (Appendix I), it is closer to a steady-state process in comparison to water column processes at each location. SSM generally predicts that shallower sites in embayments have higher SOD rates (Appendix I), which corresponds well with recent regional observations (Santana and Shull 2023).

The breakdown of the contribution of each biogeochemical process towards DO consumption in the bottom layers is shown in Figure 31 in units of kg O₂/hour and in Figure 32 in terms of g O₂/m²/day. The values in units of mass per time (kg O₂/hour) constitute the total magnitudes of DO consumed per time in each grid cell, whereas the values in units of flux (g O₂/m²/day) constitute the mass of DO consumed per area and time so that all grid cells are normalized by area. The influence of biochemical processes also changes with bottom layer thickness, as

discussed below. Figure 28 shows water column depths and areas for each location. The top plot in Figures 31 and 32 shows the heterotrophic respiration (DDOC), nitrification (NITRIF), algal production minus algal respiration (DeltaDO_Algal) and sediment oxygen demand (SOD) in terms of the annual mean oxygen utilized in the bottom two layers at each of these locations. The bottom box plots show the median, interquartile range, and outliers of hourly utilization of DO at the selected nodes in the bottom two layers over the whole year.

Sediment oxygen demand is, in all cases, the biochemical process that consumes the most DO in the bottom two layers of the water column, but the relative contribution shifts depending on the location. This is due to the differences in water column depths (bottom layers thickness) at each location as well as the relative differences of oxygen uptake by the sediments that are, among other drivers, also a function of depth, where SOD has greater influence in shallower stations.

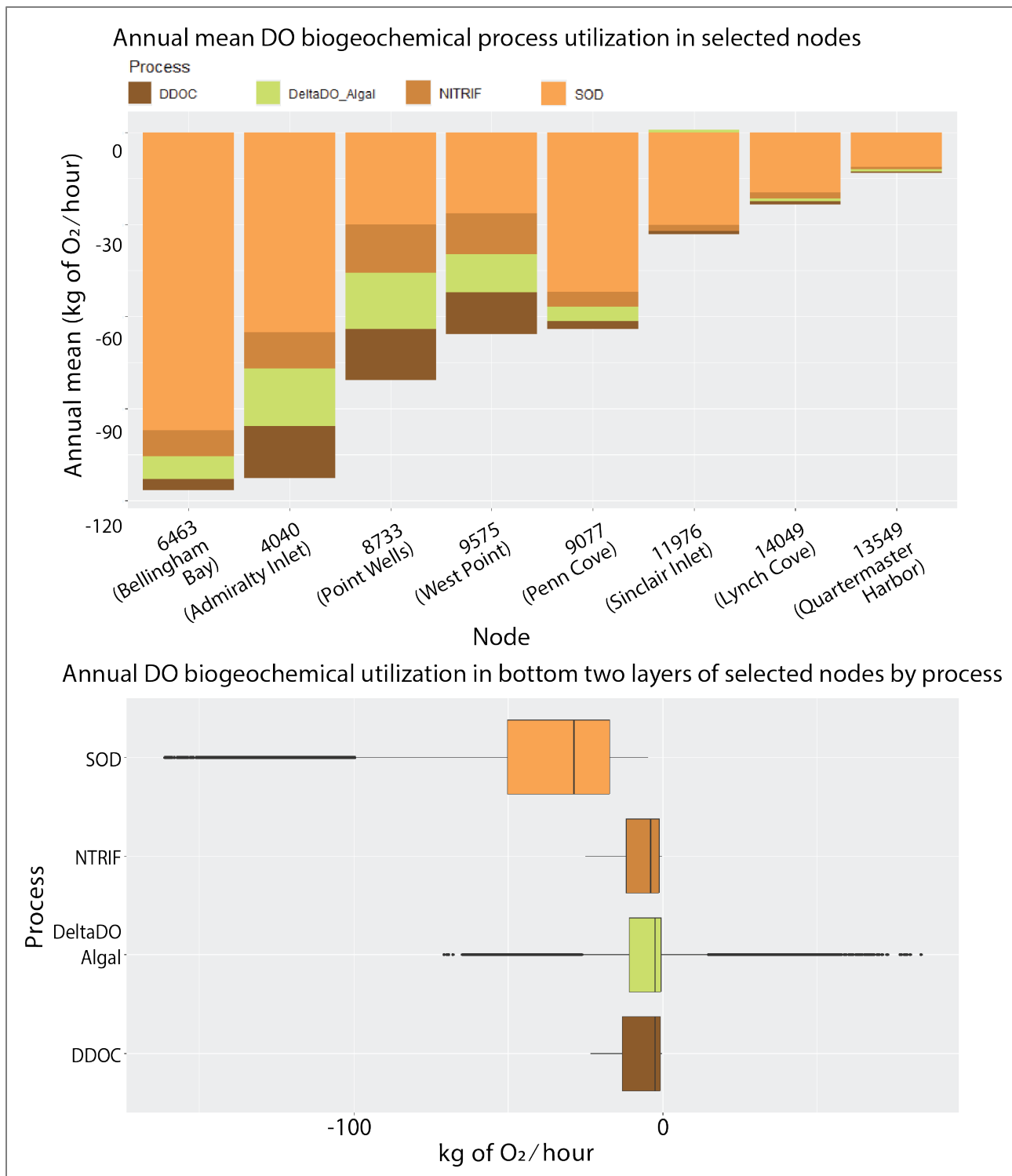


Figure 31. Comparison of dissolved oxygen (DO) consumption from SSM's bottom two layers at selected nodes by heterotrophic respiration (DDOC), nitrification (NITRIF), algal production minus algal respiration (DeltaDO_Algal) and sediment oxygen demand (SOD) in units of kg of O₂/hour.

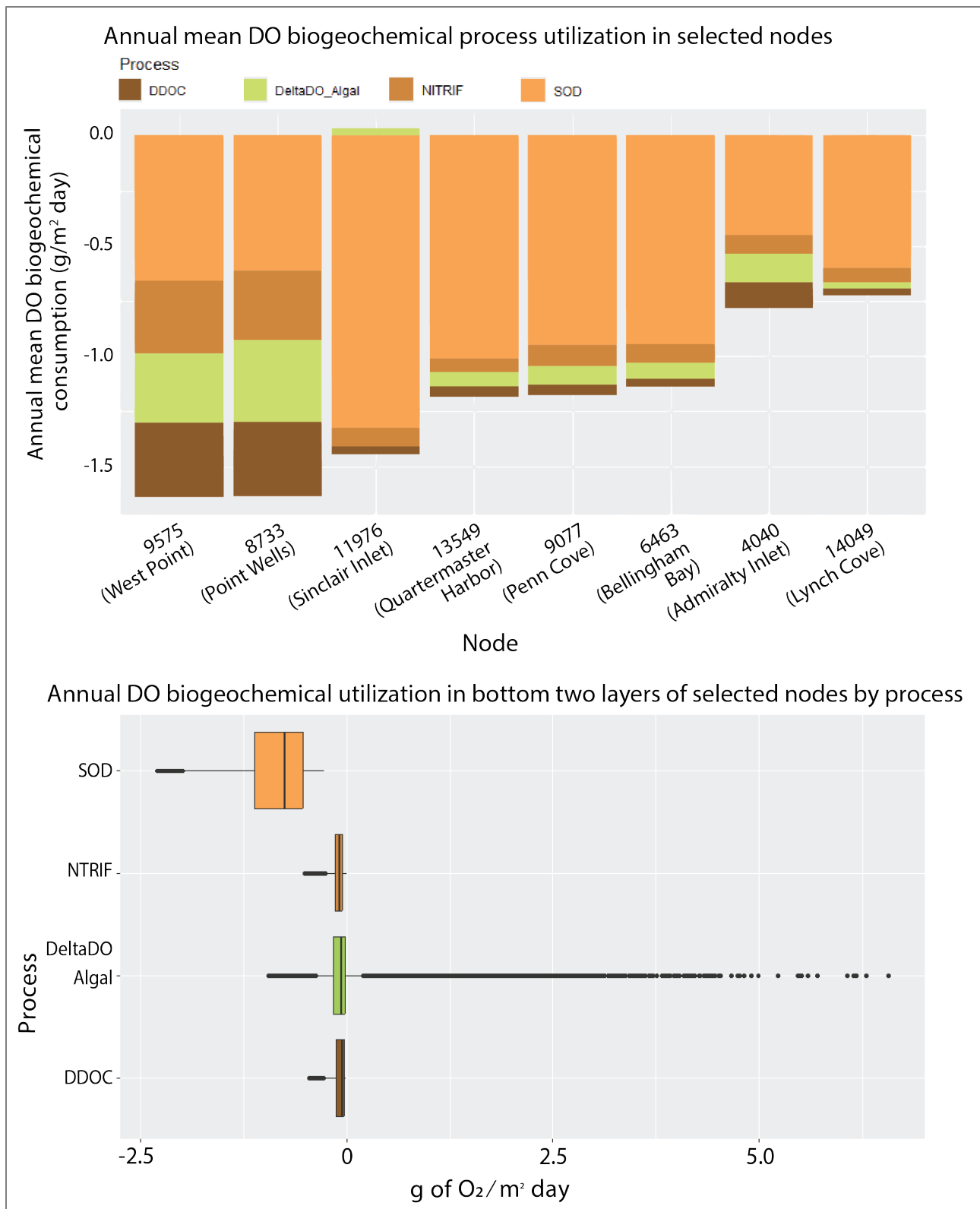


Figure 32. Comparison of dissolved oxygen (DO) consumption from SSM bottom two layers at selected nodes by heterotrophic respiration (DDOC), nitrification (NITRIF), algal production minus algal respiration (DeltaDO_Algal) and sediment oxygen demand (SOD) in units of g O₂/m²/day.

Considering only the consumptive respiration processes in the water column and SOD, Figure 33 shows that the proportion of SOD consumption to total DO consumption at the open channel locations (nodes 4040, 8733 and 9575) is lower throughout the year than that occurring at the embayment locations (11976, 6463, 13549, 9077 and 14049). The percentage of DO removed via SOD compared to the total DO consumptive processes is higher at all locations in the winter and fall, when the algal population, and accordingly algal respiration, is lower. In the spring, as algal population quickly increases and boosts the production of DO, algal respiration also increases, and SOD constitutes a smaller portion of the total DO consumptive processes.

Our results agree with an observation-based estimate of around 19.4% DO consumption by sediment oxygen demand for a site in Hood Canal in July (Shull 2022). In 2014, SSM predicts that the monthly average proportion of DO consumed by SOD in July at Lynch Cove, at the head of Hood Canal, is around 21% when estimating over the entire water column. At this location, bottom layers become very low in DO or anoxic during parts of the year (Figure 29), making less oxygen available to be consumed in any process, but if considering only the bottom layers, the proportion of DO consumed by SOD is much higher.

Importantly, as shown in the bottom portion of Figure 33, SOD can become by far the dominant biogeochemical process consuming DO in bottom layers— greater than 70% at all selected embayment locations at all times of the year when SOD influence is restricted to bottom layers of the water column due to stratification. As shown in Figure 30, such conditions occurred in varying degrees and durations, from a few days to several months in 2014 at the selected embayment locations.

To show how DO consumption processes change seasonally, Figure 34 shows time series for each process at each location in 2014 in the two bottom layers. At most locations and times, DeltaDO_Algal (shown in green) is negative, signifying that respiration overtakes algal DO production in the two bottom layers. At the selected nodes in Bellingham Bay and in Sinclair Inlet during a subset of daylight hours in the spring through early fall, DeltaDO_Algal becomes positive, signifying that during those times, more DO is being produced in the bottom two layers by photosynthesis than the amount of DO consumed by respiration. On an annual basis, however, when averaging all hours, only Sinclair Inlet has a slightly net positive DeltaDO_Algal value (around 0.74 kg O₂/hour), as shown in Figure 31 (top). The diel variation during days when photosynthesis is at a maximum, for example on 7/26/14 for the Sinclair Inlet node 11976, shows positive values for DeltaDO_Algal for eight hours and negative DeltaDO_Algal for the rest of the 24-hour day (16 hours). However, throughout the year, SOD is the predominant biochemical process consuming DO.

The SOD time series patterns in the water column are similar for the open channel locations with peak sediment consumption in the summer and fall, and lower consumption in the winter and early spring. At embayment locations, the consumption of DO via the sediment in the warm or hot months is less when less DO is available in the water column. The best example of this is in Lynch Cove.

In summary, this analysis highlights that SOD is a key driver in DO consumption and is the primary biochemical process consuming DO in the bottom water column layers at embayment locations which are vulnerable to hypoxia due to stratification and less mixing and flushing.

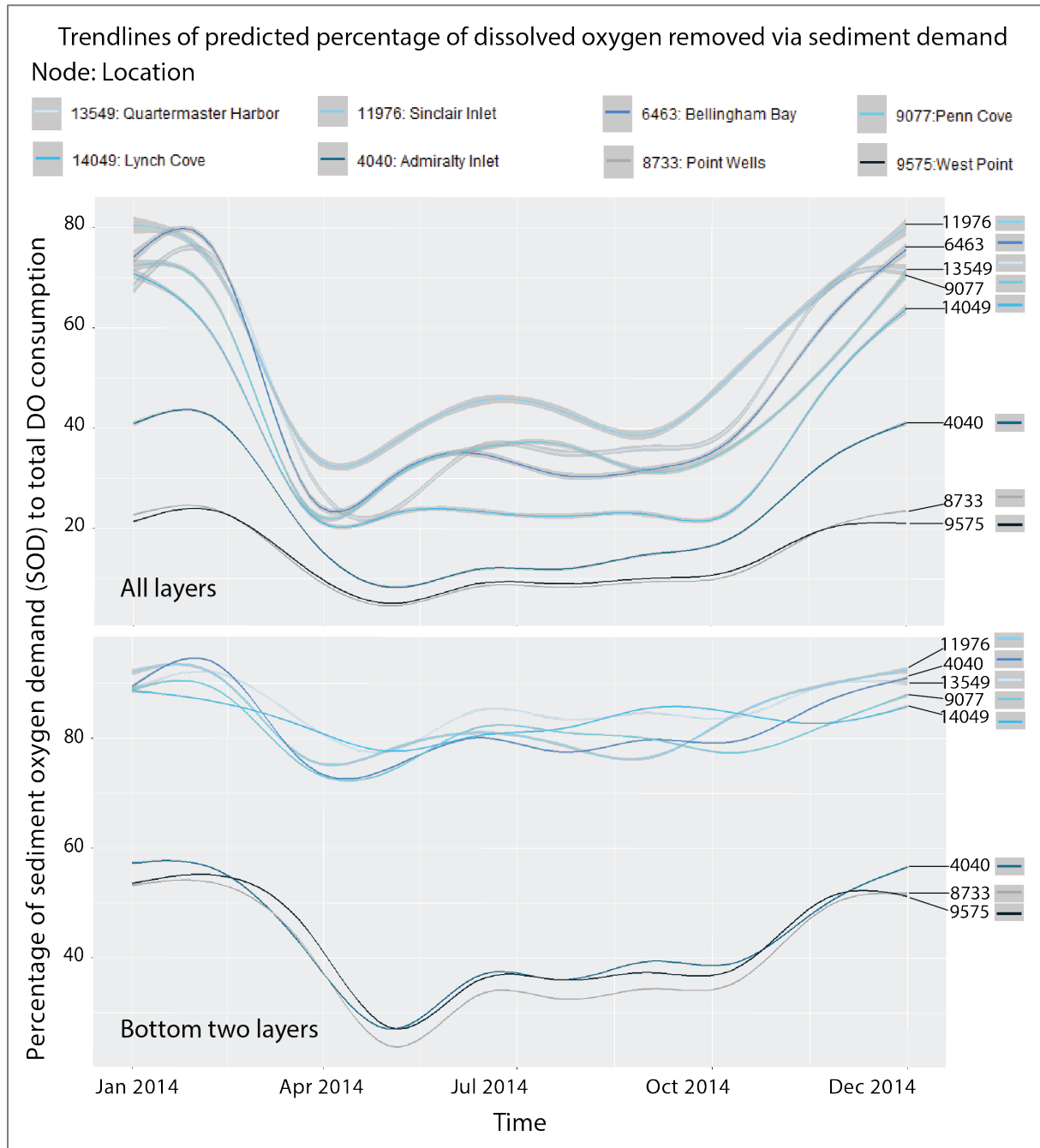


Figure 33. Trendlines (smooth time series) of predicted percentages of dissolved oxygen (DO) removed by sediment oxygen demand (SOD) at selected nodes from entire water column (top) and from the two bottom layers (bottom) in 2014.

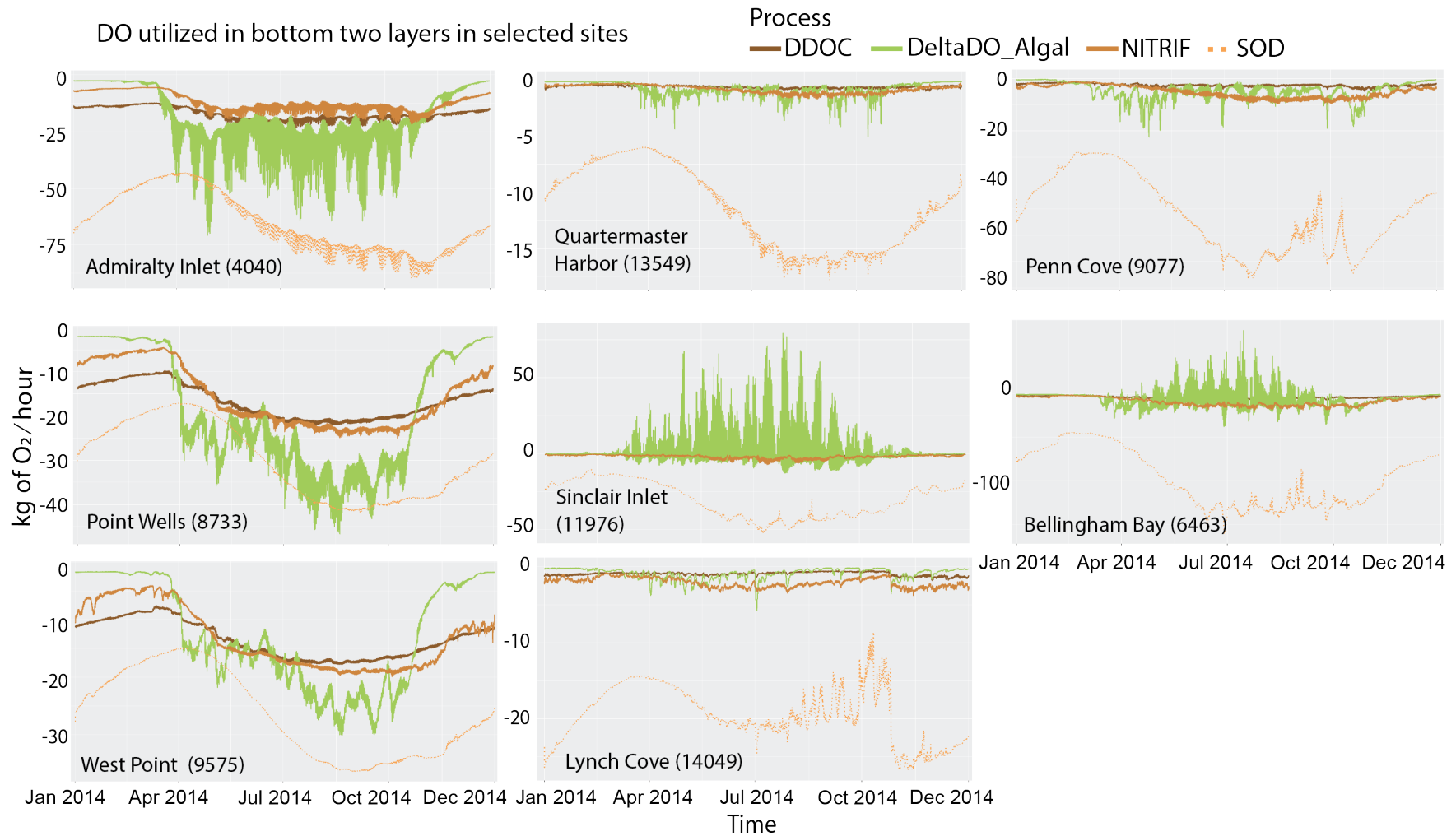


Figure 34. Time series of predicted dissolved oxygen (DO) consumed by biogeochemical processes at selected nodes in 2014.

Sensitivity and uncertainty

Sensitivity analysis, in the context of the SSM, aims to determine the model's response to an input or parameter perturbation that represents a change to a specific point(s) in the mechanistic, biogeochemical simulation. Numerous sensitivity studies were conducted during SSM development and calibration. Subsequently, Ahmed et al. (2019) conducted and reported on additional sensitivity tests, mainly one-at-a-time sensitivity tests where a single parameter is changed at a time to discern the influence of that parameter on the results. We conducted additional sensitivity tests and report on them in Appendix A.

Refining and improving inputs that the model is most sensitive to is an efficient way to attain overall model performance enhancements. For example, using HYCOM for oceanic open boundary conditions, comparing uniform versus spatially variable bottom friction and updating tidal constituents to improve water surface elevation predictions, using two different reaeration algorithms that conform better to observations and optimizing labile and refractory settling velocities to achieve close to steady state sediment fluxes after running the model for consecutive times for initialization (Appendix A) have resulted in overall improvements.

Lack of agreed terminology with respect to uncertainty can generate confusion (Morgan and Henrion 1990). Uncertainty refers to both systematic (variability from the true mean due to biases in estimation or experimental methods) and random errors (variability due to chance). Errors associated with model limitations and the representativeness of observations at the spatial scales applied in the model are systematic. Observational data can also have systematic and random errors.

Calculations involving differences between model predictions and observations, termed goodness-of-fit statistics, such as the bias and root mean square error (RMSE), are used to quantify such errors. Random errors cannot be reduced via mechanistic modeling, but systematic errors can. We aim for a model that produces not only the best goodness of fit statistics to minimize systematic errors, but that also demonstrates the ability to reproduce real-world processes, as has been shown for sediment fluxes, phytoplankton productivity, and water column respiration described in Appendices I, J, and K, respectively. By addressing these questions and improving model skill, we have successfully reduced uncertainty with respect to systematic errors.

The remainder of this section describes the following analyses we conducted to delve deeper into sensitivity and uncertainty questions:

- Sensitivity to multiple parameter adjustments.
- Uncertainty in DO depletion estimates.
- Uncertainty in comparison with DO numeric criteria.

Sensitivity to multiple parameter adjustment

SSM depends on dozens of parameters that are calibrated to match Salish Sea dynamics. A reasonable question is: How much can the ultimate outcome change if the model used an alternate set of parameterizations different from the calibration set? To fully answer this question, a mechanistic model needs to be run thousands of times with randomly varying parameter sets to determine whether any other reasonable parameterizations are feasible — that is, that can attain acceptable model skill.

Due to the computational time limitations inherent in this modeling system (three days to complete a water quality model run using 80 cores at the UW supercomputing center, Hyak, based on prior completion of the decoupled hydrodynamics run), a completely random sensitivity analysis for all parameters as described above is not feasible.

To partially address this type of situation, Bowen and Hieronymus (2000) used a “regional sensitivity analysis,” which can also be described as a modified Monte-Carlo approach. Their approach consisted of running the model many times with modified parameter subsets randomly selected to be within a percentage of literature values and then checking for any alternative parameterizations that demonstrated at least the same level of skill as the base calibration parameter set. The latter alternative parameterizations were then used to run the model using the expected level of load reductions to determine the variability of resulting outcomes and compare those with results from the base calibration set.

We used a method similar to the “regional sensitivity analysis” approach in Bowen and Hieronymus (2000). The questions that motivated this analysis were:

- Are other parameterizations feasible (that demonstrate the same level of skill or better) for this modeling system?
- How does the sensitivity of the model to changes in a subset of parameters influence noncompliances in a reduction scenario?

This analysis focused on parameters that influence DO present in the water column and algal growth including half-saturation rate for nitrogen uptake (KHN), algal settling velocities (WS), maximum photosynthetic rate (PM), minimum respiration rate of labile dissolved organic carbon (KLDC) and dissolution rate of labile particulate organic carbon (KLPC). We generated random values for these parameters within a range of $\pm 30\%$ of the values used in the existing SSM base calibration, as described in Appendix A, unless that level of change moved the parameter value outside the literature range, and in that case, the value was capped at the literature range. We conducted sixty model runs for the year 2014, each using a combination of randomly selected values, within the constraints mentioned above, for these parameters. We calculated performance statistics (R, RMSE, bias) for DO, nitrate-nitrite, ammonium, and chlorophyll-a for each of these sixty runs and compared them with those of the 2014 base calibration run.

When considering the skill in predicting the water quality variables above, no alternative parameterization produced better statistical skill metrics (R, RMSE, and bias better for all variables) than the base calibration. Pooled statistics for all 60 runs are shown in Taylor plots

for DO, ammonium, nitrate-nitrite, and chlorophyll-a (Figure 35). For DO and nitrate-nitrite, the data from the sixty runs were segregated into four distinct clusters. The cluster closest to the horizontal axis represents better skill with respect to correlation.

Although none of the 60 runs have better overall skill metrics than the base calibration, one of them has statistical skill metrics that are essentially the same as those of the base calibration. We selected this alternative parameterization for further analysis. The values of the eight different rate parameters are included in Table 12 for both the base calibration and alternative parameterization. Summary statistics for the 2014 base and alternative calibration runs are presented in Table 13. In terms of chlorophyll-a, we consider the base calibration slightly superior to the alternative.

Table 12. Values of several key parameters under the base calibration and alternative calibration for the year 2014.

| Model run | WS1 (m/d) | WS2 (m/d) | Khn1 (g N/m ³) | Khn2 (g N/m ³) | KLDC (1/d) | KLPC (1/d) | PM1 (g C/g Chl/d) | PM2 (g C/g Chl/d) |
|------------------|--------------|--------------|-------------------------------|-------------------------------|---------------|---------------|----------------------|----------------------|
| Base calibration | 0.4 | 0.2 | 0.06 | 0.06 | 0.025 | 0.01 | 350 | 450 |
| Alternative | 0.28 | 0.26 | 0.06 | 0.06 | 0.025 | 0.007 | 350 | 315 |

Table 13. Statistics for 2014 base calibration and alternative parameterization runs.

| Model run | Statistic | DO | NH ₄ | NO ₃ -NO ₂ | Chl-a |
|------------------------------|------------------------------------|-------|-----------------|----------------------------------|-------|
| Base calibration | R | 0.86 | 0.43 | 0.83 | 0.52 |
| | RMSE (mg/L, except Chl-a in µg/L) | 0.82 | 0.02 | 0.07 | 3.27 |
| | NRMSE (mg/L, except Chl-a in µg/L) | 0.53 | 1.00 | 0.68 | 0.88 |
| | Bias (mg/L, except Chl-a in µg/L) | -0.08 | 0.01 | -0.006 | 0.03 |
| | NBias | -0.05 | 0.5 | -0.06 | 0.01 |
| Alternative parameterization | R | 0.86 | 0.43 | 0.82 | 0.52 |
| | RMSE (mg/L except µg/L for Chl-a) | 0.82 | 0.02 | 0.07 | 3.28 |
| | NRMSE (mg/L, except Chl-a in µg/L) | 0.53 | 1.00 | 0.68 | 0.88 |
| | Bias (mg/L except µg/L for Chl-a) | -0.07 | 0.01 | 0.005 | -0.04 |
| | NBias | -0.05 | 0.5 | -0.04 | -0.01 |

The base calibration (red dot) and the alternative (blue dot) fall into the same cluster, and one on top of the other in the DO Taylor plot (Figure 35). They fall very close to each other in the plots for the other parameters. Both parameterizations show high skill with respect to the spread of the predictions since the normalized standard deviation falls on the ideal line (1), signifying that the spread of predictions around the DO mean is the same as the spread of observations around the DO mean. The rest of the statistics (R and uRMSE) are similar for all the variables.

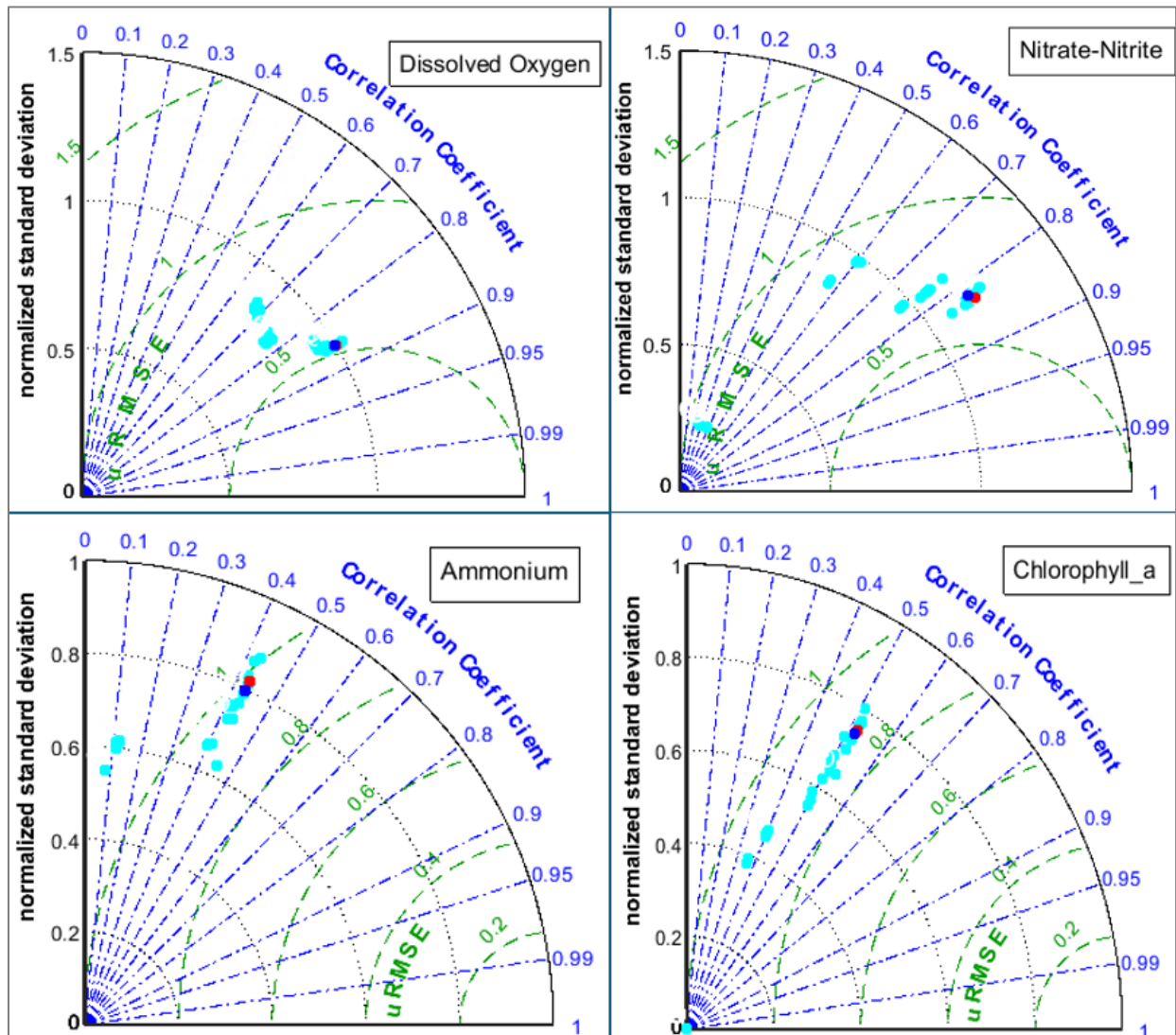


Figure 35. Taylor plots for sensitivity runs for dissolved oxygen, nitrate-nitrite, ammonium, and chlorophyll-a.

The red dot is the base calibration, the blue dot is the chosen alternative parameter set discussed above, and the cyan dots are the rest of the 60 sensitivity runs.

We calculated DO noncompliances using this alternative parameterization set (using both existing and reference condition runs with the same set of parameter values) and compared them with those for the 2014 base calibration. The run with the alternative parameterization

set gave the same maximum magnitude of noncompliance of -1.1 mg DO/L as the 2014 base calibration run. However, the non-compliant area was 2 Km² (0.4%) larger in the alternative parameter set (469 Km²) compared with the base calibration run (467 Km²). The noncompliant days in terms of grid-cell-days were 127 days less (0.16%) in the alternative parameter set (80152 days) compared with the base calibration run (80279 days). Appendix N contains planview maps for noncompliance calculated using both the base calibration run (Existing 2014) and the alternative parameter set.

As an example, we also compared DO noncompliances between the Opt2_8 scenario and Opt2_8 with the alternative parameter set. The maximum magnitude of noncompliance and the area of noncompliance are essentially the same between the two. However, the Opt2_8 scenario had 1 day of noncompliance more than the Opt2_8 scenario with the alternative parameter set. Appendix N contains noncompliance planview maps of both Opt2_8 and Op2_8 with the alternative parameter set.

In summary, the compliance results calculated using both the base calibration and the alternative parameterization for existing and Opt2_8 scenarios are very close.

Uncertainty in DO depletion estimates

One key feature of the noncompliance computations involves the difference between the existing and the reference scenario compared with the human allowance of 0.2 mg/L. This section covers how we estimate the uncertainty with respect to DO depletions resulting from subtracting the output from one scenario from that of another. As noted below, the scenarios are run with exactly the same forcings except for differences in loadings (existing condition includes all loadings, whereas the reference condition excludes local and regional anthropogenic loading).

Mechanistic models are typically used to understand the sensitivity of a system to a perturbation or change. We simulated a response using SSM to a finite, targeted change in the system, resulting from different input loads. We know the errors associated with how the model represents the existing scenario because we can compute them from differences with observations. We *accept* the errors associated with the model and *recognize that such errors are present every time the model is used*. We assume that the error associated with the existing condition is also associated with a defined reference condition, and that its magnitude is equal. This is a reasonable assumption because exactly the same model and configurations (parameterization, model year, climate, hydrology, and ocean boundary conditions) are used for the reference condition as for the existing condition. The differences between existing and reference conditions are well within the observational range and variability.

To propagate the error associated with taking the difference of two model runs, we use the standard equation for differences of variances (Snedecor and Cochran 1989). Error for the existing prediction is defined as: $P_{ex}-O_{ex}$, and error for reference prediction is defined as: $P_{ref}-O_{ref}$, where:

P_{ex} = Predicted existing condition

P_{ref} = Predicted reference condition

O_{ex} =Observation of existing condition.

O_{ref} =Observation of reference condition (an unattainable variable)

We use the square of the unbiased or centered RMSE ($RMSE_c$) to compute the variance of differences.

$$VAR_{diff} = VAR_{exist} + VAR_{ref} - 2 \times R \times RMSE_{c_{exist}} \times RMSE_{c_{ref}}$$

Where:

VAR_{diff} = variance of the difference of errors between existing and reference predictions, relevant to the DO depletion

VAR_{exist} = variance of errors of predictions under existing conditions ($RMSE_{c_{exist}})^2$

VAR_{ref} = variance of errors of predictions under reference conditions ($RMSE_{c_{ref}})^2$, which is assumed to be equal to the variance of errors under existing conditions.

R = Pearson's correlation coefficient between existing and reference condition errors, which approaches one based on the above assumption. It is approximated here with the correlation between existing and reference condition predictions, which, to three significant digits, equals 0.999 for all years.

$RMSE_{c_{diff}}$ = Unbiased root mean squared error of the DO depletion (the difference between the existing and reference scenarios) that is computed by taking the square root of VAR_{diff} .

The resulting values for $RMSE_{c_{diff}}$ are 0.04 mg/L DO for all years (2000, 2006, 2008, and 2014). In summary, when subtracting two model runs and using reasonable assumptions, we get a relatively precise answer with an estimated precision error less than the 0.2 mg/L human allowance.

Uncertainty in comparison with DO numeric criteria

Another key feature of the noncompliance computations involves comparing DO minima predicted for each grid cell and vertical layer to the established DO biologically based numeric criteria, which range from 4 to 7 mg/L, depending on location. To quantify the probability of error when computing whether predicted minima at a grid-cell-layer are above or below the DO numeric criteria, we tested whether each DO minimum prediction for each grid-cell-layer was above or below the DO numeric criteria at each location and time where observations are available. Each time predicted and observed minima are both above or both below the DO numeric criteria at a paired time within a grid-cell-layer constitutes a match between predictions and observations relevant to the applicable DO numeric threshold. With respect to

this test, false negative errors occur when the predicted minima are above the threshold and the observed minima are below it. False positive errors occur when the predicted minima are below the threshold and the observed minima are above it.

It is important to note that comparison with numeric criteria is a key feature of the noncompliance calculations, but it is not the only feature. So, a false negative or false positive result from this test does not necessarily mean that ultimately noncompliances resulted in false negatives or positives, since other parts of the noncompliance computation are also relevant in making a noncompliance calculation. The algorithm for noncompliance calculations is described in detail in Ahmed et al. 2021, Appendix F.

We conducted three tests using different groupings of observational data:

1. Using all the DO observations available for all four modeled years — 2000, 2006, 2008, and 2014
2. Using all the DO observations available for only year 2014
3. Using all the observations available for grid-cell-layers corresponding to locations that experienced noncompliances in 2014.

The results of these three tests are shown in Table 14.

Table 14. Probability of correct matches between DO predictions and observations, and of errors when comparing with DO numeric criteria threshold.

| Observations used in test | Number of data points ^a | Percent of matching cases ^b | Percent of false negative errors ^c | Percent of false positive errors ^d |
|---|------------------------------------|--|---|---|
| Observations from all modeled years | 19705 | 86.2% | 8.9% | 5% |
| Observations from 2014 | 4975 | 87.3% | 8.0% | 4.7% |
| Observations at locations that had at least one noncompliance in 2014 | 483 | 89.0% | 6.4% | 4.5% |

DO = dissolved oxygen.

^a Paired grid-cell-layers minima.

^b Prediction and observation DO minima are both above or both below the applicable DO numeric criteria.

^c Prediction minima were above DO numeric criteria, and the observed minima were below it.

^d Prediction minima were below the DO numeric criteria, and the observed minima were above it.

A proportion of an outcome is a probability. So, the numbers in Table 14 represent probabilities that SSM predictions and observations will match in terms of both being above or below the DO numeric criteria or diverge, in which case the error is considered either false negative or false positive. The calculated probabilities for a correct match between predictions and observations are high — varying from 89% to 86.2% — while the probabilities for false negative errors ranged from 6.4% to 8.9%, and for false positive errors ranged from 4.5% to 5%.

As mentioned before, this is not the only test used to determine compliance. Upon further investigation of the false negatives in the third test (row 3 in Table 14) we found that predictions of DO minima at deeper layers in the water column for that same grid-cell and date coincided with lower minima than the DO numeric criteria which was also reflected in corresponding observations, so the overall determination for the entire grid-cell for those dates often depended on the human allowance test rather than the DO numeric criteria test. We did find some false negatives that would not have been further tested with the human allowance test because the predicted reference DO concentration was high.

Conversely, for most of the false positives in row 3 in Table 14 which corresponded with a monitoring location in Hood Canal (HCB010) and contributing to 303(d) assessment units 1175 (47122G8G1) and 1176 (47122G8G2), we found that DO observational minima at vertical layers lower in the water column for that same grid-cell became lower than the DO numeric criteria. Therefore, although the grid cell had the potential to be noncompliant, none of the specific dates flagged as false positives in this test at that location were ultimately flagged as noncompliant due to the human allowance test in 303(d) assessment unit that we checked (47122G8G1).

In summary, these results show that model uncertainty with respect to the biologically based criteria is well within reasonable levels for noncompliance calculation purposes.

DO noncompliance

This section presents and compares DO noncompliance for existing conditions and for the refined Opt2 scenarios (see Glossary for definition of “noncompliance” in terms of this report). Appendix F of Ahmed et al. (2021) contains the compliance algorithm that we continue to use in this work. However, in the BSR and Opt1, DO noncompliance was calculated at every SSM grid-cell-layer. In this phase, DO noncompliance is now calculated as a volume-weighted average of all SSM grid cell-layers that fall within a 303(d) grid-cell-layer (discussed in more detail in Appendix D). Additionally, noncompliances are not evaluated in areas that are masked, which includes Budd Inlet (DO noncompliance in Budd Inlet is addressed via the Budd Inlet Dissolved Oxygen TMDL rather than via the PSNSRP).

DO noncompliances are expressed in a few different ways:

- **Area of DO noncompliance:** Aggregated area of DO noncompliance calculated by adding up the surface area of any 303(d) assessment unit that exhibits noncompliance anywhere within the ten vertical layers of the model grid at any point during the entire model year.
- **Maximum magnitude of DO noncompliance:** The maximum magnitude over the entire year of DO noncompliance at a specific location, calculated across all vertical layers of a 303(d) assessment unit over the entire year. The more negative this value is, the greater the magnitude of noncompliance.
- **Cumulative days of DO noncompliance:** The sum over the entire year of all days of DO noncompliance calculated by adding up each unique day of predicted noncompliance for a

specific 303(d) assessment unit. This value can be no more than 365 days for a single 303(d) assessment unit.

- **Total days of DO noncompliance:** The sum of all cumulative days of DO noncompliance within a larger spatial area, e.g., sum within each basin, or within all WA waters of the Salish Sea. This value can be greater than 365 (the number of days in a year) since it is calculated by adding up the cumulative days of DO noncompliance (defined above) associated with all 303(d) assessment units within the assessed area.

Noncompliance under existing conditions

Table 15 compares the total days, total area, and maximum magnitude of DO noncompliance between all four modeled years (2000, 2006, 2008, and 2014) for WA waters of the Salish Sea. In terms of interannual variability in the total number of days of noncompliance, 2006 had the most days of noncompliance, followed by 2014, 2000, and 2008. The year 2006 also had the highest area of noncompliance, followed by the years 2000, 2014, and 2008. The maximum magnitude of noncompliance is also greatest in 2006, followed by 2000, 2014, and 2008. Appendix N contains noncompliance planview maps for all four years under existing conditions.

For context, the magnitude of noncompliances is smaller than the differences in daily minima between reference and existing conditions in noncompliant areas. For instance, in 2014, the difference in daily DO minima between reference and existing conditions at noncompliant locations ranged from -0.3 to -1.3 mg/L, with a mean of -0.3 mg/L DO, whereas the noncompliance magnitude ranged from -0.1 to -1.1 mg/L, with a mean of -0.1 mg/L.

Table 15. DO noncompliance^a under existing conditions for the years 2000, 2006, 2008, and 2014 for WA waters of the Salish Sea.

| Year | Total days of noncompliance | Total area of noncompliance (km ²) | Maximum magnitude of DO noncompliance (mg/L) |
|------|-----------------------------|--|--|
| 2000 | 74,156 | 477 | -1.2 |
| 2006 | 136,367 | 621 | -1.4 |
| 2008 | 70,060 | 465 | -0.9 |
| 2014 | 80,279 | 467 | -1.1 |

^a Noncompliance excludes masked areas (e.g., Budd Inlet).

Noncompliance under Opt2 scenarios

This section presents model results in terms of DO noncompliance for all 10 refined Opt2 scenarios, which were run for the year 2014. It is important to note that PSNSRP delivers the necessary improvements in water quality to the Budd Inlet boundaries under that TMDL (refer to Appendix O).

Table 16 presents DO noncompliance results from the refined Opt2 model scenarios for all WA waters of the Salish Sea, which help answer the questions posed in Table 3 in terms of effect on noncompliance. Table 17 presents DO noncompliance results for each basin. Figure 36 compares the area and magnitude of noncompliance, and Figure 37 compares days of noncompliance across all these scenarios.

All 10 refined Opt2 scenarios significantly reduce the total days and area of DO noncompliance by over 99% relative to the noncompliance under existing 2014 conditions. All scenarios also result in the same reduction in terms of the maximum magnitude of DO noncompliance (from -1.1 mg/L under existing 2014 conditions to -0.1 mg/L DO).

Table 16. DO noncompliance^a and anthropogenic total nitrogen (TN) loads under existing conditions and for each of the refined ten Opt2 model scenarios for the year 2014.

| Opt2 scenario | Anthropogenic TN load (thousands of kg/year) | Percent reduction in anthropogenic TN load relative to existing | Total days of noncompliance | Total area of noncompliance ^a (km ²) | Maximum magnitude of DO noncompliance (mg/L) | Percent of area with zero noncompliance (relative to 2014 existing noncompliant area) |
|---------------|--|---|-----------------------------|---|--|---|
| Existing | 21,300 | 0% | 80,279 | 467 | -1.1 | 0.00% |
| Opt2_1 | 7,370 | 65.4% | 57 | 2.50 | -0.1 | 99.5% |
| Opt2_2 | 7,380 | 65.4% | 58 | 2.50 | -0.1 | 99.5% |
| Opt2_3 | 7,330 | 65.6% | 36 | 0.93 | -0.1 | 99.8% |
| Opt2_4 | 7,490 | 64.8% | 58 | 2.50 | -0.1 | 99.5% |
| Opt2_5 | 7,500 | 64.8% | 58 | 2.50 | -0.1 | 99.5% |
| Opt2_6 | 7,450 | 65.0% | 36 | 0.93 | -0.1 | 99.8% |
| Opt2_7 | 7,460 | 65.0% | 36 | 0.93 | -0.1 | 99.8% |
| Opt2_8 | 7,370 | 65.4% | 36 | 0.93 | -0.1 | 99.8% |
| Opt2_9 | 7,290 | 65.8% | 35 | 0.93 | -0.1 | 99.8% |
| Opt2_10 | 6,570 | 69.2% | 18 | 0.83 | -0.1 | 99.8% |

^a Noncompliance excludes masked areas (e.g., Budd Inlet).

Table 17. DO noncompliance associated with existing conditions and each of the refined ten Opt2 model scenarios for the year 2014 for each basin^a.

| Noncompliance (NC) metric | Basin | Existing | Opt2_1 | Opt2_2 | Opt2_3 | Opt2_4 | Opt2_5 | Opt2_6 | Opt2_7 | Opt2_8 | Opt2_9 | Opt2_10 |
|--|------------------------------------|---------------|-------------|-------------|-------------|-------------|-------------|-------------|-------------|-------------|-------------|-------------|
| Total days of NC | Northern Bays | 800 | -- | -- | -- | -- | -- | -- | -- | -- | -- | -- |
| | Whidbey Basin | 18,918 | -- | -- | -- | -- | -- | -- | -- | -- | -- | -- |
| | Main Basin | 911 | 55 | 56 | 34 | 56 | 56 | 34 | 34 | 34 | 33 | 18 |
| | South Sound | 8,220 | 2 | 2 | 2 | 2 | 2 | 2 | 2 | 2 | 2 | -- |
| | Hood Canal | 51,430 | -- | -- | -- | -- | -- | -- | -- | -- | -- | -- |
| | WA waters of the Salish Sea | 80,279 | 57 | 58 | 36 | 58 | 58 | 36 | 36 | 36 | 36 | 35 |
| Total area of NC (km²) | Northern Bays | 39.6 | -- | -- | -- | -- | -- | -- | -- | -- | -- | -- |
| | Whidbey Basin | 185 | -- | -- | -- | -- | -- | -- | -- | -- | -- | -- |
| | Main Basin | 13.4 | 2.40 | 2.40 | 0.83 | 2.40 | 2.40 | 0.83 | 0.83 | 0.83 | 0.83 | 0.83 |
| | South Sound | 80.6 | 0.11 | 0.11 | 0.11 | 0.11 | 0.11 | 0.11 | 0.11 | 0.11 | 0.11 | -- |
| | Hood Canal | 148 | -- | -- | -- | -- | -- | -- | -- | -- | -- | -- |
| | WA waters of the Salish Sea | 467 | 2.50 | 2.50 | 0.93 | 2.50 | 2.50 | 0.93 | 0.93 | 0.93 | 0.93 | 0.93 |
| Max. magnitude of DO NC (mg/L) | Northern Bays | -0.2 | -- | -- | -- | -- | -- | -- | -- | -- | -- | -- |
| | Whidbey Basin | -0.5 | -- | -- | -- | -- | -- | -- | -- | -- | -- | -- |
| | Main Basin | -1.1 | -0.1 | -0.1 | -0.1 | -0.1 | -0.1 | -0.1 | -0.1 | -0.1 | -0.1 | -0.1 |
| | South Sound | -0.8 | -0.1 | -0.1 | -0.1 | -0.1 | -0.1 | -0.1 | -0.1 | -0.1 | -0.1 | -- |
| | Hood Canal | -0.6 | -- | -- | -- | -- | -- | -- | -- | -- | -- | -- |
| | WA waters of the Salish Sea | -1.1 | -0.1 |

^a The following three basins have no DO noncompliance even under existing 2014 conditions and are not included in the table: Admiralty, SJF-US, SOG-US.
 -- = zero noncompliance.

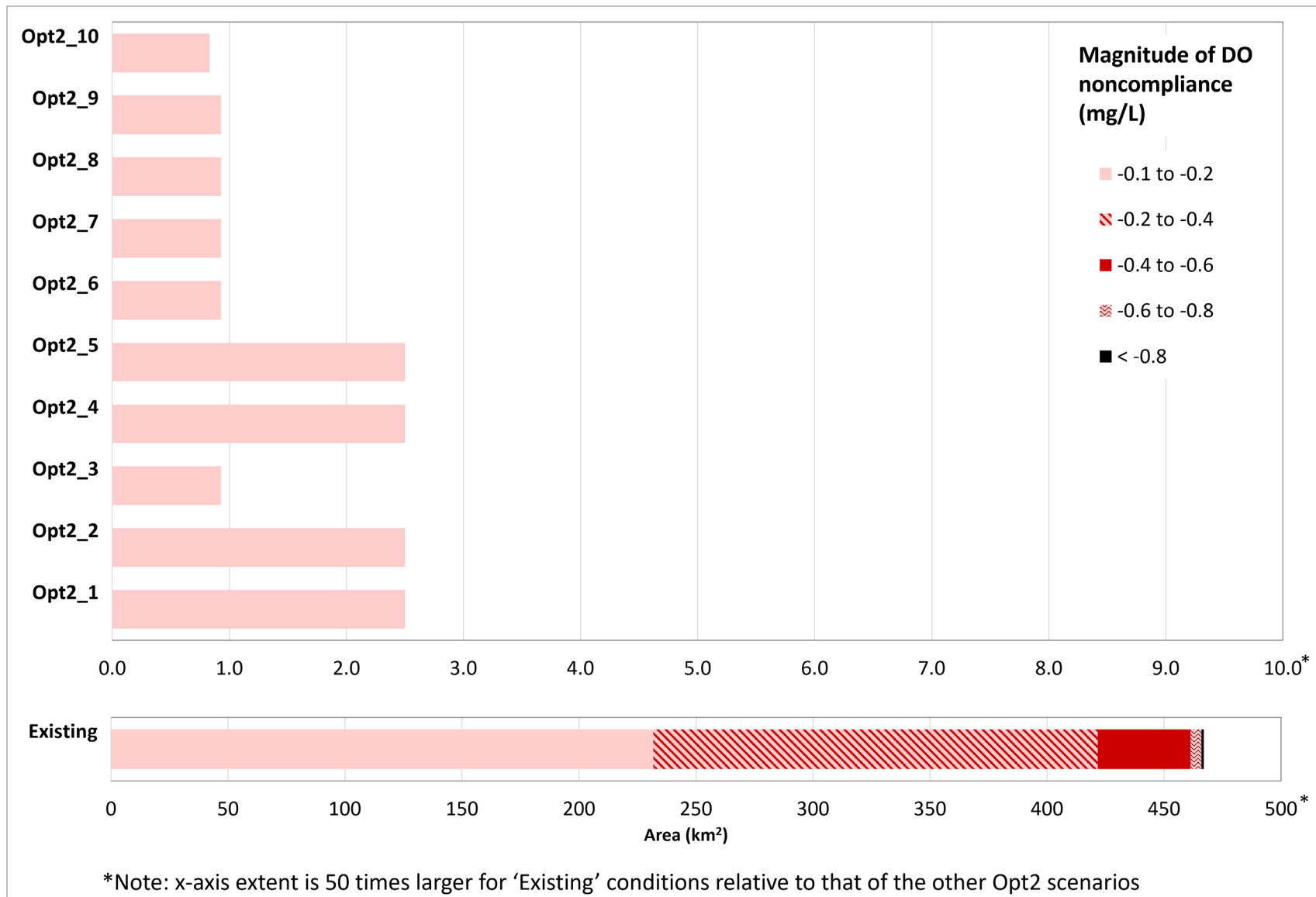


Figure 36. Area of DO noncompliance and maximum magnitude of DO noncompliance under existing conditions (bottom bar) and under each refined Opt2 model scenario for the year 2014.

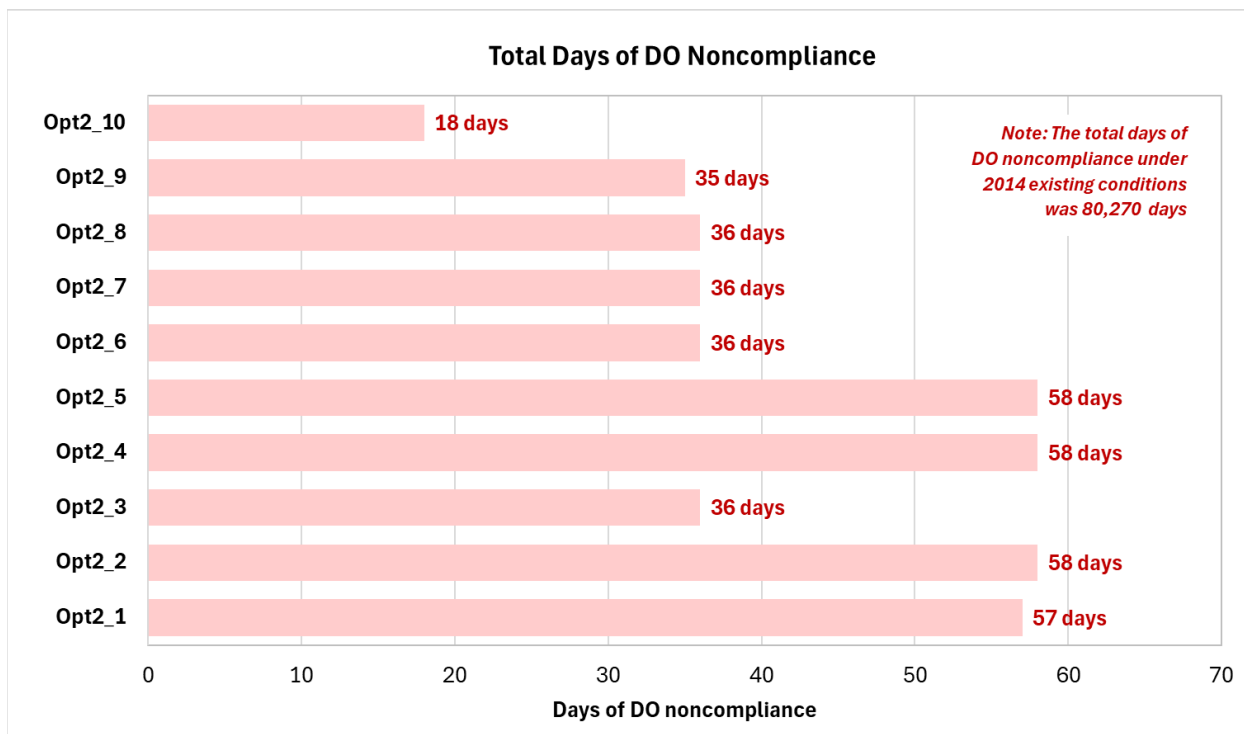


Figure 37. Total days of DO noncompliance under each refined Opt2 model scenario for the year 2014.

As a reminder, Opt2_1 through Opt2_6 test the effect of one or more of the following: holding very small WWTPs at existing 2014 loads, holding WWTPs discharging to specific basins at 2014 loads, and increasing BNR treatment for WWTPs discharging to Sinclair Inlet. Subsequently, Opt2_7 through Opt2_10 all include holding WWTPs in the very small category as well as WWTPs discharging to Hood Canal, Admiralty, SJF-US, and SOG-US at 2014 existing loads, and setting the three WWTPs within or near Sinclair Inlet at BNR 3/3/3 (while all other WWTPs are set at BNR 8/5/3). Opt2_8 and Opt2_9 then test the effect of additional BNR treatment during warm months at some or all dominant facilities discharging to Main Basin. Lastly, Opt2_10 tests the effect of all dominant facilities discharging to Main Basin at BNR3 year-round. These are described in more detail in Table 3.

Table 3 posed several questions that each of the refined Opt2_scenarios was designed to answer. Here, we present responses to those questions based on model results at the scale of WA waters of the Salish Sea.

1. **Holding nutrient loads from very small WWTPs at existing 2014 levels increased the incidence of noncompliances by 0 – 1 days:** We have three pairs of scenarios (Opt2_1 and Opt2_2, Opt2_4 and Opt2_5, and Opt2_6 and Opt2_7) where the only difference between them is that very small WWTPs are held in the latter. Opt2_2 only results in one additional day of DO noncompliance (in Sinclair Inlet) relative to Opt2_1, but the area and magnitude of noncompliance are the same between these two scenarios. Opt2_4 and Opt2_5, as well as Opt2_6 and Opt2_7, have identical DO noncompliances.

2. **Increasing BNR treatment at the three WWTPs discharging into or near Sinclair Inlet reduces DO noncompliances locally:** We have two pairs of scenarios (Opt2_1 and Opt2_3, and Opt2_4 and Opt2_6) where the latter scenario includes BNR3 year-round at all three WWTPs discharging into or near Sinclair Inlet. When comparing the noncompliances between each of the two scenario pairs, the latter scenario in each pair (which has BNR3 year-round for these three WWTPs) results in 22 fewer days and 1.57 km² less area of DO noncompliance, while the magnitudes of noncompliance remain the same at 0.1 mg/L.
3. **Holding nutrient loads from WWTPs discharging to Hood Canal, Admiralty, SJF-US, and SOG-US at existing 2014 levels increased the incidence of noncompliance by 1 day:** Opt2_4 has only one additional day of DO noncompliance relative to Opt2_1, and both scenarios show the same area and magnitude of noncompliance. The only difference between these two scenarios is that WWTPs' loads in these four basins are held in Opt2_4 at existing 2014 levels, but not in Opt2_1.
4. **Increasing BNR treatment during warm months at three of the four dominant Main Basin WWTPs (8/3/3) in Opt2_8 results in the same level of noncompliance as Opt2_7:** Opt2_7 and Opt2_8 result in the same number of days (36), area, and magnitude of DO noncompliance. The difference between these two scenarios is that in Opt2_7, all four dominant Main Basin WWTPs are at BNR 8/5/3 (BNR3 only during hot months), while in Opt2_8, three of these four dominant Main Basin WWTPs are at BNR 8/3/3 (BNR3 during warm *and* hot months — the exception is West Point, which remains at BNR 8/5/3).
5. **Increasing BNR treatment at all four dominant Main Basin WWTPs during warm months (8/3/3) in Opt2_9 results in one less day of DO noncompliance compared to Opt2_8:** The difference between these two scenarios is that in Opt2_9, West Point is set to BNR 8/3/3 (BNR3 during warm and hot months) to match the treatment levels applied to the other three dominant Main Basin WWTPs, while in Opt2_8, West Point remains at BNR 8/5/3 (BNR3 only during hot months).
6. **Increasing BNR treatment at all dominant WWTPs to 3/3/3, and all others set as in Opt2_7, resulted in the largest DO improvements.** The number of days of noncompliance (18 days) is the lowest under the Opt2_10 scenario.

These results show that all remaining DO noncompliances are in Main Basin (specifically in Sinclair Inlet) and South Sound (specifically in Henderson Inlet). The number of days of DO noncompliance and the area of DO noncompliance remain the same in South Sound across all refined Opt2 scenarios (two days of noncompliance and 0.11 km² area of noncompliance) except in Opt2_10, which resolves all remaining noncompliances in South Sound. Except for Opt2_10, all the Opt2 scenarios that involve BNR3 year-round for the three WWTPs in Sinclair Inlet result in similar days of noncompliance (33 – 34 days) and the same area of noncompliance (0.83 km²) in Main Basin. Opt_2 scenarios that do not have BNR3 year-round at these three facilities also result in a similar number of days of noncompliance (55 – 56 days) and the same area of noncompliance (2.40 km²).

Plan view maps of noncompliance

Figure 38 compares plan view maps of DO noncompliance between 2014 existing conditions and two of the 10 refined Opt2 scenarios (Opt2_5 and Opt2_10). The insets in the middle and right panel highlight remaining noncompliances in Sinclair and Henderson Inlets under both Opt2_5 and Opt2_10, except that in Opt2_10, zero noncompliances remain in Henderson Inlet. Relative to existing conditions, the area of noncompliance is reduced significantly from 467 km² under 2014 existing conditions to 2.50 km² and 0.83 km² in Opt2_5 and Opt2_10, respectively. This is a 99.5% and 99.8% reduction in noncompliant area under Opt2_5 and Opt2_10, respectively. The total number of days of noncompliance is reduced from 80,279 days under existing conditions to 36 and 18 days, respectively, under Opt2_5 and Opt2_10 (i.e., by greater than 99.9% in both scenarios). The maximum magnitude of DO noncompliance was reduced in both scenarios from -1.1 mg/L to -0.1 mg/L. This illustrates that zero noncompliance at most locations can be achieved with nitrogen and organic carbon load reductions from watersheds and WWTPs discharging into marine waters.

Figure 39 illustrates areas where remaining noncompliances persist in localized areas within Sinclair and Henderson Inlets across most of the 10 scenarios, in terms of cumulative days of noncompliance. As presented in Table 17, there are 18 to 56 remaining days of noncompliance in Sinclair Inlet, and two remaining days of noncompliance in Henderson Inlet across all scenarios except Opt2_10 (where no noncompliances remain in Henderson Inlet).

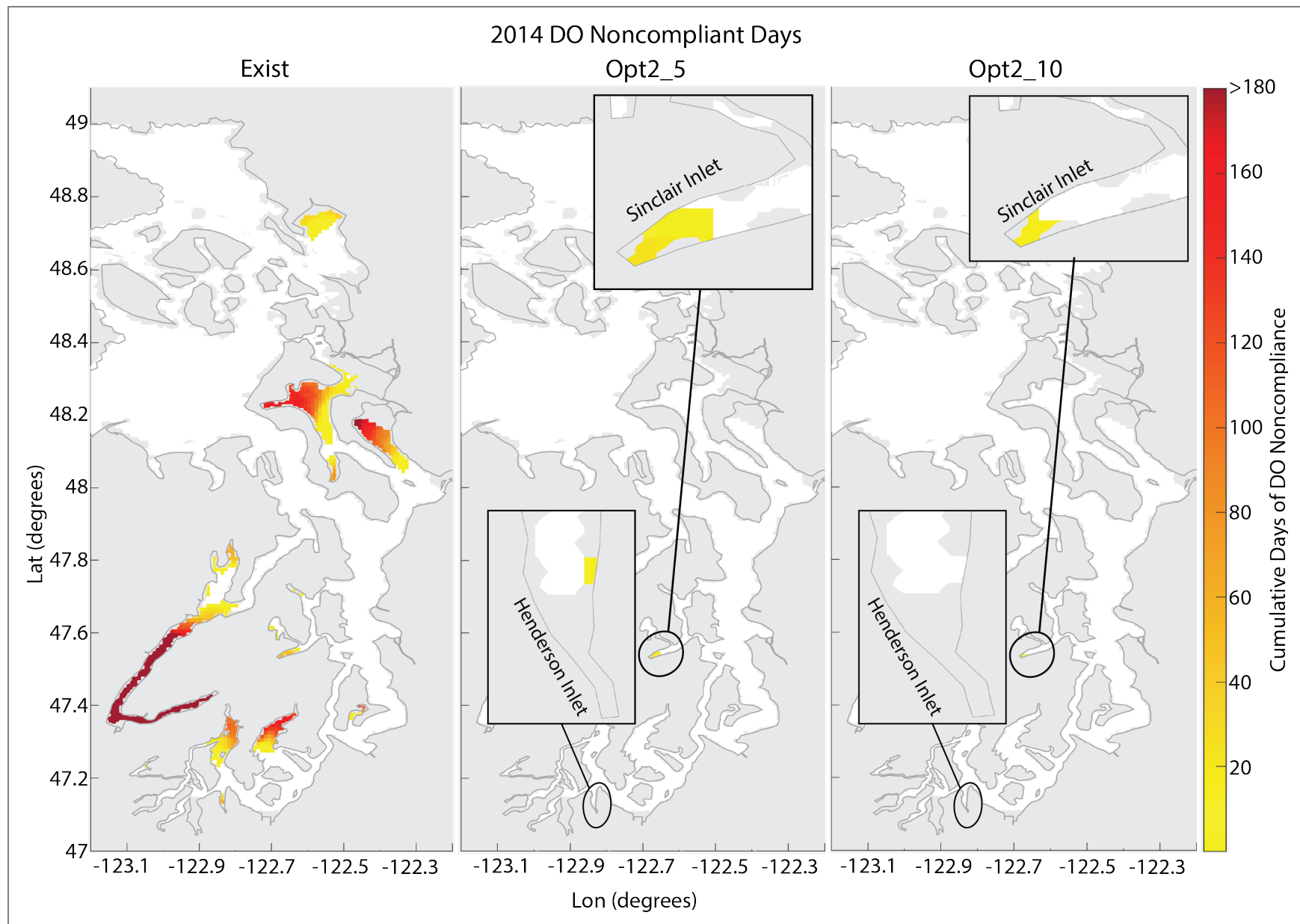


Figure 38. Cumulative days of DO noncompliance for 2014 existing (left), Opt2_5 (center), and Opt2_10 (right).

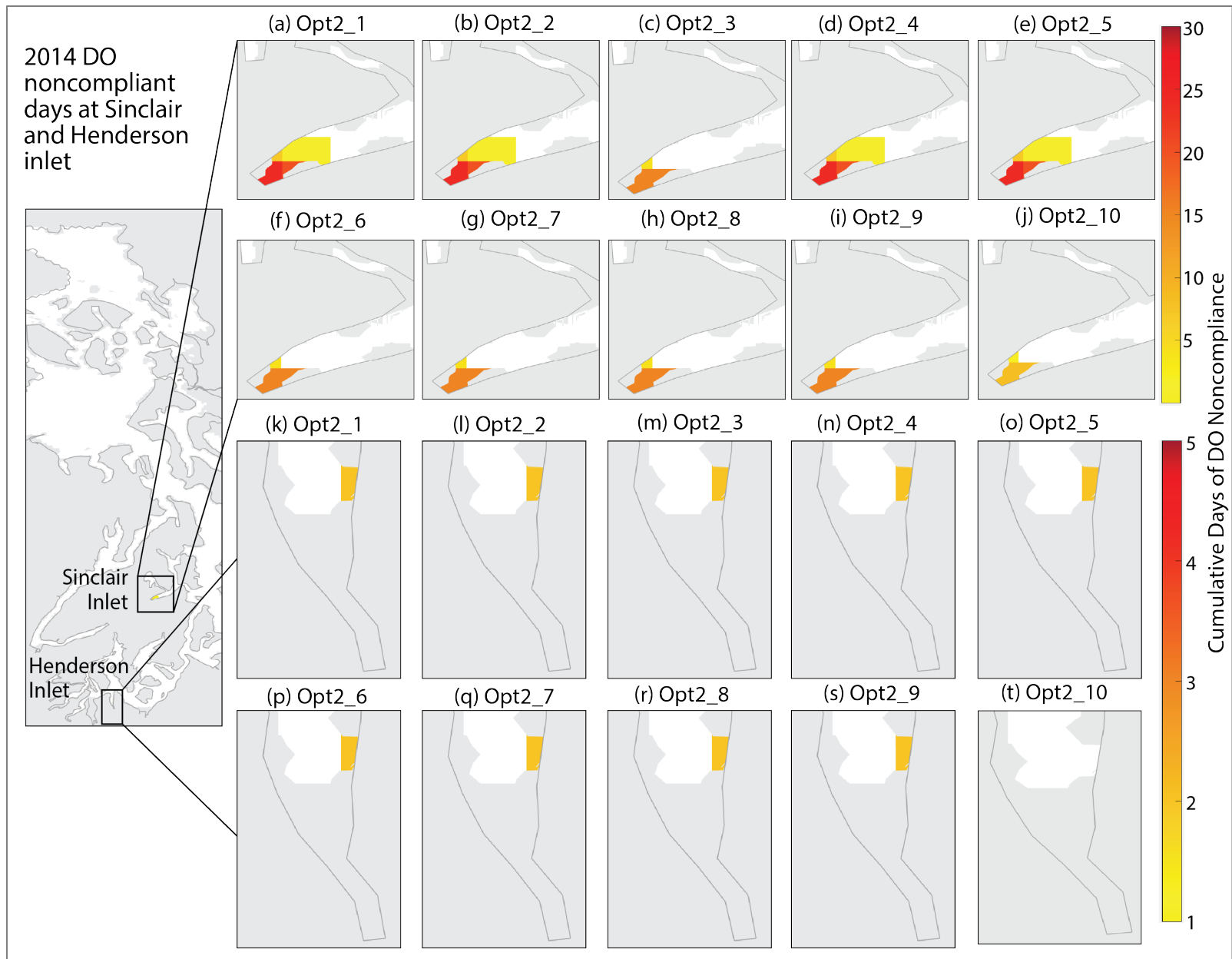


Figure 39. Cumulative days of DO noncompliance for all 10 refined Opt2 scenarios in Sinclair and Henderson Inlets.

Comparing noncompliance at specific locations

We compared noncompliance at three specific locations (Henderson Inlet, Sinclair Inlet, and Lynch Cove) to illustrate differences between various embayments. In the noncompliance calculations, comparisons are made to the biologically based numeric DO criteria and predicted reference DO concentrations, and rounding to the closest tenth mg/L DO is applied to each noncompliance per Appendix F of Ahmed et al. 2021, which contains a step-by-step description of the algorithm used.

Figures 40 – 42 each show the following information:

- The top left quadrant shows a location map of the site that the plots focus on. All plots are for the bottom water column layer in 2014. It also contains a legend that applies to all plots. The line labeled as the numeric criteria line refers to the biologically based numeric criteria that correspond to each location. The line labeled “Human Use Allowance (rounded)” (or HUA, defined in the glossary) refers to 0.2 mg/L depletion below the reference condition, rounded to the nearest 0.1 mg/L.
- The top right quadrant shows time series for the existing condition.
- The bottom left quadrant presents time series for Opt2_5, the refined scenario with the least amount of anthropogenic nitrogen reduction.
- The bottom right quadrant presents time series for Opt2_10, the refined scenario with the greatest amount of anthropogenic nitrogen reduction.

Henderson Inlet: Figure 40 shows the daily minimum DO time series at the bottom layer of 303(d) grid #124 (47122B8D2) located in Henderson Inlet. The noncompliant period, under the existing 2014 conditions, occurs between July and November, as shown in vertical dotted lines. In the Opt2_5 scenario, the non-compliant period shrinks to only two instances (the vertical lines are not shown due to the short duration) and to zero noncompliances in Opt_10. Under existing 2014 conditions, the total number of days of noncompliance for 303(d) grid #124 (47122B8D2) was 99 days, with the maximum magnitude of noncompliance at -0.8 mg/L DO. This was reduced to two days of noncompliance under Scenario Opt2_5, with a maximum magnitude of -0.1 mg/L, or a 98% reduction in days and 88% reduction in magnitude of noncompliance, and 100% reduction in both magnitude and days of noncompliance under Opt2_10.

Sinclair Inlet: Figure 41 shows the daily minimum DO time series at the bottom layer of 303(d) grid # 936 (47122F6D7) located in Sinclair Inlet. The non-compliant period under existing conditions occurs during the second half of 2014. In the Opt2_5 scenario, the non-compliant period shrinks down to two events between mid-July and September 2014. In Opt2_10, noncompliances occur between mid-July and mid-August. Under existing 2014 conditions, the total number of noncompliant days for 303(d) grid #936 (47122F6D7) was 58 days, with a maximum noncompliant magnitude of -1.1 mg DO/L. The noncompliance reduction at this assessment unit is about 59% (down to 24 days) and 86% (down to 8 days) under Opt2_5 and Opt2_10, respectively. The reduction of the maximum noncompliance magnitude is around 90% for both Opt2_5 and Opt2_10, as both of those scenarios have a maximum magnitude of noncompliance of -0.1 mg DO/L at this location.

Lynch Cove: Figure 42 shows the daily minimum DO time series at the bottom layer of 303(d) grid # 651 (47122D9J3) located in Lynch Cove. This is an interesting location to focus on because Hood Canal is the basin with the longest flushing time, and Lynch Cove, located at the head of Hood Canal, is the embayment with the longest residence time among the set we analyzed and reported on (see Residence and flushing times section).

As a result of the physical constraints at this location, the top left panel shows that noncompliances occurred in 2014 in Lynch Cove throughout the year, rather than seasonally. The low to no flushing and mixing conditions allow ample time for DO consumption due to biochemical processes in the sediments and in the water column itself to proceed until close to anoxic (0 mg/L DO) levels in the bottom layer. Under both Opt2_5 and Opt2_10, there are zero noncompliances at this location, and the minimum DO daily concentrations are improved by around 50% (Figure 43), but the extreme physical constraints which limit flushing time and produce long-term stratification, result in a singular pattern in which improved conditions means stepping away from anoxic, but still within hypoxic conditions, during the critical summer period at this location.

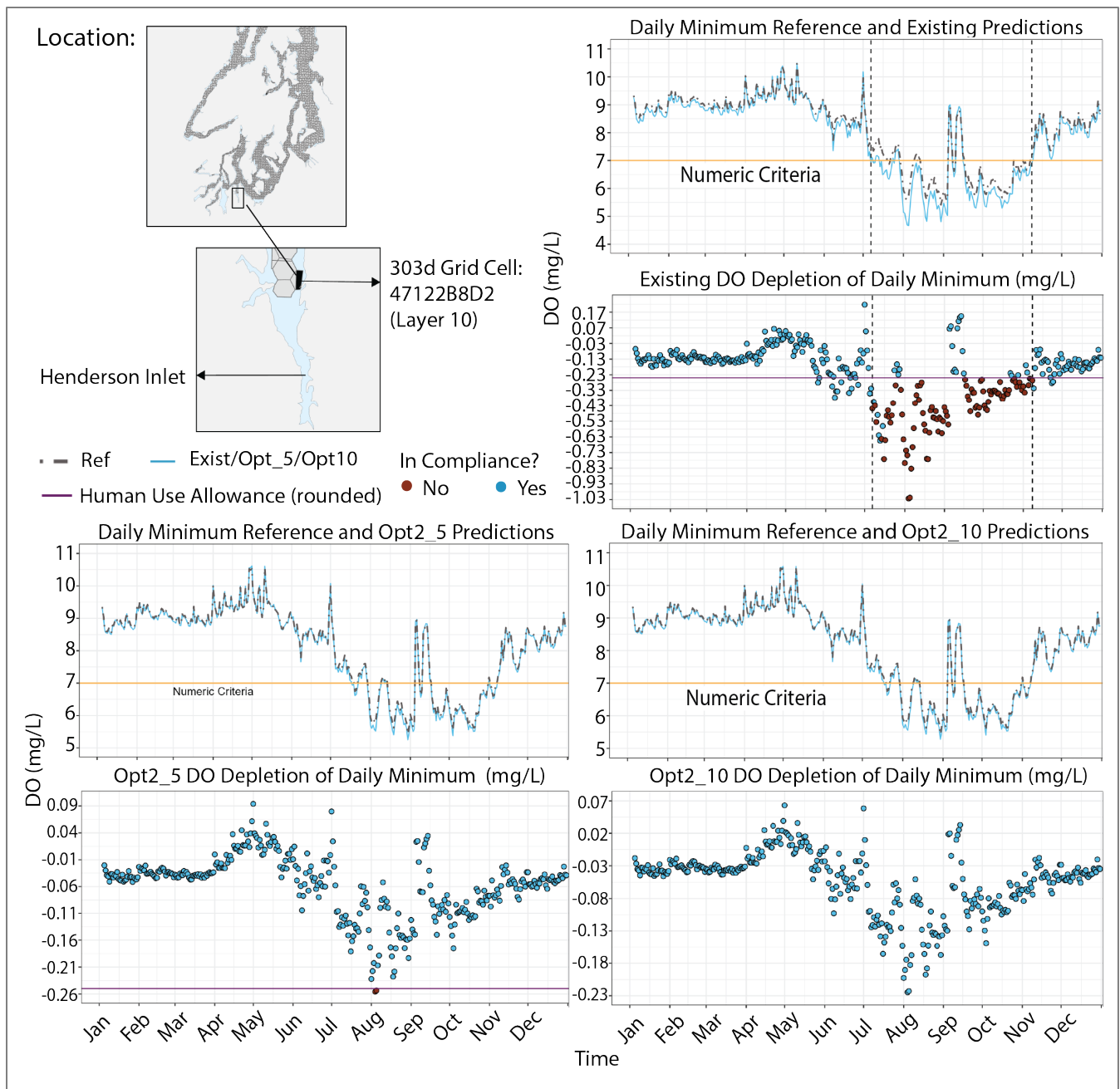


Figure 40. Predicted 2014 time series at Henderson Inlet 303(d) assessment units under reference, existing, and Scenario Opt2_5 and Opt2_10.

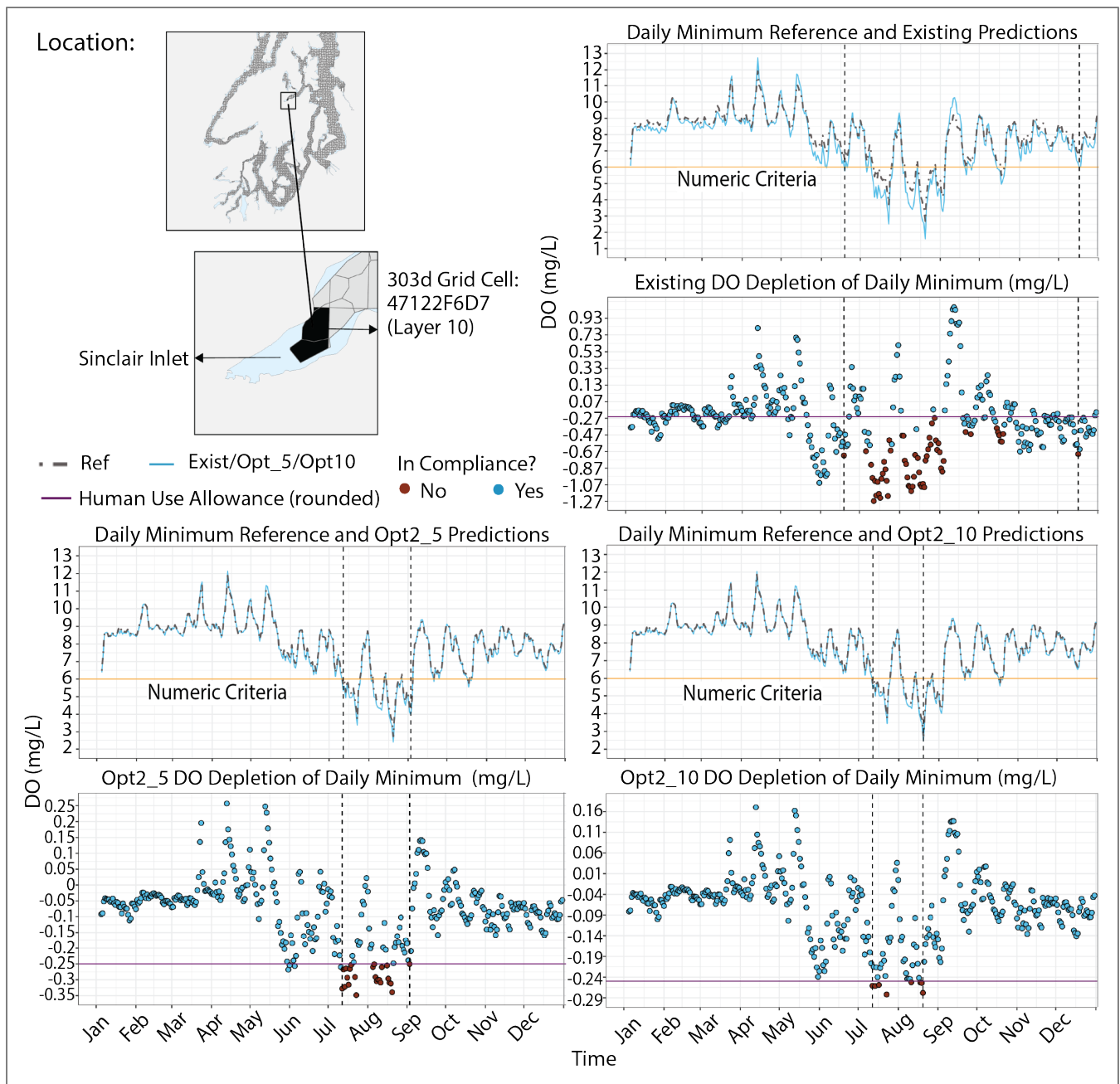


Figure 41. Predicted 2014 time series at Sinclair Inlet 303(d) assessment unit under reference, existing, and Scenarios Opt2_5 and Opt2_10.

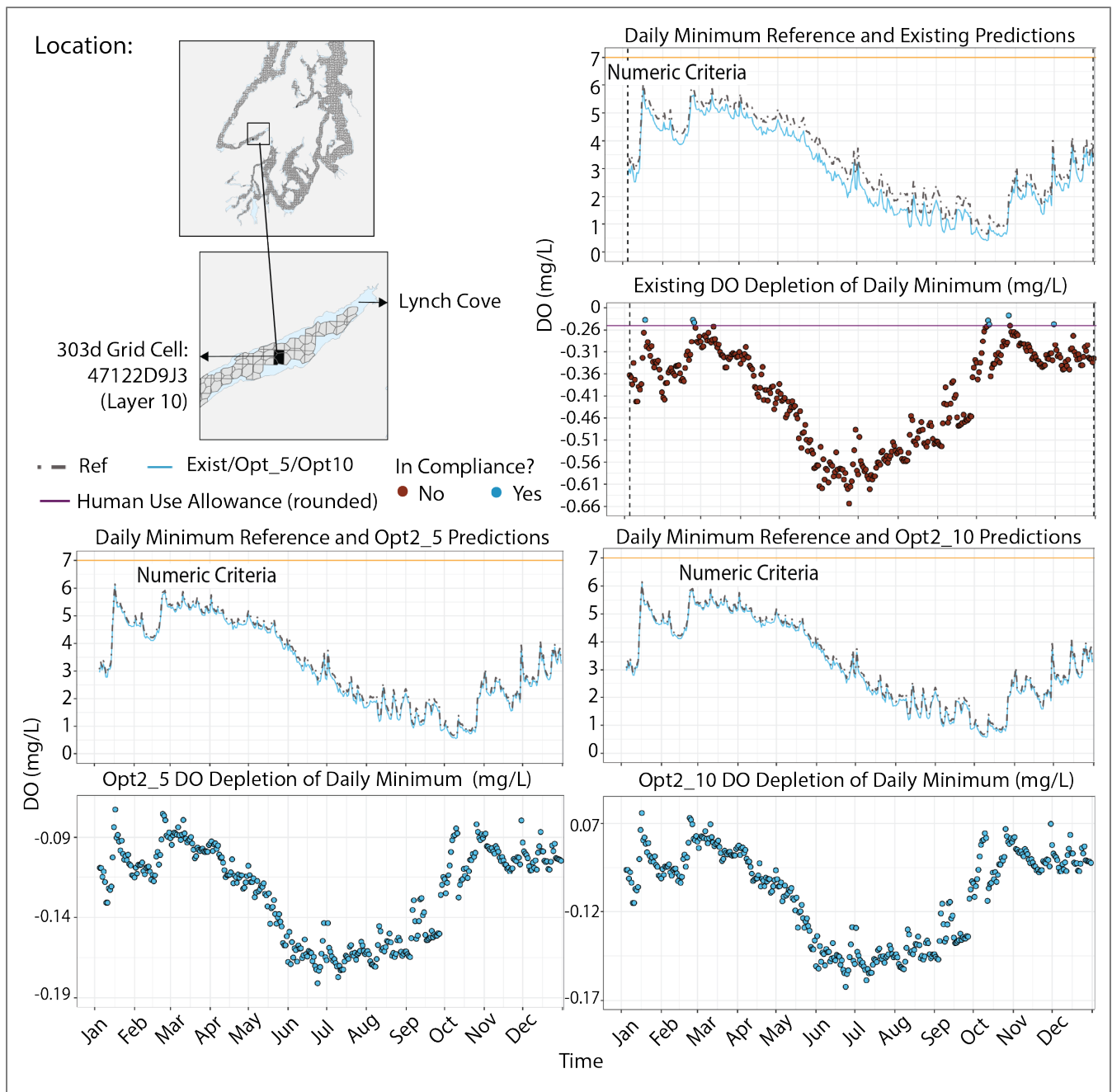


Figure 42 Predicted 2014 time series at Lynch Cove (Hood Canal) 303(d) grid assessment units under reference, existing, and Scenario Opt2_5 and Opt2_10.

Improvements in minimum DO in bottom layer and SOD

We present here results from Opt2_5 and Opt2_10 scenarios to show improvements, compared to existing conditions, in bottom layer minimum DO and sediment oxygen demand (SOD). In both scenarios, very small WWTPs and WWTPs in the Straits of Juan de Fuca and Georgia, Admiralty Inlet, and Hood Canal were left at existing conditions. In scenario Opt2_5, DIN in all other WWTPs was reduced to 8 mg/L, 5 mg/L, and 3 mg/L in cold, warm, and hot months, respectively. Scenario Opt2_10 was the same as Opt2_5 except that three WWTPs near Sinclair Inlet, as well as the dominant WWTP in Main Basin, had DIN reduced to 3 mg/L in all seasons.

Relative to 2014 existing conditions, SSM predictions in daily minimum DO improve in scenario Opt2_5 and Opt2_10. Maximum improvements of 1.06 (Opt2_5) and 1.11 (Opt2_10) DO mg/L are relatively large. The top panel in Figure 43 shows the difference in minimum DO concentration in the bottom layer of each grid cell between existing 2014 conditions and scenario Opt2_5 (left panel) and Opt2_10 (right panel). Note that the scale in this plot is truncated to 1 mg/L DO. Most of the bottom DO improvements under Opt2_5 and Opt2_10 scenarios are in the terminal inlets, with as much as 55% improvement in scenario Opt2_5 (lower left panel, Figure 43) and 58% improvement in scenario Opt2_10 (lower right panel in Figure 43).

We previously discussed that SOD is the biochemical process that consumes the largest percentage of DO in bottom layers of shallow inlets. The top panel in Figure 44 shows the reduction in maximum SOD between 2014 existing conditions and scenarios Opt2_5 (left panel) and Opt2_10 (right panel).

Although the scale in Figure 44 is truncated at $-0.7 \text{ g O}_2/\text{m}^2/\text{d}$, the maximum reduction in SOD under scenario Opt2_5 was $-0.73 \text{ g O}_2/\text{m}^2/\text{d}$ while that under scenario Opt2_10 was $-0.76 \text{ g O}_2/\text{m}^2/\text{d}$. This equates to 21.7% and 22.5% reduction in maximum SOD under scenario Opt2_5 (bottom left panel, Figure 44) and scenario Opt2_10 (bottom right panel, Figure 44), respectively, compared with existing conditions. The largest SOD reductions in Opt2_5 and Opt2_10 are in terminal inlets. The reduction in maximum SOD in Lynch Cove is near zero because that location is already hypoxic and so there is very little DO in the water column that can be taken up by sediments for aerobic decomposition of organic matter yet there is a large demand.

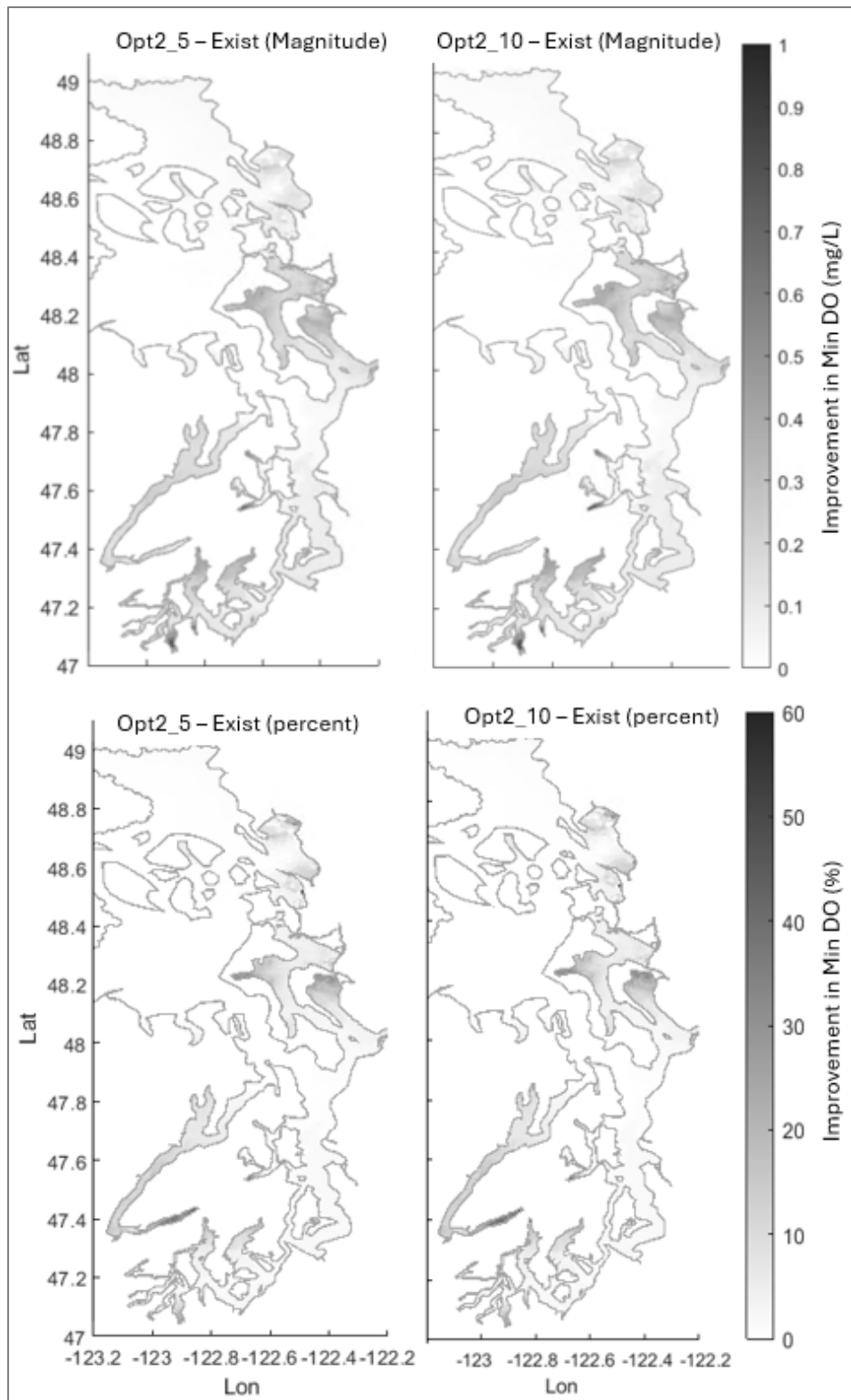


Figure 43. Planview map showing improvement in bottom layer minimum dissolved oxygen (DO) concentrations in terms of magnitude (top panel) and percent (bottom panel) between 2014 existing conditions and Scenario Op2_5 (left panel) and Scenario Opt2_10 (right panel).

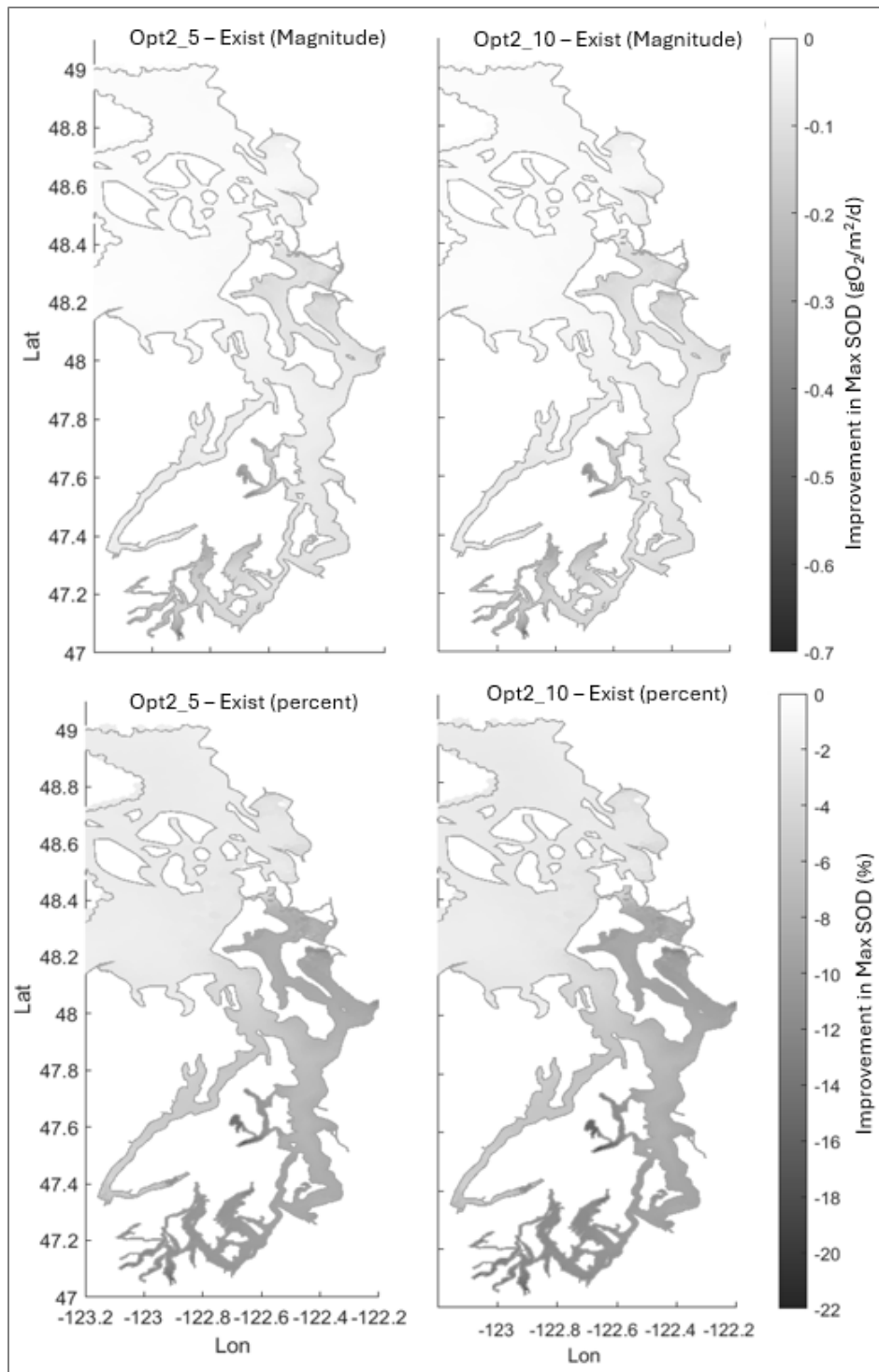


Figure 44. Planview map showing reduction in maximum sediment oxygen demand in terms of magnitude (top) and percentage (bottom) between 2014 Scenario Opt2_5 (left panel) and existing condition, and Scenario Opt2-10 (right panel) and existing condition, respectively.

Conclusions

Results of this study support the following conclusions, organized by categories:

- 1. Updates resulted in improved model skill compared to prior Salish Sea modeling work in support of the PSNSRP.** Ahmed et al. 2019 outlined steps for model improvements, which have been achieved.
 - Model performance water quality objectives for SSM applications, described in the QAPP (McCarthy et al. 2018), were met.
 - Updates to land-based loads via revised river regressions and review of point source loadings optimized inputs by providing higher sub-watershed scale resolution in some areas, and more accurately quantifying flows and daily loads for specific water quality variables in other instances.
 - The newer version of the hydrodynamic model used in this study allowed for the use of variable bottom friction. This, together with updated tidal constituents at the open boundary and the updated watershed inputs to the model, allowed for improved predictions of water surface elevations and currents.
 - In consultation with Carl Cerco, and through various model run trials, we concluded that a looped ten-year set of warm-up runs achieved stable labile POC concentrations in the sediment. In this phase of the work, all model runs followed this scheme of a looped ten-year warm-up set of runs followed by a one-year hot start run to get model outputs. This allowed for improvements in sediment flux predictions.
 - In terms of model code, we used FVCOM-ICM4 instead of FVCOM-ICM2. The newer version has a corrected photosynthetically available radiation (PAR) scheme that, in conjunction with changes to the reaeration scheme (Khangaonkar et al. 2021b), improved predictions.
- 2. The model demonstrated a high level of skill, particularly for bottom and middle layer DO predictions.**
 - SSM simulations show congruence in patterns in time and space when compared with available data.
 - The SSM reproduces seasonally low DO, particularly at inlets and bays, and reproduces its temporal variability. The model skill in the bottom and middle waters exceeds the model skill in surface layers.
 - The SSM simulates embayment locations with similar skill as open channel locations. The correlation coefficients were high (between 0.8 and 0.9) for all segregated bottom layer DO sets. The normalized, centered root mean square error, NRMSEc (or uRMSE), was 0.5 or less, and the normalized standard deviation hovered around 1. This indicates that, overall, SSM skill is high when predicting bottom water DO at either embayment or open channel stations.
 - The model predicts temperature, DO, salinity, and nitrate-nitrite within the Washington waters of the Salish Sea with higher skill than chlorophyll-a, PAR, and ammonium.

- 3. Simulated key biogeochemical processes in Salish Sea waters compare well with independent data sets.**
 - Model performance evaluation using independent data sets for sediment flux processes, gross and net primary productivity, and water column respiration demonstrated that the model produces results within expected ranges. These results add to the evidence that SSM adequately represents biogeochemical processes.
- 4. Sediment oxygen demand (SOD) can play a key role in oxygen consumption in Puget Sound's shallow inlets, particularly during periods when waters experience reduced flushing.**
 - The percentage of DO consumed via SOD compared to the total DO consumptive processes in the water column is higher in the winter and fall, when the algal populations, and accordingly algal respiration, are lower. In the spring, as algal populations quickly increase and boost the production of DO, algal respiration also increases, and SOD constitutes a lower portion of the total DO consumptive processes.
 - Of particular importance in shallow inlets during stratified conditions when mixing becomes restricted, SOD can consume the largest percentage of bottom DO (greater than 70% when considering the bottom 29% of the water column) compared to that consumed via water column biochemical processes. SOD consumes a lower percentage of DO when considering all the water column layers.
- 5. Flushing analysis points to the basins and heads of inlets with the longest flushing times.**
 - Basin flushing times in terms of e-folding times established using virtual dye suggest that Hood Canal has the longest flushing time, across all four years studied, followed by South Sound and Whidbey Basin. This aligns with results found in the literature.
 - For heads of inlets, the longest residence time was that of Lynch Cove, followed by Case Inlet, Carr Inlet, and Sinclair Inlet.
- 6. Model sensitivity analysis shows only one out of 60 parameter sets tested had skill statistics with almost identical skill to the base calibration. We did not find an alternative parameter set with better skill statistics.**
 - Of the 60 sensitivity runs that used randomly selected values of eight key parameters, only one alternative parameter set resulted in skill statistics analogous to the base calibration for the year 2014. In terms of DO noncompliance, the alternative set of parameters had the same maximum magnitude of noncompliance (-1.1 mg DO/L), fewer days (0.16%), and slightly higher area (0.4%) of noncompliance compared to the base calibration.
- 7. The difference of two model runs produces reasonably precise results with small, propagated errors.**
 - Based on reasonable assumptions about model error, when subtracting two model runs (existing and reference) to compute DO depletion, we get a precise answer with an estimated precision error (0.04 mg/L), or between 80% and 85% less than the 0.2 mg/L human allowance.

8. Model uncertainty with respect to the numeric criteria thresholds is between 11% and 14%.

- When comparing with the numeric criteria threshold, the calculated probabilities for a *correct* match between predictions and observations are high, varying from 89% to 86.2%. In comparison, the probabilities for false negative errors ranged from 6.4% to 8.9%, and for false positive errors ranged from 4.5% to 5%.

9. Opt2 scenarios results showed the potential for attaining zero noncompliance.

- Of the eight initial watershed nutrient reduction frameworks (Appendix L), the one that resulted in the least noncompliant areas and days was the framework with an overall watershed nutrient reduction of 58.9% (Framework H1, see Appendix L).
- Of the five initial WWTP reduction frameworks (Appendix L), the one that resulted in the least noncompliant areas and days was the framework where all U.S. WWTPs were set to BNR3, BNR5, and BNR8 in hot, warm, and cool months, respectively (Framework C, see Appendix L).
- Ten additional nutrient reduction scenarios were evaluated that further varied nutrient reductions from the best watershed and WWTP combination (H1_C). These 10 refined Opt2 scenarios significantly reduce the total days and area of DO noncompliance by over 99% relative to the noncompliance under existing 2014 conditions.
- Of these 10 refined scenarios, Opt2_6, Opt2_7, and Opt2_8 all resulted in the same level of DO noncompliance, but Opt2_8 involved slightly less nutrient reduction. The Budd Inlet TMDL open boundary “bubble allocation” was evaluated by holding loads entering Budd Inlet in scenario Opt2_8, as an example, to the Budd Inlet TMDL allocations. The “bubble allocation” was met for this scenario (Appendix O). The magnitude, area, and days of noncompliance were the same in this scenario compared to Opt2_8.

Recommendations

Results of this study support the following recommendations:

- The Salish Sea Model (SSM) has demonstrated adequate skill at this intermediate scale. It can be used for Total Maximum Daily Load (TMDL) or advanced restoration plan applications and during implementation.
- Model approaches developed here can be adapted to modeling historical natural conditions in the Salish Sea. SSM can be used for multiple applications, including analyses pertaining to eutrophication and quantification of human impacts.
- Consistently updating the input file database for SSM (every 2 – 3 years) is necessary to keep it ready for future work connected to implementation or other policy questions.
- Future analysis of watershed inputs can be integrated with recently completed dynamic Puget Sound SPARROW (SPATIally-Referenced Regression On Watershed attributes) results (Schmadel et al. 2025) to understand links between discharges to marine waters that are input into the SSM and upstream sources.
- Refined-scale analyses, including compiling past data and conducting future location-specific, transect-based field monitoring efforts and modeling studies, may be considered if there is a need to understand DO dynamics in areas that were masked due to model limitations.
- Collaboration with other entities to develop changes to domain-scale hydrology that would be necessary to conduct future climate scenarios. These updates may be needed to shape policy.

References

- Ahmed, A., G. Pelletier, and M. Roberts. 2017. South Puget Sound flushing times and residual flows. *Estuarine, Coastal and Shelf Science* 187: 9 – 21.
<https://doi.org/10.1016/j.ecss.2016.12.027>.
- Ahmed A., C. Figueroa-Kaminsky, J. Gala, T. Mohamedali, G. Pelletier, and S. McCarthy. 2019. Puget Sound Nutrient Source Reduction Project, Volume 1: Model Updates and Bounding Scenarios. Publication 19-03-001. Washington State Department of Ecology, Olympia.
<https://apps.ecology.wa.gov/publications/SummaryPages/1903001.html>
- Ahmed A., J. Gala, T. Mohamedali, C. Figueroa-Kaminsky, and S. McCarthy. 2021. Technical Memorandum: Puget Sound Nutrient Source Reduction Project – Optimization Scenarios Phase 1.
https://www.ezview.wa.gov/Portals/_1962/Documents/PSNSRP/TechMemoPSNSRPOptimizationScenariosPhase1.pdf
- Aura Nova Consultants, Inc., Brown and Caldwell, Evans-Hamilton, J.E. Edinger and Associates, WA Department of Ecology, and the University of Washington Department of Oceanography. 1998. Budd Inlet Scientific Study Final Report. Prepared for the LOTT Partnership, Olympia, Washington.
- Albertson, S., J. Newton, L. Eisner, C. Janzen and S. Bell. 1995. Sinclair and Dyes Inlet Seasonal Monitoring Report, Washington State Department of Ecology Publication No. 95-345
- Apple, J., and S. Bjornson. 2019. Spatial and seasonal variability in Salish Sea bottom-water microbial respiration, Final Project Report. EIM Data Link:
<https://apps.ecology.wa.gov/eim/search/Detail/Detail.aspx?DetailType=Study&SystemProjectId=99971985>.
- Barnes, C., and E. Collias. 1958. Some Considerations of Oxygen Utilization Rates in Puget Sound, University of Washington, Department of Oceanography, Technical Report 74.
- Belley, R., P. Snelgrove, P. Archambault, and S.K. Juniper. 2016. Environmental Drivers of Benthic Flux Variation and Ecosystem Functioning in Salish Sea and Northeast Pacific Sediments. *PLoS ONE* 11 (3): e0151110.
<https://doi.org/10.1371/journal.pone.0151110>
- Bernhard, A., and E. Peele. 1997. Nitrogen Limitation of Phytoplankton in a Shallow Embayment in Northern Puget Sound, *Estuaries* Vol. 20, No. 4, p. 759 – 769.
- Bowen, J., and J. Hieronymus. 2000. Neuse River Estuary Modeling and Monitoring Project Stage I: Predictions and Uncertainty Analysis of Response to Nutrient Loading Using a Mechanistic Eutrophication Model, University of North Carolina, WRRP Project No. 50222

- Burchard H., K. Bolding, R. Feistel, U. Gräwe, K. Klingbeil, P. MacCready, V. Mohrholz, L. Umlauf, and E.M. van der Lee. 2018. The Knudsen theorem and the Total Exchange Flow analysis framework applied to the Baltic Sea. *Progress in Oceanography*. Volume 165, July – August 2018, Pages 268 – 286.
<https://doi.org/10.1016/j.pocean.2018.04.004>
- Cerco, C., and T. Cole. 1993. Three-dimensional eutrophication model of Chesapeake Bay. *J Environ Eng* 119:1006 – 1025
- Cerco, C., and T. Cole. 1994. Three-Dimensional Eutrophication Model of Chesapeake Bay, US Army Corps of Engineers, Waterways Experiment Station, Technical Report EL-94-4
- Chen, C., R. Beardsley, and G. Cowles. 2006. An unstructured grid, finite-volume coastal ocean model: FVCOM User Manual, Second Edition, SMAST/UMASS-06-0602
- Cohn, T.A., L.L. Delong, E.J. Gilroy, R. M. Hirsch, and D. K. Wells. 1989. Estimating constituent loads. *Water Resources Research*. 25(5): 937 – 942.
<https://doi.org/10.1029/WR025i005p00937>.
- Cohn, T.A., D.L. Caulder, E. J. Gilroy, L D. Zynjuk, and R.M. Summers. 1992. The validity of a simple statistical model for estimating fluvial constituent loads: an empirical study involving nutrient loads entering Chesapeake Bay. *Water Resources Research*. 28(9): 2353 – 2363.
<https://doi.org/10.1029/92WR01008>.
- Di Toro, D. 2001. *Sediment Flux Modeling*, John Wiley & Sons, Inc.
- Diaz, R., and R. Rosenberg. 2008. Spreading dead zones and consequences for marine ecosystems. *Science* 321: 926 – 929.
- Ecology. 2022. Budd Inlet Dissolved Oxygen Total Maximum Daily Load, Water Quality Improvement Report and Implementation Plan, Washington State Department of Ecology, Olympia, Publication 22-10-012.
<https://apps.ecology.wa.gov/publications/SummaryPages/2210012.html>
- Ecology. 2025. Puget Sound Nutrient Source Reduction Plan: An advanced restoration approach to recovering water quality in Puget Sound, Washington State Department of Ecology, Olympia. Publication 25-10-038.
<https://apps.ecology.wa.gov/publications/SummaryPages/2510038.html>
- Glibert, P.M., S. Seitzinger, C.A. Heil, J.M. Burkholder, M.W. Parrow, L.A. Codispoti, and V. Kelly. 2005. The role of eutrophication in the global proliferation of harmful algal blooms. *Oceanography* 18 (2): 198 – 209.
<https://doi.org/10.5670/oceanog.2005.54>.
- Howarth, R., F. Chan, D. Conley, J. Garnier, S. Doney, R. Marino, and G. Billen. 2011. Coupled biogeochemical cycles: Eutrophication and hypoxia in temperate estuaries and coastal marine ecosystems. *Frontiers in Ecology and the Environment* 9(1): 18 – 26.
<https://doi.org/10.1890/100008>.

- Jolliff, J., J. Kindle, I. Shulman, B. Penta, M.A. Friederichs, R. Helber, and R.A. Arnone. 2009. Summary diagrams for coupled hydrodynamic-ecosystem model skill assessment, *Journal of Marine Sciences*, 76, 64 – 82.
<https://doi.org/10.1016/j.jmarsys.2008.05.014>.
- Khangaonkar, T., Z. Yang, T. Kim, and M. Roberts. 2011. Tidally averaged circulation in Puget Sound sub-basins: Comparison of historical data, analytical model, and numerical model. *Journal of Estuarine Coastal and Shelf Science* 93(4): 305 – 319.
<https://doi.org/10.1016/j.ecss.2011.04.016>.
- Khangaonkar, T., B. Sackmann, W. Long, T. Mohamedali, and M. Roberts. 2012. Simulation of annual biogeochemical cycles of nutrient balance, phytoplankton bloom(s), and DO in Puget Sound using an unstructured grid model. *Ocean Dynamics* 62(9): 1353 – 1379.
<https://doi.org/10.1007/s10236-012-0562-4>.
- Khangaonkar, T., W. Long, and W. Xu. 2017. Assessment of circulation and inter-basin transport in the Salish Sea including Johnstone Strait and Discovery Islands pathways. *Ocean Modelling* 109: 11 – 32.
<https://doi.org/10.1016/j.ocemod.2016.11.004>.
- Khangaonkar, T., A. Nugraha, W. Xu, W. Long, L. Bianucci, A. Ahmed, T. Mohamedali, and G. Pelletier. 2018. Analysis of hypoxia and sensitivity to nutrient pollution in Salish Sea. *Journal of Geophysical Research: Oceans* 123: 4735 – 4761.
<https://doi.org/10.1029/2017JC013650>.
- Khangaonkar, T., A. Nugraha, S.K. Yun, L. Premathilake, J. Keister and J. Bos. 2021a. Propagation of the 2014 – 2016 Northeast Pacific Marine Heatwave Through the Salish Sea. *Frontiers in Marine Science*. 8:787604.
<https://doi.org/10.3389/fmars.2021.787604>.
- Khangaonkar, T., A. Nugraha, S.K. Yun, L. Premathilake, J. Keister, and A. Borde. 2021b. Projections of algae, eelgrass, and zooplankton ecological interactions in the inner Salish Sea – for future climate, and altered oceanic states, *Ecological Modeling* 441:109420.
<https://doi.org/10.1016/j.ecolmodel.2020.109420>.
- Khangaonkar, T., and S.K. Yun. 2023. Estuarine nutrient pollution impact reduction assessment through euphotic zone avoidance/bypass considerations. *Frontiers in Marine Science*. 10:1192111.
<https://doi.org/10.3389/fmars.2023.1192111>.
- Kim, T., and T. Khangaonkar. 2012. An Offline Unstructured Biogeochemical Model (UBM) for Complex Estuarine and Coastal Environments. *Environmental Modelling & Software* 31: 47-63.
<https://doi.org/10.1016/j.envsoft.2011.11.010>.
- King County. 2025. Whidbey Bottle Data. Downloaded 1/21/2025
<https://data.kingcounty.gov/Environment-Waste-Management/Whidbey-Bottle-Data/vuu8-t6kc/data>.

- Landry, M., and B.M. Hickey, 1989. Coastal Oceanography of Washington and Oregon. Elsevier Oceanography Series, 47. Elsevier Science Publishers, New York, NY.
- Lincoln, J., and E. Collias. 1970. Skagit Bay Study, Progress Report No.3, University of Washington, Department of Oceanography, Ref. M70-111
- Lincoln, J., and E. Collias. 1975. An Oceanographic Study of the Port Orchard System, Final Report for the URS Company, M75-102, University of Washington, Department of Oceanography, Seattle, WA.
- MacCready, P., R.M. McCabe, S.A. Siedlecki, M. Lorenz, S.N. Giddings, J. Bos, S. Albertson, N.S. Banas, and S. Garnier. 2021. Estuarine circulation, mixing, and residence times in the Salish Sea. *Journal of Geophysical Research: Oceans* 126(2).
<https://doi.org/10.1029/2020JC016738>.
- Mackas, D., and P. Harrison. 1997. Nitrogenous nutrient sources and sinks in the Juan de Fuca Strait/Strait of Georgia/Puget Sound estuarine system: Assessing the potential for eutrophication. *Estuarine, Coastal and Shelf Science* 44: 1 – 21.
- McCarthy, S., C. Figueroa-Kaminsky, A. Ahmed, T. Mohamedali, and G. Pelletier. 2018. Quality Assurance Project Plan: Salish Sea Model Applications. Publication 18-03-111. Washington State Department of Ecology, Olympia.
<https://fortress.wa.gov/ecy/publications/SummaryPages/1803111.html>.
- Merritt, E. 2017. The influence of sedimentary biogeochemistry on oxygen consumption and nutrient cycling in Bellingham Bay, Washington. Thesis, Western Washington University, NSF REU at Shannon Point Marine Center, Anacortes.
- Mohamedali T., M. Roberts, B. Sackmann, and A. Kolosseus, 2011. Puget Sound Dissolved Oxygen Model Nutrient Load Summary for 1999 – 2008. Publication No. 11-03-057, Washington State Department of Ecology, Olympia, Washington.
<https://apps.ecology.wa.gov/publications/summarypages/1103057.html>
- Moore, S., N. Mantua, J. Newton, M. Kawase, M. Warner, and J. Kellogg. 2008. A descriptive analysis of temporal and spatial patterns of variability in Puget Sound oceanographic properties. *Estuarine, Coastal and Shelf Science* 80, 545 – 554.
<https://doi.org/10.1016/j.ecss.2008.09.016>.
- Morgan, M.G., and M. Henrion. 1990. *Uncertainty: A Guide to Dealing with Uncertainty in Quantitative Risk and Policy Analysis*. New York: Cambridge University.
- Newton, J., and R.A. Reynolds. 2002. Oceanographic Field Studies in South Puget Sound, Chapter 2 of South Puget Sound Water Quality Study, Phase 1. Publication 02-03-021. Washington State Department of Ecology, Olympia.
<https://apps.ecology.wa.gov/publications/SummaryPages/0203021.html>
- Newton, J., and K. Van Voorhis. 2002. Seasonal Patterns and Controlling Factors of Primary Production in Puget Sound's Central Basin and Possession Sound. Publication 02-03-059.

- Newton, J.A., M. Edie, and J. Summers. 1998. Primary productivity in Budd Inlet: Seasonal patterns of variation and controlling factors. Pp. 132 – 151 in Puget Sound Research '98 Proceedings. Puget Sound Action Team, Olympia, WA.
- Newton, J., S. Albertson, K. Van Voorhis, C. Maloy, and E. Siegel. 2002. Washington State Marine Water Quality, 1998 through 2000, Washington Department of Ecology Publication No. 02-03-056.
<https://apps.ecology.wa.gov/publications/SummaryPages/0203056.html>.
- Pamatmat, M. 1971. Oxygen consumption by the Seabed. VI. Seasonal Cycle of Chemical Oxidation and Respiration in Puget Sound. *International Review of Hydrobiology*. 56(5): 769 – 793.
<https://doi.org/10.1002/iroh.19710560505>.
- Peña, M., S. Katsev, T. Oguz, and D. Gilbert. 2010. Modeling dissolved oxygen dynamics and hypoxia. *Biogeosciences* 7(3): 933 – 957.
<https://doi.org/10.5194/bg-7-933-2010>.
- Premathilake L and T. Khangaonkar. 2022. Explicit quantification of residence and flushing times in the Salish Sea using a sub-basin scale shoreline resolving model. *Estuarine, Coastal and Shelf Science* 276 (108022).
<https://doi.org/10.1016/j.ecss.2022.108022>.
- PSEMP [Puget Sound Ecosystem Monitoring Program] Marine Waters Workgroup. 2015. Puget Sound marine waters: 2014 overview. S. K. Moore, R. Wold, K. Stark, J. Bos, P. Williams, K. Dzinbal, C. Krembs, and J. Newton (Eds).
<https://pspwa.app.box.com/s/hferayhcyzwvcxrao8uohnxjvbjxhpvt/file/96258176700>.
- PSEMP [Puget Sound Ecosystem Monitoring Program] Marine Waters Workgroup. 2016. Puget Sound marine waters: 2015 overview. S. K. Moore, R. Wold, K. Stark, J. Bos, P. Williams, K. Dzinbal, C. Krembs, and J. Newton (Eds).
https://www.nanoos.org/documents/misc/PS_Marine_Waters_2015-Overview.pdf.
- Rigby, E. 2019. Springtime benthic fluxes in the Salish Sea: Environmental parameters driving spatial variation in the exchange of dissolved oxygen, inorganic carbon, nutrients, and alkalinity between sediments and overlying water, Master of Science Thesis, Western Washington University.
- Roberts, M., S. Albertson, A. Ahmed, and G. Pelletier. 2014a. South Puget Sound Dissolved Oxygen Study: South and Central Puget Sound Water Circulation Model Development and Calibration. Publication 14-03-015. Washington State Department of Ecology, Olympia.
<https://apps.ecology.wa.gov/publications/SummaryPages/1403015.html>
- Roberts, M., T. Mohamedali, B. Sackmann, T. Khangaonkar, and W. Long. 2014b. Puget Sound and the Straits Dissolved Oxygen Assessment Impacts of Current and Future Human Nitrogen Sources and Climate Change through 2070. Publication 14-03-007. Washington State Department of Ecology, Olympia.
<https://apps.ecology.wa.gov/publications/SummaryPages/1403007.html>

- Santana, E. and D. Shull. 2023. Sedimentary Biogeochemistry of the Salish Sea: Springtime Fluxes of Dissolved Oxygen, Nutrients, Inorganic Carbon, and Alkalinity, *Estuaries and Coasts* 46:1208 – 1222
<https://doi.org/10.1007/s12237-023-01197-8>
- Schmadel, N., C. Figueroa-Kaminsky, D. Wise, J. Wasielewski, Z. Johnson, and R. Black. 2025. Preprint: Simulated seasonal loads of total nitrogen and total phosphorus by major source from watersheds draining to Washington waters of the Salish Sea, 2005 through 2020. ESS Open Archive.
<https://doi.org/10.22541/essoar.173878059.92247480/v1>
- Sheibley, R.W., and A.J. Paulson. 2014. Quantifying benthic nitrogen fluxes in Puget Sound, Washington—A review of available data: U.S. Geological Survey Scientific Investigations Report 2014 – 5033.
<https://doi.org/10.3133/sir20145033>.
- Shull, D. 2022. When and where does sediment have an important impact on nitrogen cycling and low dissolved oxygen impacts? Presentation at Puget Sound Institute event on October 17, 2022
- Snedecor, G., and W. Cochran. 1989. *Statistical Methods*, 8th ed. Iowa State University Press, Ames.
- Sutherland, D.A., P. MacCready, N. Banas, and L. Smedstad. 2011. A model study of the Salish Sea estuarine circulation. *Journal of Physical Oceanography* 41: 1125 – 1143
- Szpilka, C., K. Dresback, R. Kolar, and T.C. Massey. 2018. Improvements for the Eastern North Pacific ADCIRC tidal database (ENPAC15). *Journal of Marine Science and Engineering* 6(4) 131.
<https://doi.org/10.3390/jmse6040131>.
- Taylor, K., 2001. Summarizing multiple aspects of model performance in a single diagram, *JGR*, Vol. 106-D7
- Tetra Tech, Memorandum from John Hamrick to Mindy Roberts, March 12, 2010.
- Tetra Tech. 2011. Technical and Economic Evaluation of Nitrogen and Phosphorus Removal at Municipal Wastewater Treatment Facilities. Publication 11-10-060. Prepared for Washington State Department of Ecology, Olympia.
<https://apps.ecology.wa.gov/publications/SummaryPages/1110060.html>
- Thom, R., A. Copping, and R. Albright. 1988. Nearshore Primary Productivity in Central Puget Sound: A Case for Nutrient Limitation in the Nearshore Systems of Puget Sound. In *Proceedings, First Annual Meeting on Puget Sound Research*, Vol 2, March 18 – 19, 1988.
- USECoS Team, 2008. Eastern US continental shelf carbon budget: Integrating models, data assimilation, and analysis. *Oceanography* 21(1), pp.86 – 104.

- University of Washington NWEM Mooring Data, 2005 – 2024. Accessed June 6, 2024
<https://nwem.apl.washington.edu/>, enabled by the Northwest Association of Networked Ocean Observing Systems (NANOOS, <https://www.nanoos.org>) and the Washington State Ocean Acidification Center (WOAC, <https://oceanacidification.uw.edu/>).
- Waldichuk, M. and H. Gould. 1954. Chemistry of Puget Sound Waters and Influencing Factors, Department of Oceanography, University of Washington.
- Willmott, C. 1981. On the Validation of Models. *Physical Geography*, 2, 2, pp. 184 – 194
- Winter, D.F., K. Banse, and G.C. Anderson. 1975. The dynamics of phytoplankton blooms in Puget Sound, a fjord in the Northwestern United States. *Marine Biology* 29: 139–176.

Glossary, Acronyms, and Abbreviations

Glossary

303(d) Assessment Units (also referred to as 303(d) grid): Refers to units used to check compliance with Section 303-d of the Clean Water Act and consists of a grid of approximately 790 m × 1130 m rectangles.

Advective flux: Transport with bulk fluid flow.

Ammonium: A positively charged ion consisting of one nitrogen and four hydrogen atoms (NH_4^+).

Anoxic: Dissolved oxygen in the water column is near 0 mg/L.

Annual load: The sum of all daily loads from individual source(s) over the corresponding year.

Anthropogenic: Human-caused.

Area of DO noncompliance: Aggregated area of DO noncompliance calculated by adding up the surface area of any 303(d) assessment unit that exhibits noncompliance anywhere within the ten vertical layers of the model grid at any point during the entire model year.

Average annual load: The average of the daily loads from individual source(s) over the corresponding year.

Basin: Term used to describe distinct marine areas within WA waters of the Salish Sea, generally separated by shallow sills. In this report, we refer to the following eight basins: Northern Bays, Whidbey Basin, Main Basin, South Sound, Hood Canal, Admiralty, the U.S. portions of the Strait of Juan de Fuca (SJF-US), and Strait of Georgia (SOG-US).

Bias: Systematic error. See the equation for calculating this model skill statistic in Appendix D.

Biologically-based numeric criteria: See 173- 210A-210.

Biological Nitrogen Removal (BNR): General term for a wastewater treatment process that removes nitrogen through the manipulation of oxygen within the treatment train to drive nitrification and denitrification. Nitrogen removal efficiency depends on site-specific conditions, such as treatment processes, climate, and the overall strength of the raw wastewater.

BNR3: BNR treatment process resulting in no more than 3 mg/L DIN and no more than 8 mg/L carbonaceous BOD in WWTP effluent.

BNR5: BNR treatment process resulting in no more than 5 mg/L DIN and no more than 8 mg/L carbonaceous BOD in WWTP effluent.

BNR8: BNR treatment process resulting in no more than 8 mg/L DIN and no more than 8 mg/L carbonaceous BOD in WWTP effluent.

Bounding Scenarios Report (BSR): The first volume of the Salish Sea Model results for the Puget Sound Nutrient Source Reduction Project (Ahmed et al. 2019).

Centered (or unbiased) RMSE ($RMSE_c$): The portion of the total root mean squared error that does not include model bias. A perfect model would have zero centered RMSE. See the equation for calculating this model skill statistic in Appendix D.

Centered and normalized RMSE ($NRMSE_c$ or $uNRMSE$): Consists of the ratio of the centered RMSE (defined above) and the standard deviation of observations. See the equation for calculating this model skill statistic in Appendix D.

Clean Water Act: A federal act passed in 1972 that contains provisions to restore and maintain the quality of the nation's waters. The Clean Water Act requires states to establish water quality standards (Section 303(c)), identify impaired waters, and develop plans to clean up waters (Section 303(d)).

Compliance: For the purposes of this report, compliance refers to model predictions that meet the location-specific, local, and regional human allowance of the DO water quality criteria (WAC 173-201A-210(1)(d)(i)). See Appendix F in Ahmed et al. (2021).

Correlation coefficient (R): A measure of the closeness of a linear relationship between two variables (Snedecor and Cochran 1989). See the equation for calculating this model skill statistic in Appendix D.

Cumulative days of DO noncompliance: The sum over the entire year of all days of DO noncompliance calculated by adding up each unique day of predicted noncompliance for a specific 303(d) assessment unit. This value can be no more than 365 days for a single 303(d) assessment unit.

Diel: Of, or pertaining to, a 24-hour period.

Dissolved oxygen (DO): A measure of the amount of oxygen (O_2) dissolved in water.

Dominant wastewater treatment plants: Defined in Puget Sound Nutrient General Permit as facilities discharging loads greater than 2,000 lbs/day of Total Inorganic Nitrogen, which includes the following facilities: Everett, Brightwater, South King, Tacoma Central, West Point, Chambers Creek, and Bellingham.

Dominant Main Basin wastewater treatment plants: subset of dominant WWTPs (defined above) that discharge to the Main Basin, which includes the following facilities: Brightwater, South King, Tacoma Central, and West Point.

Euphotic zone: Vertical layer in the water column where light is available and photosynthesis takes place.

Effluent: An outflow of water from a natural body of water or from a man-made structure. For example, the treated outflow from a wastewater treatment plant.

Framework: Different reductions in anthropogenic TN and TOC mass loads from WWTPs and watersheds. There are WWTP frameworks and watershed frameworks.

Greater Puget Sound: Includes Samish, Padilla, and Bellingham Bays, as well as South Sound, Main Basin, Whidbey Basin, Admiralty Inlet, and Hood Canal (see also Puget Sound).

Grid-cell-layer: For the purposes of this report, refers to each individual longitudinal and vertical spatial representation of marine waters used in the SSM.

Gross primary productivity (GPP): The rate at which algae produce organic carbon via photosynthesis.

Halocline: a layer of rapidly changing salinity within a body of water that forms a boundary between the lower salinity near the surface layer and the higher salinity below.

Hindcast: Historical model run.

Human use allowance: A DO decrease from the modeled reference condition of no more than 0.2 mg/L (rounded to the nearest 0.1 mg/L). In this report, the HUA is applied when the reference condition is lower than the biologically based numeric criteria to account for the cumulative impact of local and regional human sources.

Hydrodynamic: Pertaining to the physics of fluid motion and the forces acting upon the fluid.

Hypoxic: Dissolved oxygen in the water column is lower than 2 to 3 mg/L.

Integrated Compartment Model (ICM): a biogeochemical water quality model, originally developed by Cerco and Cole (1993,1994).

Local and regional human-caused pollution: Pollution caused by human actions, and the pollution originates from: (1) Within the boundaries of the state; or (2) Within the boundaries of a U.S. jurisdiction abutting the state that impacts surface waters of the state (WAC 173-201A-020).

Marine point source: Point sources (see “point source” definition below) represented in the SSM that discharge directly to the Salish Sea or to a major river down gradient of the freshwater monitoring station used to represent watersheds. In most cases, these river discharges are to estuarine waters that are considered marine by definition in WAC 173-201A-260(3)(e).

Masked areas: Model nodes within the Salish Sea Model domain that are removed from analysis because of model limitations that do not allow for adequate predictions at these locations.

Maximum magnitude of DO noncompliance: The maximum magnitude of DO noncompliance at a specific location, calculated across all vertical layers of a 303(d) assessment unit over the entire year. The more negative this value is, the greater the magnitude of noncompliance.

Mean absolute error (MAE): A measure of model skill that consists of the average of the absolute differences between predictions and observations. See the equation for calculating this model skill statistic in Appendix D.

National Pollutant Discharge Elimination System (NPDES): National program for issuing, modifying, revoking and reissuing, terminating, monitoring, and enforcing permits, and imposing and enforcing pretreatment requirements under the Clean Water Act. The NPDES program regulates discharges from wastewater treatment plants, large factories, and other facilities that use, process, and discharge water back into lakes, streams, rivers, bays, and oceans.

Natural condition: Surface water quality present before any human-caused pollution (WAC 173-201A-020).

NetCDF: Network Common Data Form is a file format for storing multidimensional scientific data.

Net primary productivity (NPP): Rate at which algae produce organic carbon via photosynthesis minus the organic carbon used for respiration and metabolic activity.

Nitrate-nitrite: Includes both forms ($\text{NO}_3\text{-NO}_2$) of negatively charged ions consisting of nitrogen and three (nitrate) or two (nitrite) oxygen atoms.

Node: An SSM computational point defined in space to represent a location in the water column. The intermediate scale SSM grid consists of 16,012 nodes. Computation at each node is done for an area of influence (grid cell) surrounding it. The model predicts average water quality concentrations for each grid cell and layer for each time step.

Noncompliance: For the purposes of this report, noncompliance refers to a modeled excursion from the location-specific DO water quality criteria. See Appendix F in Ahmed et al. (2021).

Nonpoint source: Pollution that enters any waters of the state from any unpermitted dispersed land-based or water-based activities, including but not limited to atmospheric deposition, unregulated stormwater runoff from agricultural lands, urban areas, or forest lands; groundwater and unregulated interflow; and discharges from boats or marine vessels not otherwise regulated under the NPDES program. Generally, any unconfined and diffuse source of contamination. Legally, any source of water pollution that does not meet the legal definition of “point source” in section 502(14) of the Clean Water Act.

Normalized bias: A statistic that consists of the ratio between the bias and the standard deviation of the observations. See the equation for calculating this model skill statistic in Appendix D.

Normalized RMSE (NRMSE): A statistic that consists of the ratio between the root mean squared error and the standard deviation of the observations. See the equation for calculating this model skill statistic in Appendix D.

Normalized standard deviation (N_{sd}): A statistic that consists of the ratio between the simulated standard deviation and the observed standard deviation. See the equation for calculating this model skill statistic in Appendix D.

Optimization Phase 1 (Opt1): Optimization Phase 1 of the Puget Sound Nutrient Source Reduction Project (PSNSRP), which consisted of an analysis of an initial set of nutrient reduction scenarios. The first optimization phase was published as a technical memorandum (Ahmed et al. 2021).

Optimization Phase 2 (Opt2): Optimization Phase 2 of the Puget Sound Nutrient Source Reduction Project (PSNSRP), which consists of a refined set of nutrient reduction scenarios. The results of the second phase are published in this report.

Oxycline: A layer of rapidly changing DO concentration in a water body that forms a boundary between higher oxygen near the surface and lower oxygen below it.

PAR: Photosynthetically active radiation.

Parameter: Water quality constituent being measured (analyte). A physical, chemical, or biological property whose values determine environmental characteristics or behavior.

Performance-based approach: A defined approach that may be chosen to establish aquatic life water quality criteria for natural condition scenarios, development of these criteria values must follow the procedures per WAC 173-201A-470(1)(b).

pH: A measure of the acidity or alkalinity of water. A low pH value (0 to 7) indicates that an acidic condition is present, while a high pH (7 to 14) indicates a basic or alkaline condition. A pH of 7 is considered neutral. Since the pH scale is logarithmic, a water sample with a pH of 8 is ten times more basic than one with a pH of 7.

Point source: Any discernible, confined, and discrete conveyance, including but not limited to any pipe, ditch, channel, tunnel, conduit, well, discrete fissure, container, rolling stock, concentrated animal feeding operation, or vessel or other floating craft, from which pollutants are or may be discharged. This term does not include agricultural stormwater discharges and return flows from irrigated agriculture. Examples of point source discharges include domestic wastewater treatment plants, regulated stormwater, and industrial wastewater.

Pollution: Contamination or other alteration of the physical, chemical, or biological properties of any waters of the state. This includes changes in temperature, taste, color, turbidity, or odor of the waters. It also includes the discharge of any liquid, gaseous, solid, radioactive, or other substance into any waters of the state. This definition assumes that these changes will, or are likely to create a nuisance or render such waters harmful, detrimental, or injurious to (1) public health, safety, or welfare; (2) domestic, commercial, industrial, agricultural, recreational, or other legitimate beneficial uses; or (3) livestock, wild animals, birds, fish, or other aquatic life.

PSNSRP: Puget Sound Nutrient Source Reduction Project.

Primary production: Biomass production due to photosynthesis by phytoplankton.

Puget Sound: Includes South Sound, Main Basin, Whidbey Basin, Admiralty Inlet, and Hood Canal (see also Greater Puget Sound).

Region: Groupings of marine geographic areas within WA waters of the Salish Sea. In Ahmed et al. (2021), the regions include: South Sound Basin, Main Basin, Whidbey Basin, Hood Canal, the combined Strait of Juan de Fuca and Admiralty Inlet (aka SJF and Admiralty), and the combined Strait of Georgia, Bellingham, Samish, and Padilla Bays (aka SOG/Northern Bays).

Reference Condition: Surface water quality present before regional and local human-caused pollution.

Relative error (RE): A statistic that consists of the ratio of the absolute sum of the difference between observations and predictions and the sum of the observations. See the equation for calculating this model skill statistic in Appendix D.

Riparian: Relating to the banks along a natural course of water.

Rivers/streams: A freshwater pathway that delivers nutrients and drains watershed areas. In the context of this report, “river inputs” and “river inflows” are used interchangeably with “watersheds,” “watershed inputs,” and “watershed inflows” to represent the delivery of flow and nutrient inputs into the Salish Sea Model. In the model, these estimates are for the mouth of each river, stream, or watershed and represent loading at the point at which the freshwater inflow enters the Salish Sea. These estimates include but do not distinguish between various upstream point and nonpoint sources in the watersheds that contribute to the loading at the mouth.

Root mean square error (RMSE): A measure of model skill that gives more weight to larger errors because it is computed by taking the square root of the average squared differences of predictions and observations. A perfect model would have zero RMSE. See the equation for calculating this model skill statistic in Appendix D.

Salish Sea: Puget Sound, Strait of Georgia, and Strait of Juan de Fuca, including their connecting channels and adjoining waters.

Sediment Oxygen Demand: Dissolved oxygen that fluxes from the water column to the sediments to serve as an oxidant in biochemical processes.

Stormwater: The portion of precipitation that does not naturally percolate into the ground or evaporate but instead runs off roads, pavement, and roofs during rainfall or snow melt. Stormwater can also come from hard or saturated grass surfaces, such as lawns, pastures, playfields, and from gravel roads and parking lots.

Surface waters of the state: Lakes, rivers, ponds, streams, inland waters, salt waters, wetlands, and all other surface waters and water courses within the jurisdiction of Washington State.

Thermocline: A layer of rapidly changing temperature within a water body that forms a boundary between warmer water near the surface and cooler water below.

Tidal forcing: Tidal elevation time series at open boundary.

Tidal range: The difference between NOAA’s minimum and maximum water surface elevations for a given year.

Thalweg: The deepest portion of a stream or navigable channel.

Total days of DO noncompliance: The sum of all cumulative days of DO noncompliance within a larger spatial area, e.g., sum within each basin, or within all WA waters of the Salish Sea. This value can be greater than 365 (the number of days in a year) since it is calculated by adding up the cumulative days of DO noncompliance (defined above) associated with all 303(d) assessment units within an area.

Total nitrogen (TN): Total nitrogen; includes the organic and inorganic fractions.

Total Maximum Daily Load (TMDL): Water cleanup plan. A distribution of a substance in a water body that is designed to protect it from not meeting water quality standards. A TMDL is equal to the sum of all of the following: (1) individual wasteload allocations for point sources, (2) the load allocations for nonpoint sources, (3) the contribution of natural sources, and (4) a

Margin of Safety to allow for uncertainty in the wasteload determination. A reserve for future growth is also generally provided.

Very small wastewater treatment plants: A wastewater treatment facility that discharged not more than 10 kg/day TN or 6 kg/day DIN in terms of maximum monthly loads in 2014.

Washington Waters of the Salish Sea: Puget Sound, Strait of Georgia, and Strait of Juan de Fuca, the Northern Bays (Bellingham Bay, Samish Bay, and Padilla Bay), including their connecting channels and adjoining waters.

Watershed: A drainage area or basin in which all land and water areas drain or flow toward a central collector, such as a stream, river, or lake at a lower elevation.

Watershed inflows: See definition of “rivers” above.

Watershed load: Nutrient inputs originating in a watershed and primarily discharged into the Salish Sea via rivers and streams. Watershed loads can be composed of both point and nonpoint sources.

Willmott skill score (WSS): An index proposed by Willmott (1981) to measure agreement of model predictions compared to observations. A value of 1 indicates perfect agreement. See the equation for calculating this model skill statistic in Appendix D.

303(d) list: Section 303(d) of the federal Clean Water Act requires Washington State to periodically prepare a list of all surface waters in the state for which beneficial uses of the water, such as for drinking, recreation, aquatic habitat, and industrial use, are impaired by pollutants. These are water quality limited estuaries, lakes, and streams that fall short of state surface water quality standards and are not expected to improve within the next two years.

Acronyms and Abbreviations

| | |
|-------------------|--|
| BNR | biological nitrogen removal |
| BSR | Bounding Scenario Report (Ahmed et al. 2019) |
| CBOD ₅ | carbonaceous 5-day biological oxygen demand |
| DFO | Department of Fisheries and Oceans Canada |
| DIN | dissolved inorganic nitrogen |
| DO | dissolved oxygen |
| DOC | dissolved organic carbon |
| BMP | best management practice |
| Ecology et al. | Washington State Department of Ecology and others |
| EIM | Environmental Information Management database |
| EPA | U.S. Environmental Protection Agency |
| GIS | Geographic Information System software |
| HYCOM | Hybrid Coordinate Ocean Model |
| MAE | mean absolute error |
| MEL | Manchester Environmental Laboratory |
| MLLW | mean lower low water |

| | |
|--------|--|
| N | number of observations |
| NOAA | National Oceanic and Atmospheric Administration |
| NPDES | National Pollutant Discharge Elimination System (see glossary) |
| NRMSE | normalized root mean square error (normalized by dividing by the standard deviation of the observations) |
| NRMSEc | centered, normalized root mean square error (symbology also used is uRMSE) |
| OBC | ocean boundary condition |
| OFM | Office of Financial Management |
| Opt1 | Optimization Phase 1 Technical Memorandum (Ahmed et al. 2021) |
| Opt2 | Optimization Phase 2 Report (this work) |
| POC | particulate organic carbon |
| POM | particulate organic matter |
| PSEMP | Puget Sound Ecosystem Monitoring Program |
| QAPP | Quality Assurance Project Plan |
| R | correlation coefficient |
| RE | relative error |
| RMSE | root mean squared error |
| RMSEc | centered (or unbiased) root mean square error |
| RPD | relative percent difference |
| RSD | relative standard deviation |
| SD_obs | standard deviation of observations |
| SJF | Strait of Juan de Fuca |
| SOG | Strait of Georgia |
| SOD | sediment oxygen demand |
| SOP | standard operating procedures |
| SRM | standard reference materials |
| SSM | Salish Sea Model |
| TCE | triangular control element used in SSM |
| TMDL | Total Maximum Daily Load (see glossary) |
| TN | total nitrogen |
| TOC | total organic carbon |
| USGS | U.S. Geological Survey |
| WA | Washington State |
| WQS | water quality standard |
| UW | University of Washington |
| SSMC | Salish Sea Modeling Center |
| WAC | Washington Administrative Code |
| WRIA | Water Resource Inventory Area |
| WSS | Willmott skill score |
| WWTP | wastewater treatment plant |
| WWU | Western Washington University |

Units of Measurement

| | |
|---------------------------------------|---|
| °C | degrees centigrade |
| cfs | cubic feet per second |
| cms | cubic meters per second, a unit of flow |
| dw | dry weight |
| E-m ² /day | Einsteins (mole of photons) measured in a square meter per day, a measure of the amount of available light or photosynthetically active radiation |
| ft | feet |
| g | gram, a unit of mass |
| g O ₂ /m ² /day | grams of oxygen per square meter per day, a measure of flux, particularly sediment oxygen demand |
| kcfs | 1,000 cubic feet per second |
| kg | kilograms, a unit of mass equal to 1,000 grams |
| kg O ₂ /hour | kilograms of oxygen per hour, a measure of dissolved oxygen consumption |
| kg/d | kilograms per day |
| km | kilometer, a unit of length equal to 1,000 meters |
| L/s | liters per second (0.03531 cubic foot per second) |
| m | meter |
| mg | milligram |
| mgd | million gallons per day |
| mg/d | milligrams per day |
| mg/kg | milligrams per kilogram (parts per million) |
| mg/L | milligrams per liter (parts per million) |
| mg/L/hr | milligrams per liter per hour |
| mL | milliliters |
| mm | millimeters |
| mmol | millimole or one-thousandth of a mole |
| mole | an International System of Units (IS) unit of matter |
| ng/g | nanograms per gram (parts per billion) |
| ng/kg | nanograms per kilogram (parts per trillion) |
| ng/L | nanograms per liter (parts per trillion) |
| NTU | nephelometric turbidity units |
| pg/g | picograms per gram (parts per trillion) |
| pg/L | picograms per liter (parts per quadrillion) |
| psu | practical salinity units |
| s.u. | standard units |
| µg/g | micrograms per gram (parts per million) |
| µg/kg | micrograms per kilogram (parts per billion) |
| µg/L | micrograms per liter (parts per billion) |
| µm | micrometer |
| µM | micromolar, a chemistry unit |
| µmhos/cm | micromhos per centimeter |
| µS/cm | microsiemens per centimeter, a unit of conductivity |
| ww | wet weight |

Appendices

Appendices A through O are available online and are linked to this report at <https://apps.ecology.wa.gov/publications/SummaryPages/2503003.html>.

Appendix A. Modeling Approach, Parameter, and Rate Updates

Appendix B. Watershed and Open Boundary Condition Updates

Appendix B1. Updates to Watershed Delineations as well as Freshwater Flows, Water Quality Data, and Regressions

Appendix B2. Changes to Watershed Loading due to updates

Appendix B3. Time Series Plots of Flow and Water Quality for Watersheds

Appendix B4. Evaluation of Inorganic Nitrogen Watershed Regressions on Continuous Data.

Appendix B5. Open boundary tides and water quality.

Appendix C. Point Source Updates

Appendix C1. Point Source Water Quality Updates

Appendix C2. Point Source Inflows and Water Quality

Appendix D. Miscellaneous

Appendix E. Model Performance Plots for 2000

Appendix E1. Water Quality Model Performance Plots for 2000

Appendix E2. Dissolved Oxygen Scatterplots for Surface, Middle, and Bottom Waters for 2000

Appendix E3. Hydrodynamic Model Performance Plots for 2000

Appendix F. Model Performance Plots for 2006

Appendix F1. Water Quality Model Performance Plots for 2006

Appendix F2. Dissolved Oxygen Scatterplots for Surface, Middle, and Bottom Waters for 2006

Appendix F3. Hydrodynamic Model Performance Plots for 2006: Water Surface Elevations

Appendix F4. Hydrodynamic Model Performance Plots for 2006: Tidal Velocities

Appendix G. Model Performance Plots for 2008

Appendix G1. Water Quality Model Performance Plots for 2008

Appendix G2. Dissolved Oxygen Scatterplots for Surface, Middle, and Bottom Waters for 2008

Appendix G3. Hydrodynamic Model Performance Plots for 2008

Appendix H. Model Performance Plots for 2014

Appendix H1. Water Quality Model Performance Plots for 2014

Appendix H2. Dissolved Oxygen Scatterplots for Surface, Middle, and Bottom Waters for 2014

Appendix H3. Hydrodynamic Model Performance Plots for 2014

Appendix I. Sediment Fluxes

Appendix J. Microalgal Biomass and Primary Productivity

Appendix K. Microbial Respiration in Bottom Waters

Appendix L. Initial Optimization Phase 2 (Opt2) Model Scenarios

Appendix M. Residence and Flushing Times

Appendix N. Additional Opt2 Scenario Results

Appendix O. Assessment of Budd Inlet TMDL Open Boundary Load Allocation